SampleID: exome_MG16413
Platform: illumina
Platform unit: C8EU1ANXX
Library: NexteraExomeCapture
Phenotype: HP:0012234
Barcode: 180215_D00183_0091_AC8EU1ANXX
Genome: Homo_sapiens.GRCh38.dna.primary_assembly_titled.fa
Bam file: exome_MG16413.bam

Minimal coverage per bases
Coverage 10x: 82180482
Coverage 20x: 57883116
Coverage 30x: 41875615
Coverage 50x: 22569174
Coverage 100x: 5912973
Coverage 1000x: 49830
Coverage 8000x: 0

Reads statistics
49031717 + 0 in total (QC-passed reads + QC-failed reads)
503085 + 0 secondary
0 + 0 supplementary
0 + 0 duplicates
48974337 + 0 mapped (99.88% : N/A)
48528632 + 0 paired in sequencing
24264316 + 0 read1
24264316 + 0 read2
46383450 + 0 properly paired (95.58% : N/A)
48434364 + 0 with itself and mate mapped
36888 + 0 singletons (0.08% : N/A)
1738344 + 0 with mate mapped to a different chr
1412947 + 0 with mate mapped to a different chr (mapQ>=5)

Alignment metrics

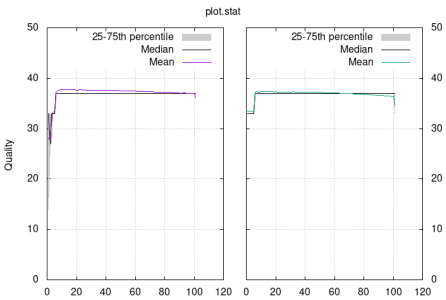

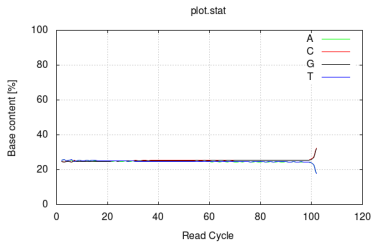

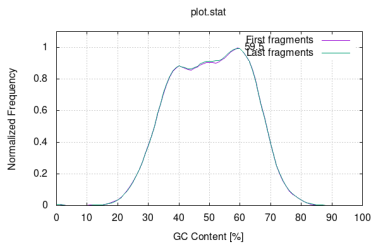

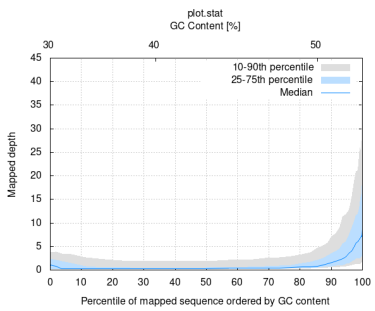

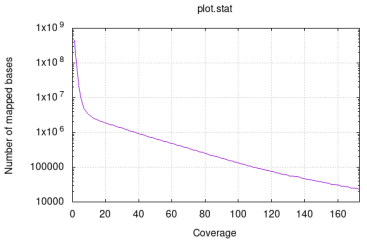

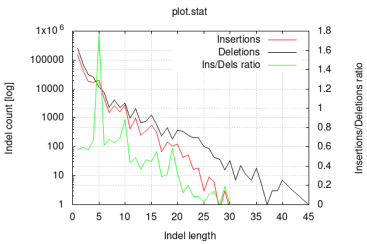

Variants with pathogenic clasification

Gene name	Genome level	Region	Protein level	Genotype	ExAC freq	ClinVar rs	ClinVar phenotype
F5	g[1:169549811_C>T]	exon:10	.	reference heterozygous	.	rs6025	Budd-Chiari_syndrome/susceptibility_to|Ischemic_stroke /susceptibility_to|Recurrent_abortion|Factor_V_deficiency|Thrombophilia_due_to_activated_protein_C_resistance|Thrombophilia_due_to_factor_V_Leiden
F5	g[1:169549811_C>T]	CDS:10	534:2_R>Q	reference heterozygous	.	rs6025	Budd-Chiari_syndrome/susceptibility_to|Ischemic_stroke /susceptibility_to|Recurrent_abortion|Factor_V_deficiency|Thrombophilia_due_to_activated_protein_C_resistance|Thrombophilia_due_to_factor_V_Leiden
MBL2	g[10:52771475_C>T]	exon:1	.	reference heterozygous	.	rs1800450	Mannose-binding_protein_deficiency
MBL2	g[10:52771475_C>T]	CDS:1	54:2_G>D	reference heterozygous	.	rs1800450	Mannose-binding_protein_deficiency
ABCC6	g[16:16198014_G>C]	intron:10	.	reference heterozygous	.	rs9940089	Pseudoxanthoma_elasticum
SLC9A3R1	g[17:74749174_C>G]	exon:1	.	reference heterozygous	.	rs35910969	Nephrolithiasis/osteoporosis/hypophosphatemic/2
SLC9A3R1	g[17:74749174_C>G]	CDS:1	110:1_L>V	reference heterozygous	.	rs35910969	Nephrolithiasis/osteoporosis/hypophosphatemic/2
RYR1	g[19:38499961_T>A]	exon:45	.	reference heterozygous	.	rs118192174	Talipes_equinovarus|EMG_abnormality|Lower_limb_amyotrophy|Minicore_myopathy_with_external_ophthalmoplegia|not_provided
RYR1	g[19:38499961_T>A]	CDS:45	2423:2_M>K	reference heterozygous	.	rs118192174	Talipes_equinovarus|EMG_abnormality|Lower_limb_amyotrophy|Minicore_myopathy_with_external_ophthalmoplegia|not_provided
KLKB1	g[4:186236880_G>A]	exon:5	.	non-reference homozygous	.	rs3733402	Prekallikrein_deficiency
KLKB1	g[4:186236880_G>A]	CDS:4	143:2_S>N	non-reference homozygous	.	rs3733402	Prekallikrein_deficiency
KLKB1	g[4:186236880_G>A]	exon:6	.	non-reference homozygous	.	rs3733402	Prekallikrein_deficiency
KLKB1	g[4:186236880_G>A]	CDS:3	105:2_S>N	non-reference homozygous	.	rs3733402	Prekallikrein_deficiency
GATA4	g[8:11748803_T>C]	UTR5	.	reference heterozygous	.	rs3735819	Congenital_heart_disease
GATA4	g[8:11748803_T>C]	intron:2	.	reference heterozygous	.	rs3735819	Congenital_heart_disease
GATA4	g[8:11748803_T>C]	intron:1	.	reference heterozygous	.	rs3735819	Congenital_heart_disease
GATA4	g[8:11748803_T>C]	intron:4	.	reference heterozygous	.	rs3735819	Congenital_heart_disease
GATA4	g[8:11758186_A>G]	intron:6	.	reference heterozygous	.	rs745379	Congenital_heart_disease
GATA4	g[8:11758186_A>G]	intron:5	.	reference heterozygous	.	rs745379	Congenital_heart_disease
GATA4	g[8:11758186_A>G]	intron:8	.	reference heterozygous	.	rs745379	Congenital_heart_disease
C1GALT1C1	g[X:120626774_A>T]	exon:2	.	non-reference homozygous	.	rs17261572	Polyagglutinable_erythrocyte_syndrome
C1GALT1C1	g[X:120626774_A>T]	exon:3	.	non-reference homozygous	.	rs17261572	Polyagglutinable_erythrocyte_syndrome
C1GALT1C1	g[X:120626774_A>T]	CDS:1	131:3_D>E	non-reference homozygous	.	rs17261572	Polyagglutinable_erythrocyte_syndrome

Variants selected by phenotype

Gene name	Genome level	Region	Protein level	Genotype	ExAC freq	dbSNP	Phenotype
ELANE	g[19:853279_G>C]	CDS:3	81:2_R>P	reference heterozygous		.	Autosomal dominant severe congenital neutropenia^CYCLIC NEUTROPENIA^RNA polymerase II transcription corepressor activity^negative regulation of transcription from RNA polymerase II promoter in response to UV-induced DNA damage^NEUTROPENIA SEVERE CONGENITAL 1 AUTOSOMAL DOMINANT

RESEARCH PAPER

New Biotechnology • Volume 33, Number 5 • September 2016

Research Paper

Transgenic barley overexpressing a cytokinin dehydrogenase gene shows greater tolerance to drought stress

Hana Pospíšilová[1], Eva Jiskrová[1], Petr Vojta[1,2], Katarína Mrízová[1], Filip Kokáš[1], Mária Majeská Čudejková[1], Veronique Bergougnoux[1], Ondřej Plíhal[1], Jana Klimešová[3], Ondřej Novák[4], Lenka Dzurová[1], Ivo Frébort[1] and Petr Galuszka[1]

[1] Department of Molecular Biology, Centre of the Region Haná for Biotechnological and Agricultural Research, Faculty of Science, Palacký University in Olomouc, Šlechtitelů 27, 783 71 Olomouc, Czech Republic
[2] Institute of Molecular and Translational Medicine, Faculty of Medicine and Dentistry, Palacký University Olomouc, Hněvotínská 1333/5, 779 00 Olomouc, Czech Republic
[3] Department of Crop Science, Mendel University in Brno, Zemědělská 1, 613 00 Brno, Czech Republic
[4] Department of Metabolomics, Centre of the Region Haná for Biotechnological and Agricultural Research, Institute of Experimental Botany AS CR, Šlechtitelů 27, 783 71 Olomouc, Czech Republic

Together with auxins, cytokinins are the main plant hormones involved in many different physiological processes. Given this knowledge, cytokinin levels can be manipulated by genetic modification in order to improve agronomic parameters of cereals in relation to, for example, morphology, yield, and tolerance to various stresses. The barley (*Hordeum vulgare*) cultivar Golden Promise was transformed using the cytokinin dehydrogenase 1 gene from *Arabidopsis thaliana* (*AtCKX1*) under the control of mild root-specific β-glucosidase promoter from maize. Increased cytokinin degradation activity was observed positively to affect the number and length of lateral roots. The impact on morphology depended upon the recombinant protein's subcellular compartmentation. While assumed cytosolic and vacuolar targeting of AtCKX1 had negligible effect on shoot growth, secretion of AtCKX1 protein to the apoplast had a negative effect on development of the aerial part and yield. Upon the application of severe drought stress, all transgenic genotypes maintained higher water content and showed better growth and yield parameters during revitalization. Higher tolerance to drought stress was most caused by altered root morphology resulting in better dehydration avoidance.

Introduction

Barley (*Hordeum vulgare*) is an economically important crop plant used primarily in producing malt, food, feed, and pharmaceutical products. Stable genetic modification of model barley cultivars is a well-developed method used for testing various approaches which might lead to better agronomic traits in cereals from the Triticeae tribe. Plant architecture can be modified by disturbing cytokinin homeostasis. Cytokinins (CKs) are plant hormones [1] that in addition to being involved in morphogenesis also participate in the regulation of many physiological processes, including tolerance to drought stress [2,3].

CK-mediated tolerance to drought stress could be acquired through two approaches. The first is based on the knowledge that increased CK concentration promotes plant acclimatization and survival rate and minimizes yield losses. This approach could be realized by stress-inducible overexpression of adenylate isopentenyl transferase (IPT), which is a key enzyme in isoprenoid CKs biosynthesis within plants [4–8]. Another successful approach

Corresponding author: Galuszka, P. (petr.galuszka@upol.cz)

http://dx.doi.org/10.1016/j.nbt.2015.12.005

decreases CK content in roots by overproduction of CK-degradation enzymes, thus resulting in modified root morphology or enhanced root biomass [9,10].

Degradation of CKs is catalyzed by a family of cytokinin dehydrogenases (CKX; [11]). CKX isoenzymes vary in their localization to different subcellular compartments [12,13] or in the temporal pattern of their expression [14]. Substrate specificity and localization of individual CKXs are best characterized in Arabidopsis (*Arabidopsis thaliana*), which contains two vacuolar CKXs (AtCKX1 and AtCKX3), one cytosolic (AtCKX7), and four probably apoplastic CKXs [13]. Secreted (apoplastic) CKX forms prefer free CK bases as substrate, whereas vacuolar CKXs prefer CK nucleotides, which are primary products of *de novo* biosynthesis [15]. Because the various CKX forms have different biological functions, a combination of desired enzyme activity, signal sequence, and a suitable tissue- or organ-specific promoter can selectively affect the plant phenotype.

Transgenic dicotyledonous plants with constitutively overexpressed CKX exhibit a CK-deficient phenotype which manifests in a smaller aerial part, lower fertility, and a larger root system [9,16] as was in details shown on the transgenic Arabidopsis with overexpressed AtCKX1–6 [13]. Generally, plants overexpressing vacuole-targeted CKXs (AtCKX1 and 3) showed stronger phenotype than overexpressors of apoplastic forms (AtCKX2 and 4). Arabidopsis plants with root-specific overproduction of AtCKX3 have up to 40% increased root mass without any negative impact on inflorescence, fertility, or seed formation. Moreover, these plants have shown greater tolerance to drought stress [17]. Similar phenotype and increased tolerance to drought have been observed also in tobacco with overexpressed AtCKX1 [10]. In contrast to dicotyledonous plants, constitutive overexpression of the maize apoplastic *ZmCKX1* gene under the control of the maize ubiquitin promoter in barley has a lethal effect [14]. During transformation, CKX as a transgene significantly reduces ability to regenerate from *in vitro* culture and causes in transformants premature senescence and inability to transit into inflorescence [14]. To avoid the lethal or strongly CK-deficient phenotype, the weaker maize β-glucosidase promoter (*bGLU*; [18]) has been used to regulate the *ZmCKX1* transgene in barley (our unpublished data). However, the resulting transgenic plants also had reduced ability to regenerate from tissue cultures and strongly CK-deficient phenotype. Additionally, enhanced expression of rice *OsCKX4* under the control of the ubiquitous promoter in *Oryza sativa* led to the formation of a robust root system with increased numbers of crown roots and significantly reduced plant height and yield at the mature stage [19]. These data indicate that the results obtained during the studies of CKX overexpression in dicotyledonous plants cannot be easily applied to such monocotyledonous plants as cereals, which may differ in control of CK metabolism and homeostasis [20].

The main objective of the present study was to introduce an appropriate intracellular form of CKX into the barley genome under control of the weak *bGLU* promoter to regulate CK homeostasis ectopically in the root tissue. Plants generated with the transgene stably integrated manifested a changed root architecture and increased tolerance to drought stress without a negative effect on yield.

Material and methods

Plasmid construction

A region 905 bp long of the maize β-glucosidase promoter (DQ333310.1; [18]) linked to the secretion signal sequence of the *AtCKX2* gene (NM_127508.2) and a coding sequence of *AtCKX1* trimmed of its native vacuolar targeting signal (NM_129714.3) was synthesized by Mr. Gene GmbH (Regensburg, Germany). The second construct was prepared by cutting off the signal sequence flanked with *Bst*BI and self-ligating. The third construct was obtained by subcloning of the full-length *AtCKX1* cDNA into the synthesized plasmid. Sequences of all three expected transcribed proteins are summarized in Fig. S4. The functional segments of DNA were inserted into the plant binary pBRACT209 vector (www.bract.org) and electrotransferred into *Agrobacterium tumefaciens* strain AGL1.

Barley transformation

All procedures from the collection of immature grains to regeneration of transgenic plantlets were performed according to the protocol described in Harwood *et al.* [21]. Plants of the spring barley cultivar Golden Promise were grown in an environmental chamber with photoperiod of 15°C/16 h/light and 12°C/8 h/dark. The light source was a combination of mercury tungsten lamps and sodium lamps providing intensity of 300 μmol m^{-2} s^{-1}. Plants were cultivated in a 2:1 mixture of soil and perlite (Perlit Ltd., Czech Republic) and were fertilized every 14 d. Soil composition was 1:1 professional substrate for plant growth (Rašelina Soběslav, Czech Republic) and soil from arable land of the Olomouc Region.

Real-time PCR analysis

Isolation of total RNA was performed with an RNAqueous kit (Life Technologies); the isolated RNA was treated using a TURBO DNA-free kit (Life Technologies) and purified by magnetic beads (Agencourt RNA-CLEAN XP, Beckman Coulter). Preparation of cDNA and real-time PCR was set up according to [14]. Primers are listed in Table S1.

RNA-seq analysis

Working with 2.5 μg of total RNA from each sample, extracted as described above, Illumina® TruSeq® Stranded mRNA Sample Preparation Kit (Illumina) was used for cDNA library preparation. Library concentration was assessed with a Kapa Library Quantification Kit (Kapa Biosystem) and all libraries were pooled to the final 8 pM concentration for cluster generation and sequencing. In the first sequencing run (the first technical replicate), the clusters were generated using an Illumina® TruSeq® PE Cluster Kit v3 cBot HS and sequenced on HiSeq PE Flow Cell v3 with a HiSeq 2500 Sequencing System. The same library was used for a second sequencing run (second technical replicate) with cluster generation using a TruSeq® SR Cluster Kit v3 cBot HS and HiSeq SR Flow Cell v3. Two biological and two technical replicates were sequenced for each sample.

The reads generated by sequencing were mapped to the reference genome of *Hordeum vulgare* v.25 (Ensembl) using a Tohat v.2.0.12 splice-read mapper [22] at default parameters. The reads mapped to the transcripts annotated in the reference genome, were quantified by using HTSeq v.0.6.0 [23] with respect to the stranded library. The tests for differential gene expression were

performed using the DESeq2 package [24] implemented in R [25]. The technical replicates were at first analyzed as two independent experiments, which yielded the same results. Afterwards, technical replicates were merged into one technical replicate to obtain higher coverage of reference transcriptome. Gene ontology (GO) annotation of the reference genome was improved by using the Blas2GO v.3.0 program [26] and nt database (b2g_Jan15), as well as the ncbi-blast+ v.2.2.28 program [27] and the UniProKB (http://www.uniprot.org/, 2015_02) and PGSB (http://pgsb.helmholtz-muenchen.de/plant/, 2014_07_31) databases. This additional GO annotation helped to increase the number of GO annotated genes to 17,885 (from the total of 26,074 genes). To draw the KEGG pathway diagrams of molecular interactions, reactions, and relations [28,29], the reference genome was blasted against the *Zea mays* genome downloaded from http://www.genome.jp/kegg/genome.html (Entry number: T01088) while accepting the first best blast hit with *e*-value $< 10^{-3}$. The blast results were then filtered to accept only those results having >80% identity, and 20,108 genes of the reference genome were definitely assigned to the *Zea mays* genes.

CKX activity assay

The CKX activity was determined spectrophotometrically [30] using 0.5 mM 2,3-dimetoxy-5-methyl-1,4-benzoquinone as an electron acceptor and 0.25 mM substrate iPR in McIlvaine buffer (pH 5.5). All measurements were performed in three biological replicates.

Measuring of CK content

The procedure used for CK purification and quantification was described in Vyroubalová *et al.* [31]. Measurement for each line consisted of at least four biological replicates.

Phenotypic analysis of transgenic plants

For phenotype determination, plants were grown hydroponically in a modified Hoagland solution [32] within an environmental chamber and with photoperiod of 22°C/16 h/light and 20°C/8 h/dark. Root length and area were determined by digital image analysis with program WinRHIZO (Regent Instruments, Québec, Canada). To determine dry mass of the aerial parts and roots, drying was carried out at 70°C for 48 h.

Drought stress

Mild drought stress was applied to plants 3 months old grown in a greenhouse in pots (0.3 m × 0.2 m × 0.2 m; composition of soil is described above). This soil was allowed to dry at regular intervals and the plants were watered according to plant age and temperature conditions, which corresponded to 1–3 waterings per week (200 mL per 1 kg of growing substrate). Control plants were watered on a daily basis.

The severe drought stress study was carried out using hydroponically grown plants. Fifteen plants from each genotype were cultivated with half of each vessel being filled with transgenic plants and the other half with WT plants. The experiment was performed twice in two time-independent replications. Stress was induced by draining the modified Hoagland solution out of the growth vessel. Plants were returned to the vessel, where they were further grown for another 24 h. During the 24 h period, leaves were collected for the determination of RWC [33].

Drought stress during revitalization studies was applied to barley plants 4 and 6 weeks old grown on trays (30 cm × 20 cm with depth of 0.5 cm) filled with growing substrate under controlled phytotron conditions (15°C/16 h/light and 10°C/8 h/dark, light intensity of 260 μmol m^{-2} s^{-1} at the top level of plants).

Plants were kept without watering for the following 3 d and then regularly watered on a daily basis. The youngest fully developed leaves were collected for the determination of RWC. Aerial parts of plants 8 weeks old were collected to estimate dry mass. At least 30 plants per genotype were grown in each experiment.

Statistical analysis

Two-sample *t*-test and ANOVA (Tukey and Bonferroni tests) at significance level 0.05 were performed using OriginPro 8.5.1 (OriginLab Corporation, Northampton, MA, USA). Some of the *t*-tests were carried out with STATISTICA 12 (StatSoft CR, Czech Republic).

Results

The spring barley cultivar Golden Promise was transformed using constructs enabling overexpression of the *AtCKX1* gene with native vacuolar sorting signal experimentally approved in Arabidopsis plants [9], engineered secretion signal sequence, and without any signal sequence. Transformation was approved on the genomic DNA, transcript, and protein levels. The stability of transgenic homozygotic lines was confirmed in three consecutive generations without any negative effect on transgene expression. Three independent transgenic lines of both cytosolic (*bGLU::cAtCKX1*) and vacuolar (*bGLU::vAtCKX1*) genotypes as well as one line with apoplastic AtCKX1 (*bGLU::aAtCKX1*) genotype were selected for further work. All studied lines were confirmed to be diploid and contain only a single T-DNA insertion (data are not shown).

Level of AtCKX1 *expression driven by* bGLU *promoter*

Real-time PCR analysis was used to clarify the function of the maize *bGLU* promoter in *bGLU::vAtCKX1* barley. Although in earlier works [18,34] *bGLU* promoter activity had been associated mainly with root tissue, further research had revealed less tissue-specific behavior [35,36]. The greatest expression of *AtCKX1* under the control of the *bGLU* promoter was detected in the period from the 2nd to 8th week after germination (Fig. 1a and b). When expression was estimated in samples collected from the whole root system and the aerial part, only 2–3-fold higher expression of AtCKX1 was detected in roots during the first 5 weeks of development. Significantly higher expression (14-fold) in roots than in leaves was observed later, in the 8th week after germination (Fig. 1a). Plants 14 or 16 weeks old had lower numbers of *AtCKX1* transcripts in roots as well as in other organs (data not shown).

When compared to the strength of the *bGLU* promoter with the 35S constitutive promoter, which had been integrated into the barley genome as a part of the T-DNA to drive expression of the hygromycin selection cassette (*hpt*), the *bGLU* promoter was 100–500-fold less effective (Fig. 1a and b).

CKX activity in transgenic tissues

At the level of total CKX activity, the T1 generation of transgenic plants with one T-DNA insertion had up to 10-fold increased CKX

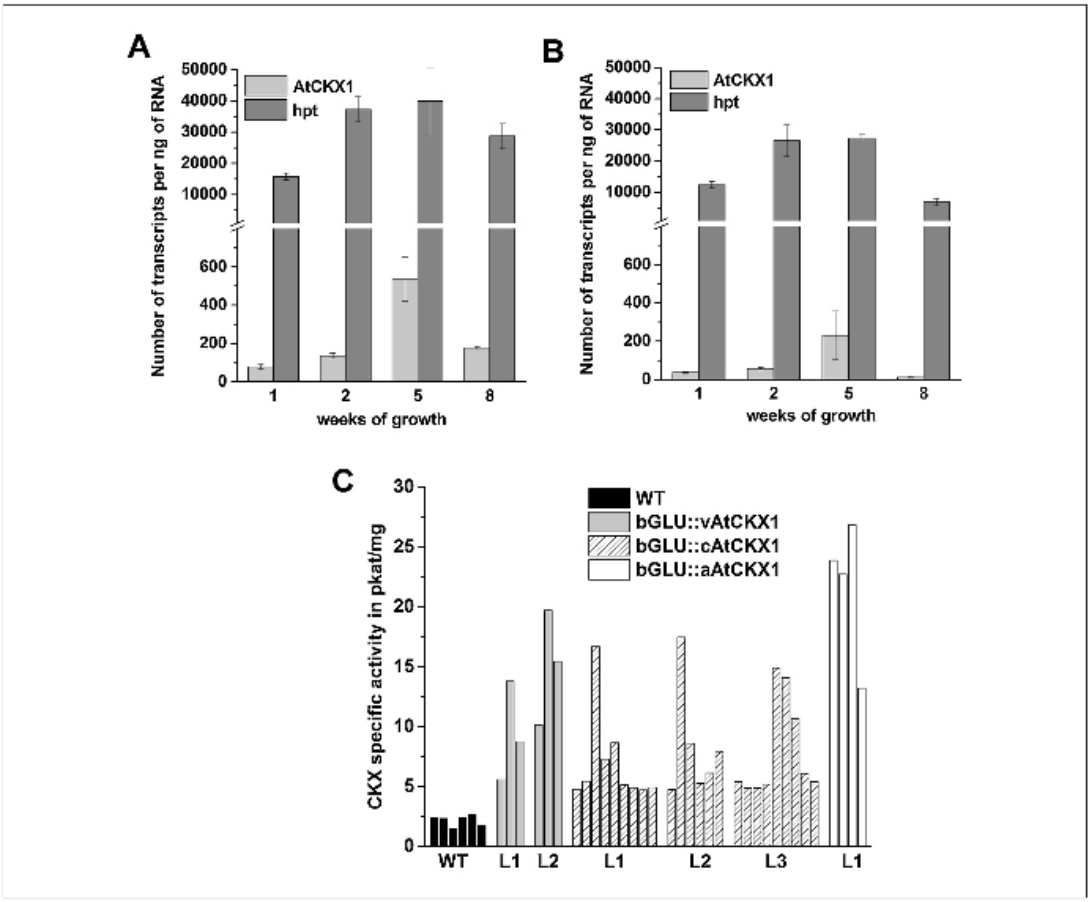

FIGURE 1

AtCKX1 gene expression and increased enzymatic activity of CKX. **(a)** Number of *AtCKX1* and *hpt* transcripts in 1 ng of RNA isolated from the whole root system. **(b)** Number of *AtCKX1* and *hpt* transcripts in 1 ng of RNA isolated from the aerial part. **(c)** CKX activity (pkat/mg) in T1 generation plant roots of two independent lines of *bGLU::vAtCKX1* (L1, 2), three independent lines of *bGLU::cAtCKX1* (L1, 2, 3), and one independent line of *bGLU::aAtCKX1* (L1) are compared to WT plants. Each bar represents a sample from a single plant 1 month old.

activity in roots compared to wild-type (WT) tissue (Fig. 1c). Variability of CKX activity among plants in the same transgenic line is caused by Mendelian segregation, as the tested plants could be heterozygous or homozygous (WT plants were excluded from the measurement). No significant differences in CKX activity in leaves and grains were detected between the control and transgenic barley.

Regulation of cytokinin biosynthetic and cytokinin degradation genes in transgenic barley

Expression profiles of native barley genes involved in CK *de novo* biosynthesis (HvIPT) and CK degradation (HvCKX) were examined in roots and the aerial part of two independent *bGLU::vAtCKX1* lines and compared to WT levels (Fig. 2). The most abundant genes in vegetative tissues during the juvenile phase of development were measured on the basis of our previous work [14].

Generally, *bGLU::vAtCKX1* plants during the vegetative growth phase down-regulate the majority of *HvCKX* genes in both the roots and the aerial part (Fig. 2). There are a few deviations from this tendency, as expression of *HvCKX11* in the 10-week-old leaves of both independent lines and of *HvCKX4* in the 8-week-old leaves of one line were up-regulated. In the roots, expression of *HvCKX4* and *HvCKX5* was significantly up-regulated 6 weeks after germination. At the same time point, the lowest levels of *HvCKX1*, *3*, and *9* were detected in the roots. On the other hand, expression of the two most abundant *HvIPT* genes (*HvIPT2* and *HvIPT5*) was up-regulated in the leaves. In the root, *HvIPT2* was also up-regulated at several time points, while expression of *HvIPT5* was more or less comparable with that of WT with the exception that it was down-regulated in roots of plants 2 and 10 weeks old. The presented results indicate that the plant overexpressing *AtCKX1* tends to maintain a natural CK homeostasis by regulation of endogenous

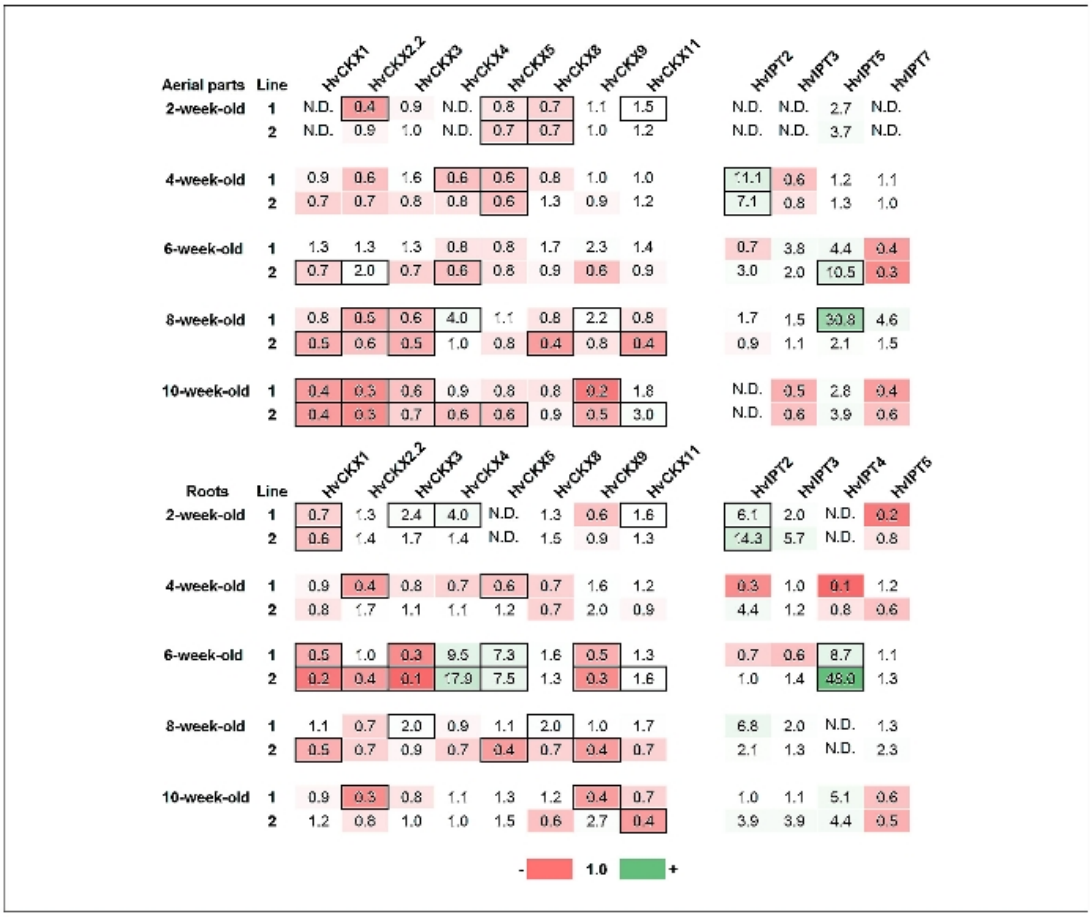

FIGURE 2

Relative quantity of *HvIPT* and *HvCKX* transcripts in roots and aerial parts of transgenic *bGLU::vAtCKX1* barley 2–10 weeks old. Quantity values are relative to WT levels (assigned as 1). Values are color-coded from red to green (from the most down-regulated to the most up-regulated). Genes encoding *HvCKX 2.2, 4, 5, 8,* and *11* and *HvIPT 2* and *5* in the aerial part and *HvCKX 1, 3, 4, 5, 8,* and *11* and *HvIPT 2* and *5* in roots are considered as abundant, in accordance with [14]. Each measurement consisted of three biological (2–5 pooled plants) and two technical replicates. Black-framed values indicate significant difference between WT and transgenic tissue according to unpaired Student's *t*-test at $P \leq 0.05$. N.D., not detected.

CK biosynthesis and degradation genes. This observation is further supported by results from CK content determination.

Cytokinin content in transgenic barley

The contents of all CK metabolites were determined separately in the roots and aerial parts of T2 homozygous progeny of *bGLU::vAtCKX1* (Fig. 3). Storage and deactivated forms of CKs, mainly *O*-glucosides of *cis*-zeatin (*cZ*) and its riboside (*cZR*) together with *N9*-glucoside of *trans*-zeatin (*tZ*), were the most predominant CKs detected in both the root and aerial parts (Fig. S1). Isopentenyladenine (iP) was prevalent primarily in the form of its nucleotide (iPR5MP). On the other hand, levels of *cZ* nucleotide (*cZR5MP*) were lower and those of *tZ* nucleotide were beneath the limit of detection. Levels of free bases and ribosides, considered as only active CK forms, were generally lower than were those considered as for storage and transport (*O*-glucosides) or as deactivated (*N*-glucosides). *tZ* free base prevailed over its riboside in whole seedlings while iP was prevalent in the form of riboside in roots and to a lesser extent also in the aerial part. Levels of *cZ* forms slightly exceeded those of the two other isoprenoid CKs. Levels of dihydrozeatin metabolites were generally lower (Fig. S1). Figure 3a makes clear that alteration of CK homeostasis in the two independent *bGLU::vAtCKX1* lines is in good accordance, an exception being isopentenyladenine riboside (iPR) content in plants 4 weeks old. The most reduced level of iP was detected in the aerial part especially in the youngest plants. On the other hand, the most reduced *tZ* content was detected in 6-week-old roots. Levels of isopentenyladenine-*N9*-glucoside (iP9G), which is considered as an irreversible inactivation product, continuously dropped in comparison to WT with increasing age of plants.

A

Biologically active forms in % of WT

Aerial parts	Line	tZ	tZR	cZ	cZR	iP	iPR
2-week-old	1	80 ± 14	104 ± 4	84 ± 7	71 ± 13	12 ± 3	278 ± 9
	2	58 ± 16	79 ± 16	104 ± 13	105 ± 14	14 ± 4	110 ± 22
4-week-old	1	200 ± 30	182 ± 5	68 ± 14	61 ± 14	99 ± 13	54 ± 11
	2	161 ± 11	241 ± 49	45 ± 15	75 ± 10	89 ± 11	112 ± 14
6-week-old	1	111 ± 12	134 ± 17	89 ± 24	91 ± 16	87 ± 12	83 ± 7
	2	117 ± 13	170 ± 18	88 ± 20	253 ± 28	90 ± 4	72 ± 14
Roots							
2-week-old	1	142 ± 15	120 ± 16	165 ± 20	119 ± 8	480 ± 18	180 ± 11
4-week-old	1	99 ± 15	161 ± 27	129 ± 20	94 ± 18	225 ± 33	18 ± 5
	2	57 ± 8	123 ± 21	127 ± 8	151 ± 24	470 ± 12	223 ± 18
6-week-old	1	25 ± 6	478 ± 43	65 ± 16	124 ± 34	108 ± 9	287 ± 28
	2	11 ± 5	929 ± 29	71 ± 13	137 ± 15	145 ± 26	407 ± 50

Storage, biologically inactive and transport forms in % of WT

Aerial parts	Line	tZOG	tZROG	tZ9G	cZOG	cZROG	cZ9G	cZR5MP	DHZOG	DHZROG	iP9G	iPR5MP
2-week-old	1	114 ± 8	118 ± 9	96 ± 5	93 ± 2	83 ± 2	78 ± 5	58 ± 18	125 ± 4	121 ± 12	77 ± 3	68 ± 13
	2	118 ± 8	77 ± 15	104 ± 18	113 ± 6	102 ± 18	142 ± 1	88 ± 14	105 ± 12	165 ± 25	101 ± 1	84 ± 8
4-week-old	1	109 ± 12	40 ± 15	108 ± 6	97 ± 5	88 ± 6	43 ± 4	100 ± 28	110 ± 8	61 ± 6	81 ± 6	58 ± 11
	2	117 ± 5	42 ± 8	132 ± 6	99 ± 9	86 ± 6	73 ± 1	511 ± 38	122 ± 9	42 ± 10	42 ± 6	60 ± 15
6-week-old	1	89 ± 5	68 ± 10	96 ± 7	101 ± 6	92 ± 6	71 ± 14	76 ± 21	93 ± 7	67 ± 18	105 ± 5	77 ± 11
	2	89 ± 11	93 ± 1	71 ± 8	108 ± 10	95 ± 10	89 ± 15	152 ± 15	81 ± 17	75 ± 5	79 ± 6	113 ± 20
Roots												
2-week-old	1	99 ± 7	120 ± 23	74 ± 18	140 ± 7	121 ± 2	92 ± 15	5577 ± 74	93 ± 13	138 ± 15	87 ± 18	182 ± 12
4-week-old	1	121 ± 10	132 ± 16	109 ± 11	102 ± 15	114 ± 11	59 ± 11	122 ± 20	118 ± 18	127 ± 10	108 ± 14	99 ± 8
	2	105 ± 11	128 ± 6	109 ± 18	124 ± 6	111 ± 2	78 ± 2	278 ± 14	176 ± 12	137 ± 5	119 ± 12	74 ± 15
6-week-old	1	127 ± 7	124 ± 4	98 ± 16	93 ± 10	92 ± 9	49 ± 8	90 ± 17	136 ± 7	133 ± 15	83 ± 6	287 ± 46
	2	136 ± 11	179 ± 29	91 ± 11	109 ± 11	111 ± 10	105 ± 8	138 ± 22	137 ± 17	137 ± 5	89 ± 6	318 ± 75

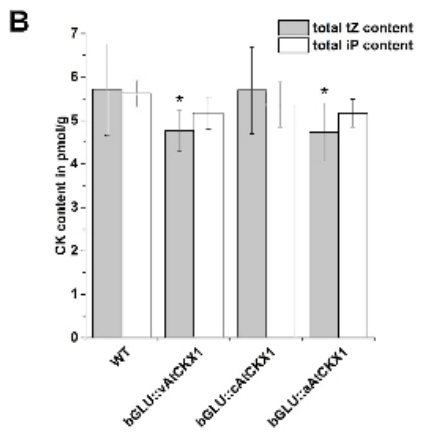

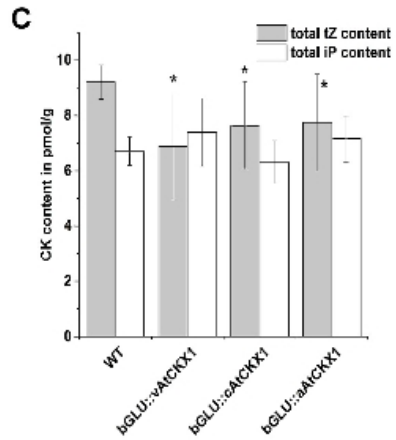

FIGURE 3

Changes in CK content of transgenic and WT plants grown hydroponically. **(a)** Changes in CK content in 2-, 4-, and 6-week-old plants from two independent *bGLU::vAtCKX1* lines of T2 generation expressed as percentages of WT CK levels. Absolute CK concentrations for WT plants are summarized in Fig. S1. CK content in aerial parts **(b)** and roots **(c)** of 6-week-old WT, *bGLU::cAtCKX1*, *bGLU::vAtCKX1*, and *bGLU::aAtCKX1* T3 generation plants expressed as sum of all iP and *tZ* forms. *tZ*, *trans*-zeatin; *tZR*, *trans*-zeatin riboside; *cZ*, *cis*-zeatin; *cZR*, *cis*-zeatin riboside; iP, isopentenyladenine; iPR, isopentenyladenine riboside; *tZOG*, *trans*-zeatin *O*-glucoside; *tZROG*, *trans*-zeatin riboside-*O*-glucoside; *tZ9G*, *trans*-zeatin *N9*-glucoside; *cZOG*, *cis*-zeatin *O*-glucoside; *cZROG*, *cis*-zeatin riboside-*O*-glucoside; *cZ9G*, *cis*-zeatin *N9*-glucoside; *cZR5MP*, *cis*-zeatin riboside 5′-monophosphate; DHZOG, dihydrozeatin-*O*-glucoside; DHZROG, dihydrozeatin riboside-*O*-glucoside; iP9G, isopentenyladenine *N9*-glucoside; iPR5MP, isopentenyladenine riboside 5′-monophosphate. Not listed CKs were below the detection limit.

CK content was also determined in *bGLU::vAtCKX1*, *bGLU::cAtCKX1*, and *bGLU::aAtCKX1* genotypes in an independent experiment on T3 generation plants 6 weeks old. A significant decrease in total content of all *tZ* forms in whole plants of all three genotypes was a main feature visible also in the T2 generation with the exception of *bGLU::cAtCKX1* aerial parts (Fig. 3b and c).

Phenotype of transgenic plants

The phenotype of the transgenic plants differed according to the target location of AtCKX1. The heights of plants with AtCKX1 targeted to vacuoles (Fig. 4a) was slightly reduced and transgenic plants had longer roots (Fig. 4c; expressed as total length of all seminal and adventitious roots) and a greater number of lateral roots (Fig. 4b). Transgenic plants with cytosolic AtCKX1 did not exhibit the typical CK-deficient phenotype (Fig. 4a). The *bGLU::cAtCKX1* roots were slightly shorter than were WT roots (Fig. 4c) and had a greater number of longer lateral roots (Fig. 4b). AtCKX1 targeted to apoplast had the strongest effect on the development of the aerial part (Fig. 4a). The heights of *bGLU::aAtCKX1* plants were distinctively reduced, but, mainly due to their substantially higher number of tillers, the total dry weight of their aerial part was slightly greater than in the case of WT barley (Table 1). Total root length of *bGLU::aAtCKX1* plants was reduced, and the number of longer lateral roots was increased compared to that of WT plants (Fig. 4b). A very similar phenotypical manifestation was observed for the T1 generation of transgenic plants transformed by the *ZmCKX1* gene under the control of the *bGLU* promoter (data

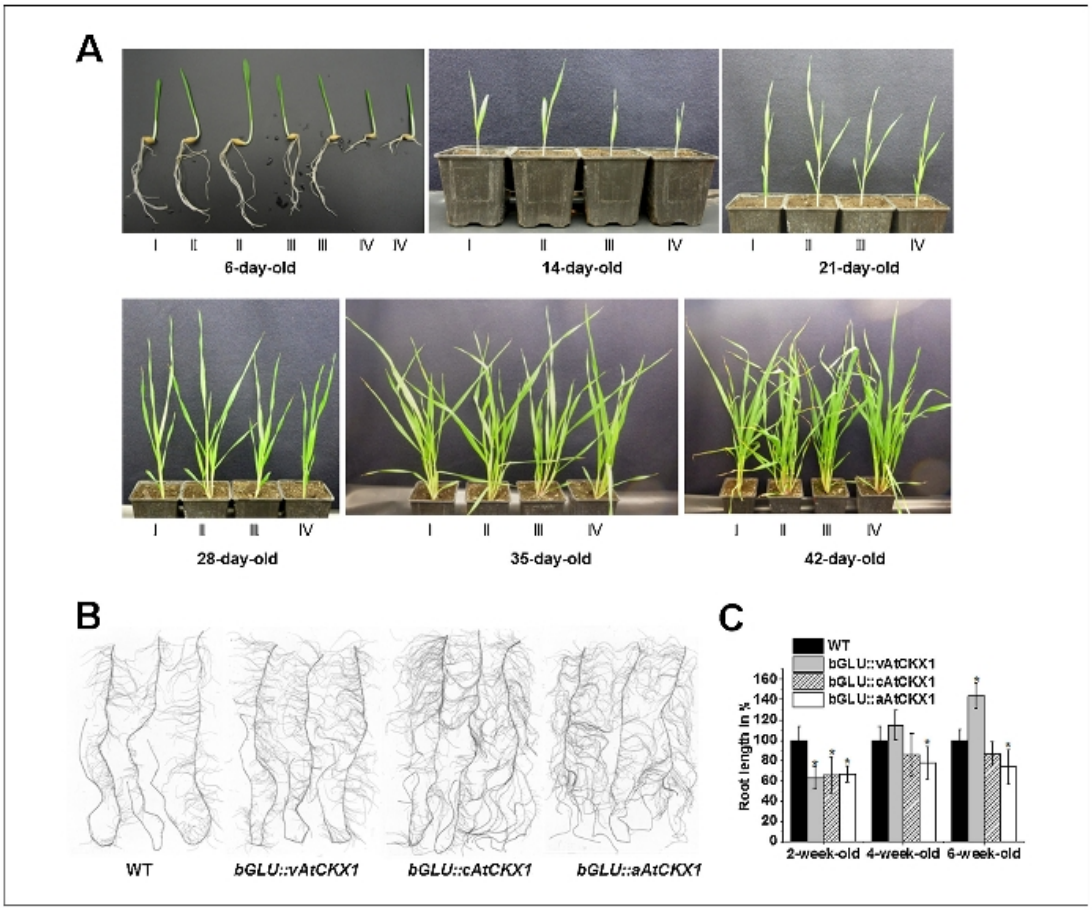

FIGURE 4

Phenotype of homozygous T2 generation transgenic barley. **(a)** Phenotype of aerial parts of WT and transgenic barley captured at 1-week intervals. I, WT; II, *bGLU::cAtCKX1*; III, *bGLU::vAtCKX1*; IV, *bGLU::aAtCKX1*. **(b)** Root architecture of 6-week-old primary (seminal) root of transgenic and control barley plants. Each root originates from a different plant. **(c)** Vegetative growth parameters of transgenic lines with overexpressed *AtCKX1* gene. Root length is expressed as total length of all seminal and adventitious roots. Values are relative to WT parameters, which were assigned as 100%. At least 20 plants for each independent line were measured. *, significant difference between WT and transgenic tissue according to unpaired Student's *t*-test at $P \leq 0.05$.

not shown). The ZmCKX1 protein is naturally targeted to apoplast [37].

Yield parameters

To evaluate the effect of *AtCKX1* overexpression on grain yield, the T2 homozygous generation was grown under optimal conditions and three independent lines of *bGLU::vAtCKX1* and *bGLU::cAtCKX1* were evaluated. Generally, yields of all independent lines of both genotypes oscillated around WT yields. Regarding *bGLU::vAtCKX1*, 1000-grain weight tended to be reduced to between 73% and 91% of that for WT (Table 1). On the other hand, *bGLU::vAtCKX1* plants contained as many as 30% more grains per plant. Hence, *bGLU::vAtCKX1* transgenic plants produced a larger number of smaller grains and average yield (grain weight per plant) was comparable to yield from WT plants. In contrast to *bGLU::vAtCKX1*, the 1000-grain weight parameter of *bGLU::cAtCKX1* lines was comparable to that of WT plants, which together with the higher number of grains per plant resulted in slightly increased grain weight per plant for 2 of 3 independent lines (Table 1). Even though *bGLU::aAtCKX1* produced significantly more tillers, spikes were more often empty or poorly filled with grains. Therefore, total yield was dramatically (8-fold) reduced compared to WT (Table 1). An even more negative effect on fertility was observed in transgenic plants overexpressing *ZmCKX1* with apoplastic targeting (data not shown), in which case only a few grains per plant were obtained in the T0 generation.

TABLE 1

Yield parameters of transgenic barley plants compared to wild type (WT) plants. Plants were grown in a greenhouse for 7 months with regular watering and fertilization reproducing natural annual conditions (February–August). Values are presented as percentage relative to WT parameters. Lines marked as bold (one for each genotype) were used for drought stress experiments. DW, dry weight.

	Line	Number of plants	Grain number per plant (%)	Grain weight per plant (%)	Weight of 1,000 grains (%)	Grain number per spike (%)	Spike number per plant (%)	Tiller number per plant (%)	Leaf DW (g) per plant (%)
Wild type	1	35	100	100	100	100	100 ± 18	100 ± 21	100 ± 15
bGLU::vAtCKX1	1	50	116	85	73	106	109 ± 19	116 ± 22	136 ± 12
	2	**50**	**120**	**109**	**91**	**111**	**109 ± 21**	**99 ± 17**	**97 ± 15**
	3	24	130	112	86	116	113 ± 14	97 ± 14	96 ± 14
bGLU::cAtCKX1	1	10	97	96	100	114	85 ± 25	86 ± 27	88 ± 10
	2	**17**	**107**	**111**	**103**	**116**	**92 ± 19**	**100 ± 9**	**106 ± 14**
	3	18	113	110	97	96	117 ± 27	119 ± 21	115 ± 18
bGLU::aAtCKX1	**1**	**30**	**18**	**13**	**73**	**54**	**33 ± 24**	**145 ± 51**	**108 ± 26**

Whole transcriptome analysis of barley plants transformed with bGLU::vAtCKX1

Transcriptome sequencing of 10 libraries prepared from the 6-week-old root tissue of two independent *bGLU::vAtCKX1* lines and the upper part of one transgenic line together with WT tissues produced a total of 329,323,385 pair-end reads, which were mapped to barley reference genome cv. Morex. Analysis confirmed that the *AtCKX1* transgene was expressed predominantly in the root (2.7-fold stronger than in the upper part). Of the total 26,067 annotated genes, 2444 and 3655 genes were significantly altered (adjusted P-value ≤ 0.01) in their expression compared to WT in the root tissue of lines 1 and 2, respectively (significantly up- and down-regulated genes are listed in Tables S2 and S3. There was an overlap between the two lines in the case of 75.5% of significantly altered genes (adjusted P-value ≤ 0.05). The *AtCKX1* transcript level in line 1 was 2.5-fold lower than that in line 2, which is in accordance with the lower number of regulated genes. The effect of the transgene in the upper part was far less pronounced than it was in the root, as only 444 genes detected in the library from line 1 were significantly deregulated (Table S4). Among the genes most up-regulated in the roots were those categorized into different responses to hormones, phenylpropanoid biosynthetic pathway, response to unfolded and topologically incorrect proteins, phosphatidylinositol signal transduction pathway, glucosyltransferase activity, and others (Table 2). Genes which are significantly down-regulated were categorized as, for instance, those for amine metabolic processes and negative regulation of cell cycle.

Mild drought stress

Relative water content (RWC) was estimated in the youngest fully developed leaves of 5-month-old *bGLU::vAtCKX1* and WT plants cultivated in soil exposed to 2 months of periodic drought. In comparison with WT plants, transgenic plants had greater than 10% higher RWC during long-term application of mild stress (Fig. S2). Moreover, the calculated drought resistance index for *bGLU::vAtCKX1* was 7% higher than that of WT plants. The drought resistance index expresses the ratio of yield reduction due to stress in a given genotype compared to the mean reduction over all genotypes tested [38].

Severe drought stress

All three transgenic genotypes together with WT barley were cultivated hydroponically under optimal conditions until the 4th week, when severe stress was applied for 24 h. RWC was measured at the end of the stress period and plants were subsequently regenerated under optimal conditions for the following 2 weeks, when growth rate parameters were evaluated.

The *bGLU::vAtCKX1* did not show altered RWC in comparison to WT (Fig. 5e), although apparently faster recovery was observed after 4 h of revitalization (Fig. 5a). On the other hand, the RWC of both *bGLU::aAtCKX1* and *bGLU::cAtCKX1* was significantly greater than that for WT during or after severe drought stress (Fig. 5e). Moreover, the two lines seemed to be more tolerant of short severe drought later as their leaves showed faster regeneration than did WT barley (Fig. 5b and c). The results provide a good comparison for the *bGLU::vAtCKX1* and *bGLU::cAtCKX1* lines, as they had height and leaf size comparable to those of WT plants. The *bGLU::aAtCKX1* plants had significantly reduced growth of the aerial part. This caused slower evaporation of water from the leaves that probably led to the delayed drought stress and faster recovery.

After a 2-week regeneration period, *bGLU::vAtCKX1* and *bGLU::cAtCKX1* genotypes exhibited as much as 32% and 17% greater mass of the aerial part, respectively, than did WT plants (Fig. 5e). In both cases, this was mainly due to faster growth of new tillers (Fig. 5e) and, in the case of *bGLU::cAtCKX1*, also due to prolonged leaves (Fig. 5b). Although the *bGLU::aAtCKX1* line showed the best immediate response to severe drought (Fig. 5c), its dry root and aerial masses were even more reduced in comparison to WT after the long regeneration period than under optimal conditions (Fig. 5c and e).

Revitalization after drought stress

All three transgenic barley genotypes were tested for their ability to recover after drought stress when growing in a small volume of substrate, which enabled rapid change of water content. Thirty plants of each genotype were grown on trays (30 cm × 20 cm with depth of 0.5 cm) filled with the growth substrate. Transgenic plants were grown mixed with WT plants on the same tray to ensure the same level of soil desiccation. Watering was eliminated 4 weeks after germination and restored to a daily basis following a

TABLE 2

The 20 most affected gene ontology (GO) terms at GO level 6 found in differentially expressed genes (adjusted *P*-value ≤ 0.01) in the root of two bGLU::vAtCKX1 lines. Percentage of affected genes shows percentage of differentially expressed genes with same GO number (100% = total number). MF, molecular function; BP, biological process.

GO number	Category	GO term	Total number	% of affected genes	
				Line 1	Line 2
Up-regulated					
GO:0045548	MF	Phenylalanine ammonia-lyase activity	8	63	63
GO:0016307	MF	Phosphatidylinositol phosphate kinase activity	18	33	28
GO:0006986	BP	Response to unfolded protein	21	33	48
GO:0035967	BP	Cellular response to topologically incorrect protein	21	33	48
GO:0009699	BP	Phenylpropanoid biosynthetic process	22	32	41
GO:0006984	BP	ER-nucleus signaling pathway	24	29	42
GO:0035091	MF	Phosphatidylinositol binding	23	26	26
GO:0004620	MF	Phospholipase activity	28	25	36
GO:0046527	MF	Glucosyltransferase activity	81	22	42
GO:0060548	BP	Negative regulation of cell death	24	21	29
GO:0010026	BP	Trichome differentiation	39	21	21
GO:0008081	MF	Phosphoric diester hydrolase activity	40	20	30
GO:0015405	MF	P–P-bond-hydrolysis-driven transmembrane transporter activity	145	20	23
GO:0043067	BP	Regulation of programmed cell death	40	18	25
GO:0009850	BP	Auxin metabolic process	29	17	21
GO:0080135	BP	Regulation of cellular response to stress	36	17	22
GO:0009753	BP	Response to jasmonic acid	55	16	20
GO:0009751	BP	Response to salicylic acid	31	16	23
GO:0009733	BP	Response to auxin	102	14	20
GO:0005096	MF	GTPase activator activity	38	13	26
Down-regulated					
GO:0004792	MF	Thiosulfate sulfurtransferase activity	8	38	13
GO:0008131	MF	Primary amine oxidase activity	6	33	17
GO:0010039	BP	Response to iron ion	8	25	25
GO:0016538	MF	Cyclin-dependent protein serine/threonine kinase regulator activity	8	25	13
GO:0045786	BP	Negative regulation of cell cycle	24	17	17
GO:0019901	MF	Protein kinase binding	12	17	17
GO:0003756	MF	Protein disulfide isomerase activity	6	17	17
GO:0042822	BP	Pyridoxal phosphate metabolic process	6	17	17
GO:0005315	MF	Inorganic phosphate transmembrane transporter activity	8	13	13
GO:0042744	BP	Hydrogen peroxide catabolic process	33	12	9
GO:0004568	MF	Chitinase activity	17	12	24
GO:0006026	BP	Aminoglycan catabolic process	17	12	24
GO:0046348	BP	Amino sugar catabolic process	17	12	24
GO:1901071	BP	Glucosamine-containing compound metabolic process	17	12	24
GO:0009309	BP	Amine biosynthetic process	20	10	35
GO:0051338	BP	Regulation of transferase activity	42	10	17
GO:0043086	BP	Negative regulation of catalytic activity	55	9	18
GO:1902170	BP	Cellular response to reactive nitrogen species	11	9	27
GO:0042886	BP	Amide transport	62	8	19
GO:0015925	MF	Galactosidase activity	13	8	15

drought period of 3 d. Within 1 d after watering restoration, all three transgenic lines showed significantly faster revitalization of their aerial parts compared to WT barley. Mean RWC values 19, 17, and 14% higher than those in WT were observed in the *bGLU::cAtCKX1*, *bGLU::vAtCKX1*, and *bGLU::aAtCKX1* lines, respectively (Fig. 6a).

The experiment was repeated independently in order to evaluate biomass production in an arrangement where RWC was not measured and the plants were therefore not destroyed. Dry weight of the aerial part was determined in 8-week-old plants (4 weeks after the stress was applied) and compared to optimally watered plants (Fig. 6b). The *bGLU::vAtCKX1* and *bGLU::cAtCKX1* produced as much as 25% and 17%, respectively, greater biomass compared to the stressed WT plants. Biomass production of *bGLU::aAtCKX1* was lower than was that for the stressed WT, but it was 21% higher in comparison with the dry aerial part mass of *bGLU::aAtCKX1* grown under optimal conditions. Similar results were obtained for plants stressed in the 6th week of growth (Fig. S3B).

Discussion

According to previous studies [10,17], dicotyledonous plants with root-specific AtCKX1 overproduction have longer primary roots, larger root systems, non-altered morphology of the upper parts, significantly reduced levels of active CKs, and higher tolerance to drought stress. For root-specific barley overexpression, the same Arabidopsis gene was chosen in its native form with a signal sequence resulting in vacuolar targeting [9], without the signal

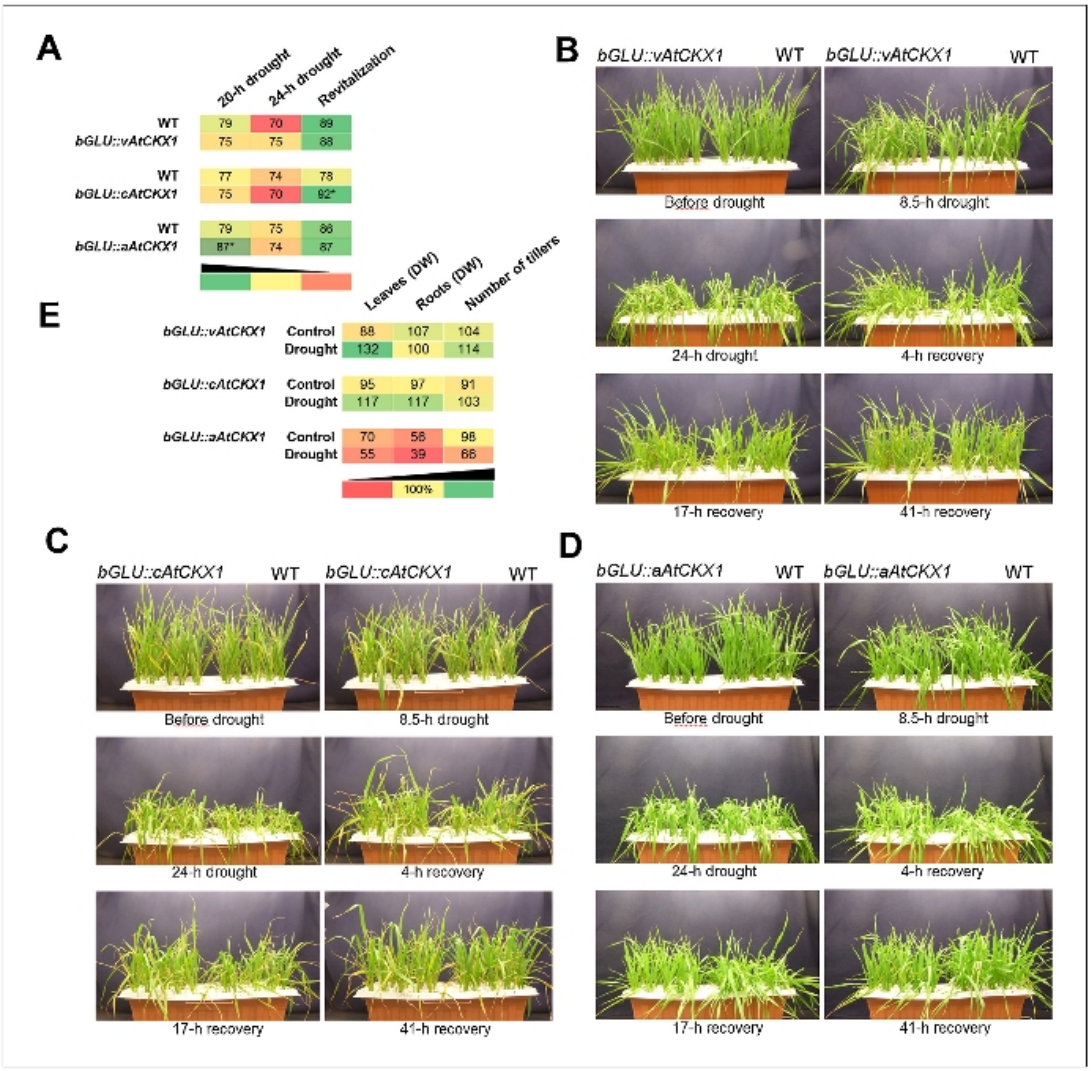

FIGURE 5

Parameters of transgenic and WT barley after application of severe drought stress. **(a)** RWC of 4-week-old barley cultivated hydroponically, measured 24 h after severe stress induction. *, significant difference between WT and transgenic tissue according to unpaired Student's *t*-test at $P \leq 0.05$. Severe drought stress applied to 4-week-old hydroponically cultivated WT and *bGLU::vAtCKX1* **(b)**, *bGLU::cAtCKX1* barley **(c)** and *bGLU::aAtCKX1* barley **(d)**. **(e)** Dry weight parameters and tiller number of 6-week-old barley cultivated hydroponically, 2-weeks after severe drought stress application. Data are expressed as percentage of corresponding WT parameters.

sequence and with anticipated cytosolic localization, and in combination with secretion sequence of the *AtCKX2* gene. Increased CKX activity (Fig. 1c) demonstrated that integration of all three constructs into the barley genome resulted in production of an active enzyme. It is known that different CKX isoforms differ in their substrate specificity and subcellular compartmentation [39]. CK content in roots of three transgenic genotypes containing differentially localized AtCKX1 was similar (Fig. 3c), which is in agreement with previously published data [13,40] showing Arabidopsis plants with overproduced vacuolar AtCKX1, apoplastic AtCKX2, and cytosolic AtCKX7 to have distinct phenotypes but similar CK content. Hence, the quantification of CKs in whole tissue may not accurately express disrupted homeostasis on the subcellular level and diminished CK content in different compartments and/or cell types might be the reason for the observed phenotypes. Constitutive overexpression of cytosolic AtCKX7 in

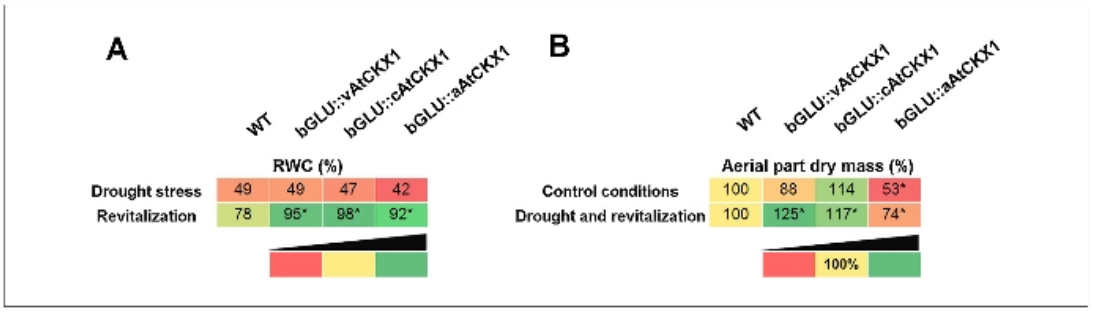

FIGURE 6

Parameters of *bGLU::vAtCKX1*, *bGLU::cAtCKX1*, *bGLU::aAtCKX1*, and WT barley grown in shallow soil after application of drought stress. **(a)** RWC in 4-week-old plants exposed to drought stress for 3 d and then 24 h into revitalization. **(b)** Dry weight of 8-week-old barley aerial parts grown in control conditions or under drought stress for 3 d with subsequent revitalization of 4 weeks. Aerial part dry mass data are expressed as percentage of corresponding WT parameters; *, significant difference between WT and transgenic tissue according to unpaired Student's *t*-test at $P \leq 0.05$.

Arabidopsis has a strong negative effect on development of the primary root, and the root system is formed only by a proliferation of adventitious roots [40]. That is in contrast with all other AtCKX overexpressors with other than cytosolic localization, which have enhanced root elongation and lateral branching [13]. Surprisingly, activation of cytosolic OsCKX4 in a rice mutant had no negative effect on primary root elongation but a substantial positive effect on crown (adventitious) root formation [19]. Moreover, silencing of OsCKX4 inhibits both primary as well as crown root growth in the seedling stage, thus pointing to the fact that CKs' role in the regulation of root architecture is different in dicotyledonous versus monocotyledonous plants.

All those transgenic barley genotypes prepared in the frame of this work had modified root morphology in terms of increased number and length of lateral roots (Fig. 4b), but (with the exception of *bGLU::vAtCKX1*) with shorter primary and seminal roots (Fig. 4c). Hence, the observed phenotypes do not clearly correspond with any of those CKX overexpressors described to date. There were not observed morphological changes in the aerial part in the case of *bGLU::cAtCKX1* and only minimal in the case of *bGLU::vAtCKX1* genotype, which fact is illustrated also by minor changes in the transcriptome of *bGLU::vAtCKX1* leaves (Table S4). Decrease in CK pool in different compartments thus affects phenotype differently in roots and aerial part. As targeting of CKX enzyme to vacuoles, cytosol or apoplast in the root causes similar alteration in morphology, the decrease in cytosolic CK pool in the aerial part does not lead to considerable alteration of phenotype contrary to decrease in vacuolar CK concentration or CKX secretion to the apoplast in the case of *bGLU::aAtCKX1* plants, which have substantially influenced shoot development in the early stage (Fig. 4a) and later also number of tillers and yield (Table 1). Using another secreted CKX isoform from maize (ZmCKX1) as a transgene under the control of the same *bGLU* promoter (data not shown) or the root-specific phosphate transporter promoter [14] had an even more profound negative effect on shoot proliferation and inflorescence. All these observations point to the ability of the CKX protein, which is produced and secreted to apoplast in the root, to be translocated to the upper part of the plant. CKX activity has been detected in the xylem sap of maize seedlings where the ZmCKX1 gene was up-regulated by the addition of CK to the nutrient solution [41]. Long-distance translocation of CK via xylem from root to shoot was proved in several studies (for review see [42]). Apoplastic CKX enzyme controls loading and transport of CKs to xylem, hence enhanced CKX activity in apoplast might substantially reduce amount of translocated root-borne CKs to the aerial part and contribute to observed stronger phenotype of the *bGLU::aAtCKX1* genotype.

When compared with the 35S promoter (Fig. 1a and b), the maize *bGLU* promoter can be classified as a weak promoter with root preference. Detailed characterization of endogenous barley genes implied in the CK biosynthesis and degradation together with cytokinin contents between the 2nd and 6th weeks of plant development, when the activity of the *bGLU* promoter is greatest, demonstrates that transgenic tissue tends to maintain natural CK homeostasis. Generally, endogenous *HvCKX* genes are down-regulated while *HvIPT* genes are up-regulated (Fig. 2 nicely correlates with RNA-seq data, Table S5), thus resulting in only slightly altered total CK content (Fig. 3). Such detailed data are not available from previous studies [10,17] done on dicotyledonous plants, but the presented significantly diminished levels for all type of CKs imply that the strength of the promoter may be the crucial factor for resulting CK homeostasis or that these plants are not able to compensate for the effect of the CKX transgene in the same way as is barley.

Targeted CK degradation by ectopic overexpression of the AtCKX1 gene not only disrupts CK homeostasis, as demonstrated by significant down-regulation of three out of seven CK primary response regulator genes of type A in both *bGLU::vAtCKX1* lines (Tables S2 and S3), but it also substantially influences homeostasis of other phytohormones. Whole-transcriptomic analysis of *bGLU::vAtCKX1* root tissue revealed that among the most up-regulated gene ontology (GO) terms in both independent lines figure those for salicylic and jasmonic acid response, ethylene biosynthesis, and auxin response (Table 2, S2, S3 and S5). Thus, the increase in the number of lateral roots can be explained by the well-established effect of increased auxin response in pericycle to initiation of lateral root primordia [43]. Up-regulation of ethylene

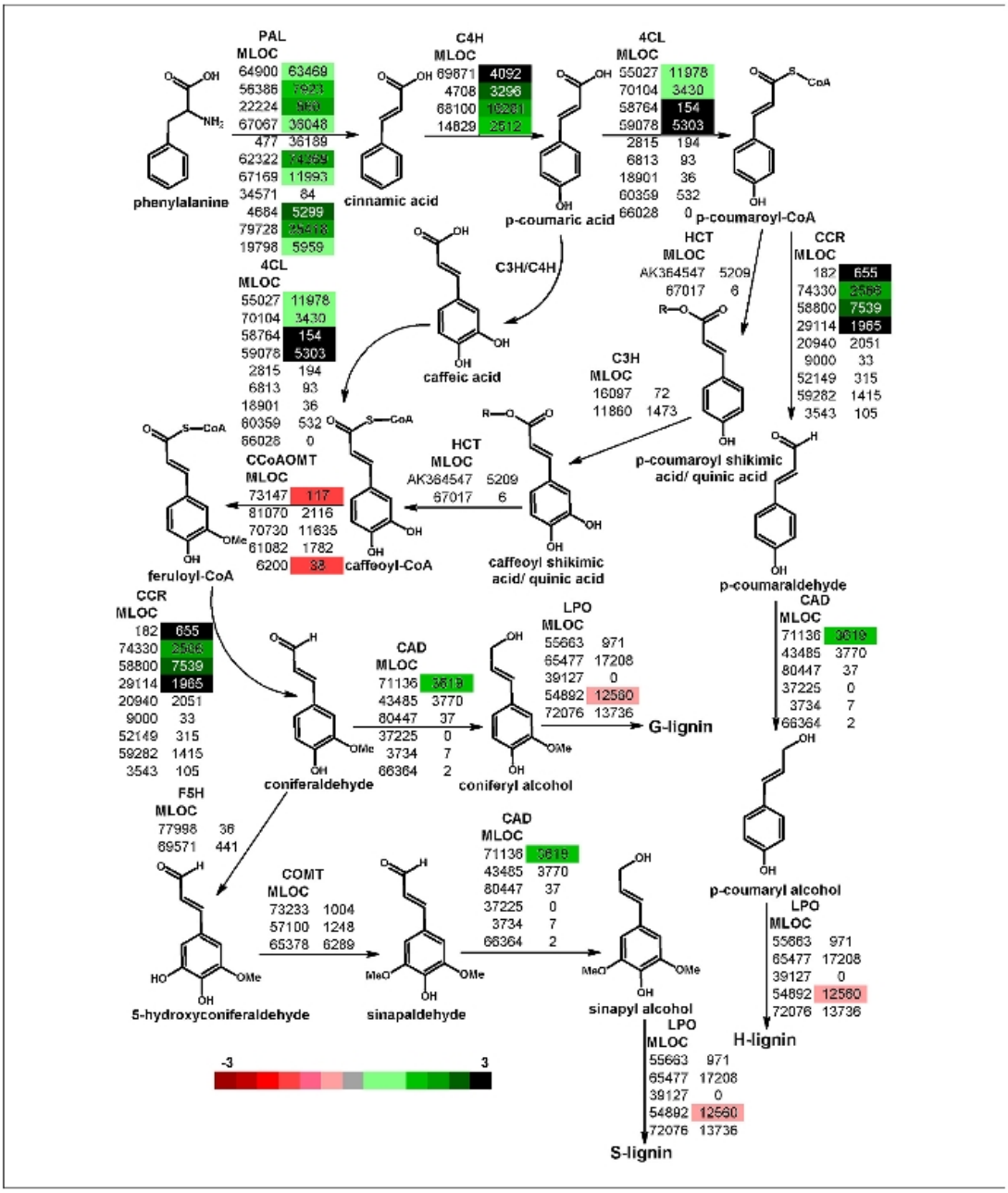

FIGURE 7

Deregulation of phenylpropanoid pathway of lignin biosynthesis. Scheme is derived from Kyoto Encyclopedia of Genes and Genomes and [49]. Accession numbers of all putative genes participating in individual metabolic conversions are listed (left number) together with their expression mean values (right number). Color code indicates significantly regulated genes (adjusted *P*-value $\leq$ 0.05). PAL, phenylalanine ammonia-lyase; C4H, cinnamate 4-hydroxylase; 4CL, 4-coumarate:CoA ligase; C3H, *p*-coumarate 3-hydroxylase; HCT, *p*-hydroxycinnamoyltransferase; CCoAOMT, caffeoyl-CoA *O*-methyltransferase; CCR, cinnamoyl-CoA reductase; F5H, ferulate 5-hydroxylase; COMT, caffeic acid *O*-methyltransferase; CAD, cinnamyl alcohol dehydrogenase; LPO, lignin-forming peroxidase; R, shikimic acid/quinic acid.

biosynthetic genes and ethylene response factors does not clearly correlate with the known effect of CK to activate ethylene production [44]. Enforced ethylene biosynthesis might be distinctive to only certain root tissue and linked to the reduction in primary root elongation observed in the early developmental stage. Nevertheless, only precise analysis of the phytohormonal dynamic in specific cell types of the cereal root system can shed more light on understanding phytohormonal cross-talk and its effect on root architecture.

During the prolonged mild drought stress applied to WT and *bGLU::vAtCKX1* barley cultivated in soil, higher RWC was detected in the leaves of transgenic plants (Fig. 5d). Since the plant growth stage most sensitive to water deficit is flowering and reproduction, the higher drought resistance index detected in *bGLU::vAtCKX1* barley confirmed tolerance of transgenic plants with altered CK homeostasis to drought. Stress tolerance is acquired by dehydration avoidance in transgenic plants due to modified root morphology (Fig. 4b). Enforced lignification and deposition of monolignols into the cell wall to cross-link oligosaccharides are among the processes described to be induced in water-stressed roots of maize and soybean [45]. Whole transcriptome analysis revealed that among the most up-regulated genes in both *bGLU::vAtCKX1* lines are these participating in lignin biosynthesis (e.g., cinnamoyl-CoA reductase, cinnamate 4-hydroxylase, and 4-coumarate:CoA ligase; Fig. 7).

For visualization of the root morphology and confirmation of the dehydration avoidance ability, transgenic plants were grown also hydroponically. During sudden drought stress, the strongest avoidance of plant dehydration was observed for *bGLU::cAtCKX1* plants (Fig. 5b) and mainly was manifested as delayed leaf rolling. Leaf wilting, expressed in cereals by leaf rolling, is an important, simple phenotypic expression of a critical stage in plant water status during drought stress [46]. Moreover, all transgenic plants showed notably faster revitalization after rewatering (Fig. 5a–c). It is known that additional and longer lateral roots promote avoidance of plant dehydration in drying soil [47]. To confirm the positive effect of modified root morphology also in soil, transgenic plants were grown in a shallow growing substrate to ensure rapid soil drying. The detected greater recovery of all tested transgenic plants in such conditions led to the faster growth rate for the aerial part (Fig. 6, Fig. S4B).

The tested transgenic plants showed better tolerance under severe and sudden drought stress due to modification of root morphology and perhaps stronger lignification. This successful strategy is probably created by a combination of dehydration avoidance and faster regeneration after plant rewatering. The *bGLU::vAtCKX1* plants were exposed also to stress over a period of 2 months in deep soil, where they displayed drought resistance index values up to 7% higher than those for WT plants. This observation is very important inasmuch as regulation differs for rapid versus prolonged drought [48]. Root morphology with a higher number of longer lateral roots could be beneficial for two soil types, namely a type wherein it is difficult for roots to penetrate in order to reach water available only at deep levels and a type wherein water is not available deep down and only a shallow soil layer undergoes seasonal wetting cycles [46].

The presented experiments clearly demonstrate that transgenic barley plants overexpressing the *Arabidopsis* AtCKX1 gene under the control of a mild promotor with root preference have higher tolerance to drought. Under stress conditions and following revitalization, transgenic plants can maintain higher yield parameters compared to WT plants. Field trials have been started with all the prepared transgenic lines, and a more detailed report regarding drought tolerance with a focus on yield and grain quality will become available in the future.

Acknowledgements

This work was supported by the Czech Science Foundation (grant no. 14-12355S) and the National Program for Sustainability (project no. LO1204).

Appendix A. Supplementary data

Supplementary material related to this article can be found, in the online version, at http://dx.doi.org/10.1016/j.nbt.2015.12.005.

References

[1] Mok DWS, Mok MC. Cytokinin metabolism and action. Ann Rev Plant Physiol Plant Mol Biol 2001;52:89–118.
[2] Dobrev PI, Vaňková R. Quantification of abscisic acid, cytokinin, and auxin content in salt-stressed plant tissues. Methods Mol Biol 2012;913:251–61.
[3] Kuppu S, Mishra N, Hu R, Sun L, Zhu X, Shen G, et al. Water-deficit inducible expression of a cytokinin biosynthetic gene IPT improves drought tolerance in cotton. PLoS One 2013;8:e64190.
[4] Rivero RM, Kojima M, Gepstein A, Sakakibara H, Mittler R, Gepstein S, et al. Delayed leaf senescence induces extreme drought tolerance in a flowering plant. Proc Natl Acad Sci U S A 2007;104:19631–36.
[5] Zhang P, Wang WQ, Zhang GL, Kamínek M, Dobrev P, Xu J, et al. Senescence-inducible expression of isopentenyl transferase extends leaf life, increases drought stress resistance and alters cytokinin metabolism in cassava. J Integr Plant Biol 2010;52:653–69.
[6] Ghanem ME, Albacete A, Smigocki AC, Frébort I, Pospíšilová H, Martinez-Andújar C, et al. Root-synthesized cytokinins improve shoot growth and fruit yield in salinized tomato (*Solanum lycopersicum* L) plants. J Exp Bot 2011;62:125–40.
[7] Merewitz EB, Gianfagna T, Huang B. Photosynthesis, water use, and root viability under water stress as affected by expression of SAG12-ipt controlling cytokinin synthesis in *Agrostis stolonifera*. J Exp Bot 2011;62:383–95.
[8] Peleg Z, Reguera M, Tumimbang E, Walia H, Blumwald E. Cytokinin-mediated source/sink modifications improve drought tolerance and increase grain yield in rice under water-stress. Plant Biotech J 2011;9:747–58.
[9] Werner T, Motyka V, Strnad M, Schmülling T. Regulation of plant growth by cytokinin. Proc Natl Acad Sci U S A 2001;98:10487–92.
[10] Macková H, Hronková M, Dobrá J, Turečková V, Novák O, Lubovská Z, et al. Enhanced drought and heat stress tolerance of tobacco plants with ectopically enhanced cytokinin oxidase/dehydrogenase gene expression. J Exp Bot 2013;64:2805–15.
[11] Galuszka P, Frébort I, Šebela M, Sauer P, Jacobsen S, Peč P. Cytokinin oxidase or dehydrogenase? Mechanism of cytokinin degradation in plants. Eur J Biochem 2001;268:450–61.
[12] Schmülling T, Werner T, Riefler M, Krupkova E, Bartrina y Manns I. Structure and function of cytokinin oxidase/dehydrogenase genes of maize, rice, Arabidopsis and other species. J Plant Res 2003;116:241–52.
[13] Werner T, Motyka V, Laucou V, Smets R, Van Onckelen H, Schmülling T. Cytokinin-deficient transgenic Arabidopsis plants show multiple developmental alterations indicating opposite functions of cytokinins in the regulation of shoot and root meristem activity. Plant Cell 2003;15:2532–50.
[14] Mrízová K, Jiskrová E, Vyroubalová Š, Novák O, Ohnoutková L, Pospíšilová H, et al. Overexpression of cytokinin dehydrogenase genes in barley (*Hordeum vulgare* cv. Golden Promise) fundamentally affects morphology and fertility. PLoS One 2013;8:e79029.
[15] Kowalska M, Galuszka P, Frébortová J, Šebela M, Béres T, Hluska T, et al. Vacuolar and cytosolic cytokinin dehydrogenases of *Arabidopsis thaliana*, heterologous expression, purification and properties. Phytochem 2010;71:1970–8.
[16] Galuszka P, Frébortová J, Werner T, Yamada M, Strnad M, Schmülling T, et al. Cytokinin oxidase/dehydrogenase genes in barley and wheat, cloning and heterologous expression. Eur J Biochem 2004;271:3990–4002.
[17] Werner T, Nehnevajova E, Köllmer I, Novák O, Strnad M, Krämer U, et al. Root-specific reduction of cytokinin causes enhanced root growth, drought tolerance,

and leaf mineral enrichment in Arabidopsis and tobacco. Plant Cell 2010;22:3905–20.
[18] Gu R, Zhao L, Zhang Y, Chen X, Bao J, Zhao J, et al. Isolation of a maize beta-glucosidase gene promoter and characterization of its activity in transgenic tobacco. Plant Cell Rep 2006;25:1157–65.
[19] Gao S, Fang J, Xu F, Wang W, Sun X, Chu J, et al. CYTOKININ OXIDASE/DEHYDROGENASE4 integrates cytokinin and auxin signaling to control rice crown root formation. Plant Physiol 2014;165:1035–46.
[20] Hirose N, Makita N, Kojima M, Kamada-Nobusada T, Sakakibara H. Plant Cell Physiol 2007;48:523–39.
[21] Harwood WA, Bartlett JG, Alves SC, Perry M, Smedley MA, Leyland N, et al. Barley transformation using Agrobacterium-mediated techniques. In: Jones HD, Shewry PR, editors. Methods in molecular biology, Vol. 478 Transgenic wheat, barley and oats. New York: Humana Press; 2008. p. 137–47.
[22] Kim D, Pertea G, Trapnell C, Pimentel H, Kelley R, Salzberg SL. TopHat2, accurate alignment of transcriptomes in the presence of insertions, deletions and gene fusions. Genome Biol 2013;14:R36.
[23] Anders S, Pyl PT, Huber W. HTSeq – a Python framework to work with high-throughput sequencing data. Bioinformatics 2015;31:166–9.
[24] Love MI, Huber W, Anders S. Moderated estimation of fold change and dispersion for RNA-seq data with DESeq2. Genome Biol 2014;15:550.
[25] R Development Core Team. R, A language and environment for statistical computing. Vienna, Austria: R Foundation for Statistical Computing; 2008 , ISBN 3-900051-07-0, URL http://www.R-project.org..
[26] Conesa A, Götz S, García-Gómez JM, Terol J, Talón M, Robles M. Blast2GO: a universal tool for annotation, visualization and analysis in functional genomics research. Bioinformatics 2005;21:3674–6.
[27] Camacho C, Coulouris G, Avagyan V, Ma N, Papadopoulos J, Bealer K, et al. BLAST+, architecture and applications. BMC Bioinformatics 2009;10:421.
[28] Kanehisa M, Goto SKEGG. Kyoto encyclopedia of genes and genomes. Nucleic Acids Res 2000;28:27–30.
[29] Kanehisa M, Goto S, Sato Y, Kawashima M, Furumichi M, Tanabe M. Data, information, knowledge and principle, back to metabolism in KEGG. Nucleic Acids Res 2014;42:D199–205.
[30] Frébort I, Šebela M, Galuszka P, Werner T, Schmülling T, Peč P. Cytokinin oxidase/dehydrogenase assay, optimized procedures and applications. Anal Biochem 2002;306:1–7.
[31] Vyroubalová Š, Václavíková K, Turečková V, Novák O, Šmehilová M, Hluska T, et al. Characterization of new maize genes putatively involved in cytokinin metabolism and their expression during osmotic stress in relation to cytokinin levels. Plant Physiol 2009;151:433–47.
[32] Vlamis J, Williams DE. Ion competition in manganese uptake by barley plants. Plant Physiol 1962;37:650–5.
[33] Turner NC, Abbo S, Berger JD, Chaturvedi SK, French RJ, Ludwig C, et al. Osmotic adjustment in chickpea (*Cicer arietinum* L.) results in no yield benefit under terminal drought. J Exp Bot 2007;58:187–94.
[34] Esen A. Purification and partial characterization of maize (*Zea mays* L.) beta-glucosidase. Plant Physiol 1992;98:174–82.
[35] Gómez-Anduro G, Ceniceros-Ojeda EA, Casados-Vázquez LE, Bencivenni C, Sierra-Beltrán A, Murillo-Amador B, et al. Genome-wide analysis of the beta-glucosidase gene family in maize (*Zea mays* L. var B73). Plant Mol Biol 2011;77:159–83.
[36] Zhao L, Liu T, An X, Gu R. Evolution and expression analysis of the β-glucosidase (GLU) encoding gene subfamily in maize. Genes Genomics 2012;34:179–87.
[37] Šmehilová M, Galuszka P, Bilyeu KD, Jaworek P, Kowalska M, Šebela M, et al. Subcellular localization and biochemical comparison of cytosolic and secreted cytokinin dehydrogenase enzymes from maize. J Exp Bot 2009;60:2701–12.
[38] Fischer RA, Maurer R. Drought resistance in spring wheat cultivars. I. Grain yield response. Aust J Agric Res 1978;29:897–907.
[39] Galuszka P, Popelková H, Werner T, Frébortová J, Pospíšilová H, Mik V, et al. Biochemical characterization and histochemical localization of cytokinin oxidases/dehydrogenases from *Arabidopsis thaliana* expressed in *Nicotiana tabaccum* L. J Plant Growth Regul 2007;26:255–67.
[40] Köllmer I, Novák O, Strnad M, Schmülling T, Werner T. Overexpression of the cytosolic cytokinin oxidase/dehydrogenase (CKX7) from Arabidopsis causes specific changes in root growth and xylem differentiation. Plant J 2014;78:359–71.
[41] Podlešáková K, Zalabák D, Čudejková M, Plíhal O, Szüčová L, Doležal K, et al. Novel cytokinin derivatives do not show negative effects on root growth and proliferation in submicromolar range. PLoS One 2012;7:e39293.
[42] Kudo T, Kiba T, Sakakibara H. Metabolism and long-distance translocation of cytokinins. J Integr Plant Biol 2010;52:53–60.
[43] Dubrovsky JG, Sauer M, Napsucialy-Mendivil S, Ivanchenko MG, Friml J, Shishkova S, et al. Auxin acts as a local morphogenetic trigger to specify lateral root founder cells. Proc Natl Acad Sci U S A 2008;105:8790–4.
[44] Cary AJ, Liu W, Howell SH. Cytokinin action is coupled to ethylene in its effects on the inhibition of root and hypocotyl elongation in *Arabidopsis thaliana* seedlings. Plant Physiol 1995;107:1075–82.
[45] Yamaguchi M, Sharp RE. Complexity and coordination of root growth at low water potentials, recent advances from transcriptomic and proteomic analyses. Plant Cell Environ 2010;33:590–603.
[46] Blum A. Drought Resistance and Its Improvement. In: Blum A, editor. Plant breeding for water-limited environments. New York: Springer Publishing; 2010 p. 53–152.
[47] White RG, Kirkegaard JA. The distribution and abundance of wheat roots in a dense, structured subsoil-implications for water uptake. Plant Cell Environ 2010;33:133–48.
[48] Barker T, Campos H, Cooper M, Dolan D, Edmeades G, Habben J, et al. Improving drought tolerance in maize. Plant Breed Rev 2005;25:173–253.
[49] Vanholme R, Demedts B, Morreel K, Ralph J, Boerjan W. Lignin biosynthesis and structure. Plant Physiol 2010;153:895–905.

Title: The first case of a missense mutation in *RPS7* as the cause of Diamond-Blackfan anaemia in humans.

Short title: Novel *RPS7* mutation in DBA

Authors: Petr Vojta[a*], Zuzana Maceckova[a*], Jana Volejnikova[a,b], Natalie Taborska[a], Pavla Koralkova[c], Alexandra Jungova[d], Zuzana Saxova[c], Renata Mojzikova[c], Ivana Hadacova[f], Jaroslav Cermak[g], Monika Horvathova[c], Dagmar Pospisilova[a,b], Marian Hajduch[a]

Affiliations:

[a]Institute of Molecular and Translational Medicine, Palacky University Olomouc, Hnevotinska 1333/5, 77900 Olomouc, Czech Republic

[b]Department of Paediatrics, Faculty of Medicine and Dentistry, Palacky University and University Hospital Olomouc, I. P. Pavlova 6, 77900 Olomouc, Czech Republic

[c]Department of Biology, Faculty of Medicine and Dentistry, Palacky University Olomouc, Hnevotinska 3, 77515 Olomouc, Czech Republic

[d]Department of Haematooncology, Charles University and University Hospital Pilsen, Alej Svobody 80, 30460 Pilsen-Lochotin, Czech Republic

[e]Department of Haemato-Oncology, Faculty of Medicine and Dentistry, Palacky University and University Hospital Olomouc, I. P. Pavlova 6, 77900 Olomouc, Czech Republic

[f]Department of Haematology, Charles University and University Hospital Motol Prague, V Uvalu 84, 15006 Prague, Czech Republic

[g]Institute of Haematology and Blood Transfusion, U Nemocnice 2094/1, 12820 Prague, Czech Republic

[*]both authors contributed equally

Corresponding author: *Clinical haematology:* Dagmar Pospisilova, Department of Paediatrics, Faculty of Medicine and Dentistry, Palacky University and University Hospital Olomouc, I. P. Pavlova 6, 77900 Olomouc, Czech Republic; E-mail: pospisid@fnol.cz; Phone: +420588442798; Fax: +420588442505

Molecular and cellular biology: Marian Hajduch, Institute of Molecular and Translational Medicine, Palacky University Olomouc, Hnevotinska 1333/5, 77900 Olomouc, Czech Republic; E-mail: marian.hajduch@upol.cz; Phone: +420 585632111; Fax: +420 585632180

Abstract

Objective: Diamond-Blackfan anaemia (DBA) is predominantly underlined by mutations in genes encoding ribosomal proteins (RP); however, its aetiology remains unexplained in approximately 25% of patients.

Methods: We performed panel sequencing of all ribosomal genes in DBA patient without previously known molecular pathology. Pathogenicity of the novel mutation was extensively studied *in vitro* in a mutation-transfected human fibroblast cell line MRC-5.

Results and conclusions: A novel heterozygous *RPS7* mutation hg38 chr2:g.3,580,153G>T coding RPS7 p.V134F was found in one female patient and subsequently confirmed in two asymptomatic family members, in whom mild anaemia and increased erythrocyte adenosine deaminase (eADA) levels were detected on further examination. We observed defects in nucleolar morphology and functions, decreased protein translational activity and ribosomal stress activation in the RPS7 p.V134F transfected cells. We also observed altered erythrocyte metabolism in the DBA patient, which may have negatively affected the lifespan of erythrocytes and contributed to the pathophysiology of the disease.

Keywords: Diamond-Blackfan anaemia (DBA); massive parallel sequencing (MPS); ribosomal proteins; ribosomal stress; *RPS7*

Introduction

Diamond-Blackfan anaemia (DBA) is a rare congenital red cell aplasia with causative mutations in genes encoding ribosomal proteins (RP), which involve small ribosomal subunit genes (*RPS19*, *RPS26*, *RPS7*, *RPS24*, *RPS17*, *RPS10*, *RPS15A*) or large ribosomal subunit genes (*RPL5*, *RPL11* and *RPL35A*) (1–3). These mutations affect translational activity, protein folding and ribosome biogenesis in an autosomal dominant manner (4). DBA may also be associated with mutations in non-ribosomal genes, such as *GATA1* (5) and *TSR2* (6). Despite intensive research, aetiology of DBA remains unexplained in approximately 25% of patients.

DBA mostly manifests during the first year after birth, but its phenotype is highly variable from silent carriers over mild (typically macrocytic) anaemia to severe transfusion dependency accompanied by short stature with skeletal abnormalities (7), mental retardation (8,9) and increased risk of tumour development (10).

Molecular pathology of DBA involves an activation of the ribosomal stress ultimately leading to induction of TP53 signalling pathway, to cell cycle arrest and apoptosis (11,12). Some ribosomal proteins (e.g., RPS7, RPL5, RPL23 and RPL11) transduce nucleolar stress signals through binding to MDM2, which results in decreased ubiquitination of TP53 (13). Furthermore, TP53 deficiency partially rescued anaemic phenotype in mouse and zebrafish DBA models (14,15). During the last years, whole transcriptome studies have been performed on *RPS19*, *RPS24*, *RPL5* and *RPL11* zebrafish knock-out models prepared by morpholino technique (16–19), where additional molecular mechanisms and pathways contributing to DBA phenotype were identified. Recently, it was also shown that ribosomal insufficiency increased oxidative stress in erythrocytes of DBA patients (19).

In this study, we performed massive parallel sequencing (MPS) of RP gene panel by selective capture hybridization to identify novel mutations among patients in the Czech National DBA Registry (20) without previously known molecular pathology. We found a novel *RPS7* mutation in three female members of one family accompanied by elevated erythrocyte adenosine deaminase (eADA) levels. Pathogenicity of the mutation was confirmed by *in vitro* studies evaluating nucleolar and ribosomal dysfunctions in transfected cells. These methods may serve as a tool to validate functional impact of novel mutations in DBA.

Patients and methods

Clinical report

The patient was an 18-year-old female born in term from second uncomplicated pregnancy with a birth weight of 2,600 g. She had no congenital malformations and presented with severe anaemia during the first month of life. Bone marrow aspirate showed a severe isolated erythroid aplasia and the diagnosis of DBA was established. The patient was transfusion dependent during the first year of life and required irregular red blood cell transfusions until 3 years of age. She was treated with small dose of prednisolone on alternate days since 3 years of age, responded well to steroid therapy and is currently in remission with haemoglobin (Hb) 101 g/L and mean corpuscular volume (MCV) 112 fL. Her body height is normal.

Patient‘s mother and older sister are both asymptomatic and their past medical history is insignificant. They harbour no somatic malformations. Normal Hb levels (120 g/L and 127 g/L, respectively) and mild macrocytosis (MCV of 97 fL and 96 fL, respectively) were detected on laboratory examination. Other family members are healthy.

DNA extraction, RNA extraction and cDNA preparation

DNA was extracted from peripheral blood by Genomic DNA Whole Blood kit (Qiagen, Germany) using MagCore HF116 robotic station (RBC Bioscience Corp., Taiwan) according to manufacturer's protocol. RNA isolation was performed from blood samples stored in Tempus Blood RNA Tubes using Tempus Spin RNA Isolation kit (Thermo Fisher Scientific, MA, USA) or from resuspended cell pellets according to manufacturer's instructions in case of *RPS7* transfected cells. RNA integrity and concentration was checked by Agilent Bioanalyzer (Agilent Technologies, CA, USA) and Nanodrop ND 1000 (Thermo Scientific, USA).

For reverse transcription, we pre-incubated 3 µg of total RNA with 0.3 µg of Random Primers (Promega, USA) at 70 °C for 5 minutes, and immediately placed the mixture on ice. Then 6 µl of RevertAid 5x RT buffer (Fermentas, Lithuania), 3 µl of 10 mM deoxyribonucleotide triphosphates (dNTPs), 0.75 µl of 40 U/µl RNAsin ribonuclease inhibitor (Promega, USA), and DEPC treated water (Ambion, USA) up to a final volume of 30 µl were added, and the mixture was incubated for 5 minutes at room temperature. During the final step, 150 U of RevertAid Moloney Murine Leukemia Virus reverse transcriptase (Fermentas, Lithuania) were added to each tube and the samples were incubated at room temperature for 10 minutes. Finally, samples were incubated at 42 °C for 60 minutes and then 70 °C for 10 minutes.

RPS7 wild-type ($RPS7^{wt}$) vs. RPS7 p.V134F ($RPS7^{mut}$) allele ratio was estimated using *RPS7* cDNA sequencing. Amplicon for target cDNA *RPS7* was obtained by PCR using primers specifically designed to 5‘ and 3‘ UTR regions of the gene (tctcgcgagatttgggtctctt, ttacaattgaaactctgggaattcaaaat).

RP panel library preparation and sequencing

NimbleGen SeqCap EZ custom targeting probes library was designed for all human exon regions of RPS and RPL genes (Suppl. Tab. 1). Sequencing library was prepared from 500 ng of nebulized genomic DNA following the supplier‘s protocol (Roche Nimblegen, WI, USA). Libraries were sequenced on 454 GS Junior platform.

Raw fastq reads were trimmed by Trimmomatic software (21) and aligned to the ensembl hg38 reference genome by BWA MEM algorithm (22). BWA-mem aligned reads were filtered for minimal mapping quality (MQ) ≥10. Subsequently, alignment was transformed to mpileup format by SAMtools (23). Variant calling format (VCF) file was generated by VarScan2 (24) (minimal coverage 10x, minimal variants supporting reads 4, minimal variant frequency 0.3, minimal Phred base quality 20) and annotated against reference genome hg38 with relevant GTF file (version 83) by in-house Python scripts. Due to the bias of the 454 sequencing in homopolymer regions (25), all indel variants were excluded and only single nucleotide variants (SNVs) were evaluated.

Annotated variants were compared with common variants in dbSNP database (build-id 146). Selected variants were checked and visualised in IGV browser (26,27) Polyphen2, I-Mutant2.0-Seq and MUpro were used to assess functional impact of DNA mutations on protein stability and function (28–30). RP gene panel sequencing revealed *RPS7* hg38 chr2:g.3,580,153G>T mutation, which was subsequently was confirmed by Sanger sequencing. DNA was amplified by PCR with following primers targeting exon 6 of *RPS7* (cattttgacttaaagaggtgc, cactaaaatccactctcactg). Results from Sanger sequencing were edited and visualized in Unipro UGENE (31).

RPS7 cDNA library preparation and sequencing

Sequencing library was prepared using Nextera XT kit (Illumina, USA) according to manufacturer's protocol and sequencing was performed on MiSeq platform (Illumina, USA). Raw fastq reads were trimmed by Trimmomatic software and aligned by STAR (32). Only unique mapped reads (MQ = 255) were used. Frequencies of *RPS7*^{mut} vs. *RPS7*^{wt} were subtracted in IGV browser.

Enzyme assays

Activity of enzymes involved in anaerobic glycolysis, oxidative defence and nucleotide metabolism, particularly pyruvate kinase (PK), hexokinase (HK), glucose 6-phosphate dehydrogenase (G6PD) and eADA, was determined according to the methods recommended by the International Committee for Standardization in Haematology (33), with the use of leukocyte- and platelet-free erythrocyte lysates as previously described (34,35). Briefly, the enzyme reaction was pre-incubated for 10 min at 37 °C, thereafter the substrate was added. Absorbance was measured at 340 nm in 1 min intervals for 20 min at 37 °C (Spectrophotometer Infinite 200 Nanoquant; Tecan, Switzerland) and specific enzyme activity was calculated using the Lambert-Beer law. All chemicals and purified enzymes were purchased from Sigma Aldrich (Germany).

Measurement of glutathione, ATP and ADP

Freshly prepared erythrocyte lysates, extracted with 5% trichloroacetic acid (Sigma-Aldrich, Germany), were used for the measurements of reduced glutathione (GSH), ATP and ADP levels by high-performance liquid chromatography-mass spectrometry (HPLC-MS) (HPLC Dionex Ultimate 3000 MS, Thermo Scientific, USA; LC/MS/MS System MDS API 3200, Applied Biosystems, USA) as previously published (34,36).

Oxidative stress and Annexin V binding

Peripheral blood erythrocytes ($2x10^7$/ml) were incubated with 0.4 mM 2',7'-dichlorofluorescein diacetate (DCF; Sigma-Aldrich, Germany) for 15 min at 37 °C as previously described (36). For a positive control, erythrocytes were exposed to 2 mM H_2O_2 for 10 min before DCF labelling. The levels of reactive oxygen species (ROS) were determined based on the DCF-dependent intensity of fluorescence measured by FACSCalibur (BD Biosciences, New Jersey, USA).

Annexin V binding to erythrocyte membrane was analysed using Annexin V/FITC kit (BD Biosciences, New Jersey, USA) following manufacturer's instructions. Fluorescence intensity was also measured by FACSCalibur.

Plasmid preparation and transfection

RPS7^{wt} cDNA was obtained from peripheral blood of healthy controls by amplification using specific primers. The resulting amplicon was then cloned into 3.3-TOPO TA vector (Life Technologies, CA, USA) according to manufacturer's instructions, followed by site-directed mutagenesis using QuikChange II kit (Agilent, CA, USA) and mutagenesis primers in order to create RPS7^{mut} cDNA.

MRC-5 human fibroblast cell line was cultured in DMEM medium supplemented with 10% FBS, 1% non-essential amino acids, penicillin (100 U/mL) and streptomycin (100 µg/mL). One million cells were transfected by 5 µg of plasmid or empty vector (control cells) using Neon transfection system (Life Technologies, CA, USA) set to 1700 V 20 ms 1x.

Western blot

Cultured cells were trypsinized, washed in PBS, resuspended and lysed in RIPA buffer (25 mM Tris-HCl pH 7.6, 150 mM NaCl, 1% NP-40, 1% sodium deoxycholate, 0.1% SDS). Protein concentration was determined by BCA kit (Sigma Aldrich, MO, USA). In total, 10 μg of cellular proteins were denatured in SDS loading buffer (5% β-mercaptoethanol, 0.02% bromophenol blue, 30% glycerol, 10% SDS, 250 mM Tris-HCl), separated on SDS-polyacrylamide gel electrophoresis and transferred onto nitrocellulose membrane. Membranes were incubated with primary antibodies against TP53 (sc-6243) and β-actin (sc-47778, both Santa Cruz Biotechnology, CA, USA) overnight at 4 °C followed by incubation with appropriate peroxidase-linked secondary antibody. Positive signals were visualised by chemiluminescence detection system (Bio-Rad, CA, USA) using the Odyssey imaging device (LI-COR Biosciences, NE, USA).

Immunofluorescence analysis

Cells were transfected with *RPS7*$^{wt/mut}$ cDNA as described above and after 3 days in culture fixed by 4% paraformaldehyde in 1x PBS for 15 min and permeabilized by 0.5% Triton X-100 in 1x PBS for 15 min at room temperature. Overnight incubation with anti-TP53 (sc-6243, Santa Cruz, CA, USA) in 5% FBS was carried at 4 °C. Samples were incubated with species-specific secondary antibody labelled by Alexa Fluor 488 (Life Technologies, CA, USA) in 5% FBS for 1 hour at room temperature. Coverslips were washed three times and placed in mounting medium with DAPI (Kreatech, Czech Republic). Localization of TP53 was examined using confocal fluorescent microscopy with super-resolution (Carl-Zeiss, Germany) at objective magnification 100x. Image quantification was calculated as a corrected spot intensity in the nucleoli using Columbus software version 2.71 (Perkin-Elmer, MA, USA).

Nucleolar morphology staining

Nucleolar morphology was evaluated by Smetana's staining (37). Transfected fibroblasts were fixed after 3 days in culture and washed with 1x PBS followed by incubation with 0.3% toluidine blue in McIlvain buffer (2.1% citric acid, 7.16% sodium phosphate dibasic; pH 6) for 10 min at room temperature and washed in McIlvain buffer. Stained nucleoli were examined at 100x magnification and divided in two categories: 1. unperturbed nucleoli - round and tight; and 2. unfolded nucleoli – with amorphous shape and loosen structure. The slides were examined by light microscope (Carl-Zeiss, Germany) at objective magnification 100x. Image quantification was calculated as a corrected spot intensity in the nucleoli using Columbus software version 2.71 (Perkin-Elmer, MA, USA).

rRNA fluorescence in situ hybridization

Cells were transfected and fixed as described above and permeabilized by 70% ethanol at -20 °C overnight. Cells were washed twice in wash buffer (2x SSC, 10% formamide), followed by hybridisation at 37 °C for 5 hours in hybridisation buffer (10% formamide, 2x SSC, 0.5 mg/mL tRNA, 10% dextran sulphate, 250 µg/mL BSA, 10 mM ribonucleoside vanadyl complexes and 0.5 ng/µL probe cgctagagaaggcttttctc conjugated with cy5). Coverslips were washed twice in wash buffer at 37 °C and mounted by mounting medium with DAPI (Kreatech, Czech Republic). The cells were examined using confocal fluorescent microscopy with super-resolution (Carl-Zeiss, Germany) at 100x magnification. Image quantification was calculated as a corrected spot intensity in the nucleolus in Columbus software version 2.71 (Perkin-Elmer, MA, USA).

Northern blot

Northern blot was used for 18S pre-RNA detection. In total, 5µg of RNA was separated on 1X MOPS denaturing gel followed by transfer to Hydrobond N^+ nylon membrane (GE Healthcare, France). Probe cgctagagaaggcttttctc was labelled with digoxigenine (DIG) using oligonucleotide 3'-end labelling kit (Sigma-Aldrich, Germany). RNA was detected using DIG-labelled probe and DIG Northern Kit (Sigma-Aldrich, Germany) according to manufacturer's protocol.

Protein synthesis assay

Fibroblasts were transfected as mentioned above, seeded on Petri dish, grown overnight and on the following day subjected to the incorporation of methionine analogue using Click-IT AHA kit (Thermo Fisher Scientific, CA, USA). Translational efficiency was measured by FACS Calibur flow cytometer and data were analysed using CellQuest software (both BD Biosciences, NJ, USA). Gate for translationally active cells was set according to control cells (gate R2). Next, cells were examined using Yokogawa CV8000 System (Yokogawa, Japan). Image quantification was calculated as cytoplasmic intensity using Columbus software version 2.71 (Perkin-Elmer, MA, USA).

Results

The Czech National DBA registry currently includes 52 patients. Previously, causative mutations were identified in 33 out of 46 patients (71.7%) in genes coding for *RPS19*, *RPS26*, *RPL5*, *RPL11* and *RPS17* using Sanger sequencing.

In study of RP gene panel sequencing, we obtained 108,774 reads after mapping quality filtration and PCR duplicates removal. The reads covered 200,696 bases of RP gene panel exons represented in bed file with minimum coverage threshold of 10x per nucleotide with average coverage 52x. 74,924 nucleotide positions were not been included into the VCF file due to insufficient coverage (10x), from which 3,379 bases included coding DNA sequence (CDS) regions (Suppl. Tab. 2.).

A novel nonsynonymous germline heterozygous transversion hg38 chr2:g.3,580,153G>T resulting in amino acid substitution p.V134F was identified by MPS in exon 6 of the *RPS7* gene in one female patient with DBA and in two of her asymptomatic relatives. The mutation was subsequently confirmed by cDNA sequencing (Fig. 1). Ultra-deep cDNA sequencing (average coverage 78,285x) revealed that expression of the mutated allele is in concordance with genotype (proband: 55% $RPS7^{wt}$ / 45% $RPS7^{mut}$, mother: 58% $RPS7^{wt}$ / 42% $RPS7^{mut}$, sister: 63% $RPS7^{wt}$ / 37% $RPS7^{mut}$).

The mentioned point mutation has not yet been published nor reported in human variants databases. Valine 134 is highly conserved in RPS7 and substitution by phenylalanine in this position is considered possibly damaging by Polyphen2 (score 0.965). *In silico* protein stability predictors I-Mutant and MUpro evaluated the substitution as decreasing RPS7 protein stability (I-Mutant reliability index 9, MUpro scores were -0.97 by Neural Network method and -1 by Support Vector Machine method).

Translational activity, nucleolar morphology, 18S rRNA precursors and TP53 activation

Electrophoretogram shows comparable levels of $RPS7^{mut}$ and $RPS7^{wt}$ transfected cells (Fig. 2A). Furthermore, using Sanger sequencing, we observed a same $RPS7^{mut/wt}$ ratio in the transfected cells as in the DBA patient and her relatives.

Protein synthesis assay showed decreased translational capacity in *RPS7*^{mut} cells: only 78.9% of *RPS7*^{mut} cells were translationally active (i.e., gated to R2 gate), compared to 97.7% of *RPS7*^{mut} cells and 92.9% of control cells. Furthermore, overall intensities of translationally active cells were significantly lower in *RPS7*^{mut} cells compared to *RPS7*^{wt} cells (mean 586.2 vs. 1874.4 fluorescence units, respectively, Fig. 2C). Cells treated with puromycin served as a positive control for the inhibition of protein synthesis. These results were confirmed by image analysis, where *RPS7*^{mut} cells had cytosolic intensity of 133.7±3 compared to 160.1±7 in *RPS7*^{wt} cells and 177.3±12.5 in control cells and (Fig. 2B).

To assess the effect of *RPS7*^{mut}, we performed a functional study in transiently transfected cells. Using 5'ITS rRNA FISH, NCL and toluidine blue staining, we detected changes in the nucleolar structure suggestive of an rRNA processing defect (Fig. 3A, D). Abnormal nucleolar morphology was more frequent in *RPS7*^{mut} compared to *RPS7*^{wt} cells and control cells: unperturbed/unfolded nucleoli ratio per 100 cells was 47/53 in *RPS7*^{mut} cells, 76/24 in *RPS7*^{wt} cells and 87/13 in control cells (Fig. 3B). Furthermore, 5'ITS rRNA staining revealed increased nucleolar spot intensity in *RPS7*^{mut} cells (118.1±0.36) compared to *RPS7*^{wt} (118.4±0.45) and control cells (119.8±0.35) (Fig. 3C). Perturbation of nucleolar structure was also apparent using NCL immunostaining (Fig. 4D). In *RPS7*^{mut} cells, NCL intensity was increased (0.31±0.0057) compared to *RPS7*^{wt} (0.317±0.0084) and control (0.36±0.011) (Fig. 3C)

The fact that *RPS7*^{mut} perturbs rRNA processing was confirmed by analysis of 18S pre-rRNA species using Northern blot. *RPS7*^{mut} accumulated of 45S pre-rRNA and decreased intensity of 30S pre-rRNA along with an increased size of this precursor compared to RPS7^{wt} and control cells (Fig. 3E).

Western blot revealed significantly increased levels of TP53 in *RPS7*^{mut} cells (Fig. 4B). Activation of TP53 and its accumulation in the nucleus in *RPS7*^{mut} cells was also confirmed using immunofluorescent staining against TP53 (Fig. 4A).

Adenosine metabolism and oxidative stress of red blood cells

Determination of eADA is considered one of the confirmatory tests for DBA, because eADA level is raised in the majority of DBA patients (39). Indeed, we detected elevated levels of eADA not only in the affected patient, but also in both asymptomatic family members harbouring the same *RPS7* mutation (patient: 4.2±0.8 IU/g Hb; mother: 3.5±0.2 IU/g Hb; sister: 4.6±0.3 IU/g Hb; reference range: 0.8-2.5 IU/g Hb) (Tab. 1).

In the following experiments, we focused on anti-oxidative defence of mature erythrocytes and on the activity of their key metabolic enzymes. As shown in Fig. 5A, increased levels of ROS were detected only in the patient‘s erythrocytes (X-mean fluorescence: 19.2), but not in erythrocytes of her asymptomatic mother (X-mean fluorescence: 13.7) and sister (X-mean fluorescence: 14.2; control range of X-mean fluorescence: 12.6-14.2). Consistently, only the patient showed increased anti-oxidative defence parameters, particularly elevated levels of reduced glutathione (GSH) and glucose 6-phosphate dehydrogenase (G6PD) compared to her mother and sister and healthy controls (Tab. 1), confirming ongoing oxidative stress and stimulated anti-oxidative defence.

Concomitant increase in the activity of hexokinase (HK; approximately 3.5x), pyruvate kinase (PK; approximately 2.5x) and in the levels of ATP (approximately 3x) in the patient‘s red blood cells also differentiated patient from healthy controls as well as from asymptomatic family members harbouring the same mutation (Tab. 1). These changes in anaerobic glycolysis suggest increased demand for ATP in patients with hypoxia caused by inadequate erythrocyte production.

Despite activated anti-oxidative defence and hyperactivated anaerobic glycolysis, flow cytometry of annexin V binding revealed increased exposure of phosphatidylserines (PS) on the membrane of patient‘s red blood cells compared to her asymptomatic family members and controls (Fig. 5B, C). This may indicate enhanced recognition and destruction of patient‘s erythrocytes by reticuloendothelial macrophages.

Discussion

Here we present the first case of a missense mutation in *RPS7* as the cause of DBA in humans. To date, five cases of *RPS7* mutations clinically associated with DBA have been published, however, in all of these patients, mutations were located at splice sites and clinical course of DBA was milder than in our case (40–43).

Previously, two ENU-induced *Rps7* mouse mutants, harbouring heterozygous sequence variants, have been reported to have impaired ribosomal biogenesis (44). Despite the fact that the murine models did not yield a phenotype analogous to DBA, the RPS7 p.V156G substitution resulted in decreased growth, abnormal skeletal morphology, mid-ventral white spotting and eye malformations - phenotypes that also occur due to haploinsufficiency of genes coding for other ribosomal subunits (44).

We identified the RPS7 p.V134F substitution in the patient and her asymptomatic mother and sister. *In silico* modelling predicted damaging effect of this variant on the RPS7 protein. To validate the causality of the mutation, we performed a number of functional tests. Decreased translational capacity caused by a lack of mature ribosomes is one of the characteristic features of DBA-mutant cells. We have previously shown that translational assay can be used to determine if given variants in ribosomal genes impair ribosomal biogenesis (45). Using this approach, we confirmed that the newly identified RPS7 p.V134F variant distorts protein synthesis.

Nucleolar disruption has been observed in ribosomal protein depletion models and nucleolar stress models (46,47). Accordingly, we detected profound changes in nucleolar morphology (i.e., loss of shape and unfolding) in *RPS7*^{mut} transfected cells, and thus assume that the RPS7 p.V134F mutation perturbs nucleolar structure and leads to nucleolar stress. In addition, we observed abnormal rRNA processing in *RPS7*^{mut} cells.

Protein TP53 is the main response element during nucleolar and ribosomal stress; several ribosomal proteins, including RPS7, bind to TP53 ubiquitin ligase MDM2 and inhibit its activity towards TP53. Significantly higher levels of TP53 in *RPS7*^{mut} cells compared to both *RPS7*^{wt} cells and control cells are consistent with the ribosomal stress theory. Slightly increased TP53 level in *RPS7*^{wt} cells compared to controls, which we observed, is in agreement with literature (48).

Increased exposure of phosphatidylserine on erythrocyte membrane in the patient compared to her asymptomatic family members and healthy controls suggests that the tendency towards redox balance restoration and membrane integrity does not completely prevent an enhanced recognition and destruction of the patient's red blood cells by reticuloendothelial macrophages. We suppose that altered red blood cell metabolism may affect the lifespan of erythrocytes in DBA and thus contribute to the worsening of the blood condition, especially during infections.

As we observed, the phenotype of family members with the identical mutation can be different, including silent carriers. All family members of patients with DBA should therefore be examined, even if asymptomatic. Testing of eADA levels could serve as a sensitive screening method for these purposes.

In conclusion, the presented functional tests revealed multiple cellular abnormalities associated with the novel RPS7 p.V134F variant, which have been previously reported in DBA and support the causality of this mutation. Analyses within larger cohort of patients are necessary to further elucidate the pathophysiology of DBA, especially in the remaining approximately 25% of cases without known underlying molecular aberration, and to better understand disease modifying conditions in symptomatic versus asymptomatic carriers.

Acknowledgements

Supported by grants of the Czech Ministry of Health (AZV16-32105A), Czech Science Foundation (GA15-13732S), Czech Ministry of Education, Youth and Sports (NPU LO 1304, EATRIS-CZ LM2015064) and Palacky University Olomouc (IGA UP LF_2017_015 and IGA UP LF_2017_013).

Conflict of interest statement

The authors declare that there is no conflict of interest.

Authors' contribution

PV performed MPS sequencing, bioinformatic analysis and annotation of genetic variants; ZM was responsible for cloning, translational analysis, nucleolar morphology analysis, immunofluorescence analysis, rRNA FISH, Western blot and Northern blot; NT performed cloning and in situ mutagenesis; JV, IH, JC and DP recruited and managed patients; PV, ZM, JV and MHo drafted the manuscript. RM and PK performed enzyme assays and were responsible for GSH, ATP and ADP measurements. ZS examined ROS levels and Annexin V binding. MHo and MHa participated in study design, data analysis and interpretation of results. DP and MHa conceived and designed the work and revised the manuscript. All authors approved the final manuscript.

References

1. Ball S. Diamond Blackfan anemia. Hematol Am Soc Hematol Educ Progr. 2011;2011(1):487–91.
2. Ikeda F, Yoshida K, Toki T, Uechi T, Ishida S, Nakajima Y, et al. Exome sequencing identified RPS15A as a novel causative gene for Diamond-Blackfan anemia. Haematologica. 2016 Mar;102(3):e93–6.
3. Errichiello E, Vetro A, Mina T, Wischmeijer A, Berrino E, Carella M, et al. Whole exome sequencing in the differential diagnosis of Diamond-Blackfan anemia: Clinical and molecular study of three patients with novel RPL5 and mosaic RPS19 mutations. Blood Cells, Mol Dis. 2017 May 6;64:38–44.
4. Cmejlova J, Dolezalova L, Pospisilova D, Petrtylova K, Petrak J, Cmejla R. Translational efficiency in patients with Diamond-Blackfan anemia. Haematologica. 2006 Nov;91(11):1456–64.
5. Sankaran VG, Ghazvinian R, Do R, Thiru P, Vergilio JA, Beggs AH, et al. Exome sequencing identifies GATA1 mutations resulting in Diamond-Blackfan anemia. J Clin Invest. 2012 Jul 2;122(7):2439–43.
6. Gripp KW, Curry C, Olney AH, Sandoval C, Fisher J, Chong JXL, et al. Diamond-Blackfan anemia with mandibulofacial dystostosis is heterogeneous, including the novel DBA genes TSR2 and RPS28. Am J Med Genet Part A. 2014 Sep;164(9):2240–9.

7. Trainor PA, Merrill AE. Ribosome biogenesis in skeletal development and the pathogenesis of skeletal disorders. Biochim Biophys Acta - Mol Basis Dis. 2014 Jun;1842(6):769–78.

8. Gustavsson P, Willig T-N, Haeringen A van, Tchernia G, Dianzani I, Donnér M, et al. Diamond-Blackfan anaemia: genetic homogeneity for a gene on chromosome 19q13 restricted to 1.8 Mb. Nat Genet. 1997 Aug;16(4):368–71.

9. Cario H, Bode H, Gustavsson P, Dahl N, Kohne E. A microdeletion syndrome due to a 3-Mb deletion on 19q13.2--Diamond-Blackfan anemia associated with macrocephaly, hypotonia, and psychomotor retardation. Clin Genet. 1999 Jun;55(6):487–92.

10. Goudarzi KM, Lindström MS. Role of ribosomal protein mutations in tumor development (Review). Int J Oncol. 2016 Feb 9;48(4):1313–24.

11. Badhai J, Fröjmark AS, J. Davey E, Schuster J, Dahl N. Ribosomal protein S19 and S24 insufficiency cause distinct cell cycle defects in Diamond-Blackfan anemia. Biochim Biophys Acta - Mol Basis Dis. 2009 Oct;1792(10):1036–42.

12. Danilova N, Sakamoto KM, Lin S. Ribosomal protein S19 deficiency in zebrafish leads to developmental abnormalities and defective erythropoiesis through activation of p53 protein family. Blood. 2008 Dec 15;112(13):5228–37.

13. Deisenroth C, Zhang Y. Ribosome biogenesis surveillance: probing the ribosomal protein-Mdm2-p53 pathway. Oncogene. 2010 Jul 29;29(30):4253–60.

14. Barlow JL, Drynan LF, Trim NL, Erber WN, Warren AJ, McKenzie ANJ. New insights into 5q- syndrome as a ribosomopathy. Cell Cycle. 2010 Nov 1;9(21):4286–93.

15. Jia Q, Zhang Q, Zhang Z, Wang Y, Zhang W, Zhou Y, et al. Transcriptome analysis of the zebrafish model of Diamond-Blackfan anemia from RPS19 deficiency via p53-dependent and -independent pathways. Sabaawy HE, editor. PLoS One. 2013 Aug 19;8(8):e71782.

16. Zhang Z, Jia H, Zhang Q, Wan Y, Zhou Y, Jia Q, et al. Assessment of hematopoietic failure due to Rpl11 deficiency in a zebrafish model of Diamond-Blackfan anemia by deep sequencing. BMC Genomics. 2013 Dec 17;14(1):896.

17. Song B, Zhang Q, Zhang Z, Wan Y, Jia Q, Wang X, et al. Systematic transcriptome analysis of the zebrafish model of diamond-blackfan anemia induced by RPS24 deficiency. BMC Genomics. 2014 Sep 4;15(759):759.

18. Wan Y, Zhang Q, Zhang Z, Song B, Wang X, Zhang Y, et al. Transcriptome analysis reveals a ribosome constituents disorder involved in the RPL5 downregulated zebrafish model of Diamond-Blackfan anemia. BMC Med Genomics. 2016 Mar 9;9(1):13.

19. Utsugisawa T, Uchiyama T, Toki T, Ogura H, Aoki T, Hamaguchi I, et al. Erythrocyte glutathione is a novel biomarker of Diamond-Blackfan anemia. Blood Cells, Mol Dis. 2016 Jul;59:31–6.

20. Pospisilova D, Cmejlova J, Ludikova B, Stary J, Cerna Z, Hak J, et al. The Czech National Diamond-Blackfan Anemia Registry: Clinical data and ribosomal protein mutations update. Blood Cells, Mol Dis. 2012 Apr 15;48(4):209–18.

21. Bolger AM, Lohse M, Usadel B. Trimmomatic: A flexible trimmer for Illumina sequence data. Bioinformatics. 2014 Aug 1;30(15):2114–20.

22. Langmead B, Trapnell C, Pop M, Salzberg SL, Dettling M, Dudoit S, et al. Ultrafast and memory-efficient alignment of short DNA sequences to the human genome. Genome Biol. 2009 Oct 27;10(3):R25.

23. Li H, Handsaker B, Wysoker A, Fennell T, Ruan J, Homer N, et al. The Sequence Alignment/Map format and SAMtools. Bioinformatics. 2009 Aug 15;25(16):2078–9.

24. Koboldt DC, Chen K, Wylie T, Larson DE, McLellan MD, Mardis ER, et al. VarScan: Variant detection in massively parallel sequencing of individual and pooled samples. Bioinformatics. 2009 Sep 1;25(17):2283–5.

25. Margulies M, Egholm M, Altman WE, Attiya S, Bader JS, Bemben LA, et al. Genome sequencing in microfabricated high-density picolitre reactors. Nature. 2005 Sep 15;437(7057):376–80.

26. Robinson JT, Thorvaldsdóttir H, Winckler W, Guttman M, Lander ES, Getz G, et al. Integrative genomics viewer. Nat Biotechnol. 2011 Jan;29(1):24–6.

27. Thorvaldsdóttir H, Robinson JT, Mesirov JP. Integrative Genomics Viewer (IGV): High-performance genomics data visualization and exploration. Brief Bioinform. 2013 Mar 1;14(2):178–92.

28. Adzhubei IA, Schmidt S, Peshkin L, Ramensky VE, Gerasimova A, Bork P, et al. A method and server for predicting damaging missense mutations. Nat Methods. 2010 Apr;7(4):248–9.

29. Capriotti E, Fariselli P, Casadio R. I-Mutant2.0: Predicting stability changes upon mutation from the protein sequence or structure. Nucleic Acids Res. 2005 Jul 1;33(SUPPL. 2):W306-10.

30. Cheng J, Randall A, Baldi P. Prediction of protein stability changes for single-site mutations using support vector machines. Proteins Struct Funct Bioinforma. 2006 Mar 1;62(4):1125–32.

31. Okonechnikov K, Golosova O, Fursov M. Unipro UGENE: a unified bioinformatics toolkit. Bioinformatics. 2012 Apr 15;28(8):1166–7.

32. Dobin A, Davis CA, Schlesinger F, Drenkow J, Zaleski C, Jha S, et al. STAR: ultrafast universal RNA-seq aligner. Bioinformatics. 2013 Jan 1;29(1):15–21.

33 Beutler E, Blume KG, Kaplan JC, Löhr GW, Ramot B, Valentine WN. International Committee for Standardization in Haematology: recommended methods for red-cell enzyme analysis. Br J Haematol. 1977 Feb;35(2):331–40.

34. Mojzikova R, Dolezel P, Pavlicek J, Mlejnek P, Pospisilova D, Divoky V. Partial glutathione reductase deficiency as a cause of diverse clinical manifestations in a family with unstable hemoglobin (Hemoglobin Haná, β63(E7) His-Asn). Blood Cells, Mol Dis. 2010 Oct 15;45(3):219–22.

35. Mojzikova R, Koralkova P, Holub D, Zidova Z, Pospisilova D, Cermak J, et al. Iron status in patients with pyruvate kinase deficiency: Neonatal hyperferritinaemia associated with a novel frameshift deletion in the PKLR gene (p.Arg518fs), and low hepcidin to ferritin ratios. Br J Haematol. 2014 May;165(4):556–63.

36. Zidova Z, Kapralova K, Koralkova P, Mojzikova R, Dolezal D, Divoky V, et al. DMT1-mutant erythrocytes have shortened life span, accelerated glycolysis and increased oxidative stress. Cell Physiol Biochem. 2014;34(6):2221–31.

37. Smetana K, Karban J, Trneny M. To the nucleolar bodies (nucleoli) in cells of the lymphocytic lineage in patients suffering from B - chronic lymphocytic leukemia. Neoplasma. 2010;57(6):495–500.

39. Vlachos A, Ball S, Dahl N, Alter BP, Sheth S, Ramenghi U, et al. Diagnosing and treating Diamond Blackfan anaemia: Results of an international clinical consensus conference. Vol. 142, British Journal of Haematology. 2008. p. 859–76.

40. Gazda HT, Sheen MR, Vlachos A, Choesmel V, O'Donohue MF, Schneider H, et al. Ribosomal Protein L5 and L11 Mutations Are Associated with Cleft Palate and Abnormal Thumbs in Diamond-Blackfan Anemia Patients. Am J Hum Genet. 2008 Dec;83(6):769–80.

41. Gerrard G, Valgañón M, Foong HE, Kasperaviciute D, Iskander D, Game L, et al. Target enrichment and high-throughput sequencing of 80 ribosomal protein genes to identify mutations associated with Diamond-Blackfan anaemia. Br J Haematol. 2013 Aug;162(4):530–6.

42. Smetanina NS, Mersiyanova I V., Kurnikova MA, Ovsyannikova GS, Hachatryan LA, Bobrynina VO, et al. Clinical and genomic heterogeneity of Diamond Blackfan anemia in the Russian Federation. Pediatr Blood Cancer. 2015 Sep;62(9):1597–600.

43. Ichimura T, Yoshida K, Okuno Y, Yujiri T, Nagai K, Nishi M, et al. Diagnostic challenge of Diamond-Blackfan anemia in mothers and children by whole-exome sequencing. Int J Hematol. 2017 Apr 23;105(4):515–20.

44. Watkins-Chow DE, Cooke J, Pidsley R, Edwards A, Slotkin R, Leeds KE, et al. Mutation of the Diamond-Blackfan Anemia Gene Rps7 in Mouse Results in Morphological and Neuroanatomical Phenotypes. Barsh GS, editor. PLoS Genet. 2013 Jan 31;9(1):e1003094.

45. Cmejla R, Cmejlova J, Handrkova H, Petrak J, Pospisilova D. Ribosomal protein S17 gene (RPS17) is mutated in Diamond-Blackfan anemia. Hum Mutat. 2007 Dec;28(12):1178–82.

46. Choesmel V, Bacqueville D, Rouquette J, Noaillac-Depeyre J, Fribourg S, Crétien A, et al. Impaired ribosome biogenesis in Diamond-Blackfan anemia. Blood. 2007 Feb 5;109(3):1275–83.

47. Choesmel V, Fribourg S, Aguissa-Touré AH, Pinaud N, Legrand P, Gazda HT, et al. Mutation of ribosomal protein RPS24 in Diamond-Blackfan anemia results in a ribosome biogenesis disorder. Hum Mol Genet. 2008 Jan 18;17(9):1253–63.

48. Chen D, Zhang Z, Li M, Wang W, Li Y, Rayburn ER, et al. Ribosomal protein S7 as a novel modulator of p53–MDM2 interaction: binding to MDM2, stabilization of p53 protein, and activation of p53 function. Oncogene. 2007 Aug 2;26(35):5029–37.

Figures:

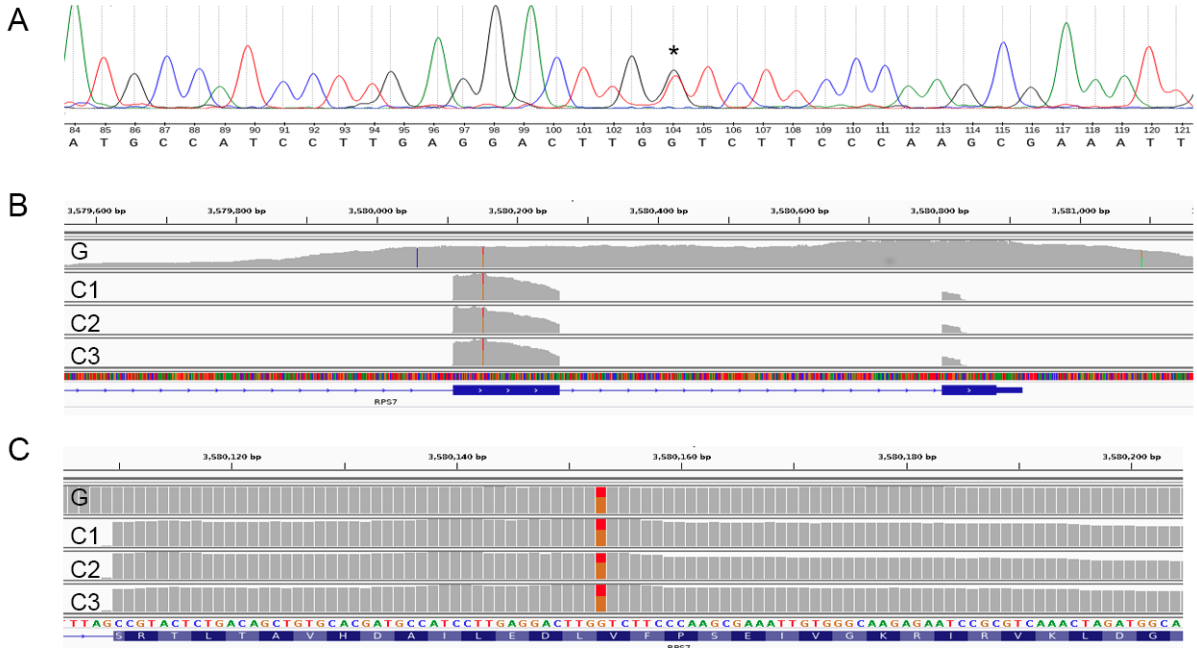

Fig. 1. *RPS7* mutation in the patient with DBA and two of her family members. The confirmation of hg38 chr2:g.3,580,153G>T heterozygous mutation in *RPS7* by Sanger sequencing technique in the patient panel (A). The mutation has been previously identified by MPS sequencing of genomic DNA (G). Mutation was later detected in patient‘s cDNA C1 as well as in her mother (C2) and sister (C3). Panel (B) visualizes alignments in last two *RPS7* exons by IGV in comparison of RP panel gene sequencing and cDNA sequencing. Panel (C) shows position of the mutation in exon 6 of *RPS7* in detail.

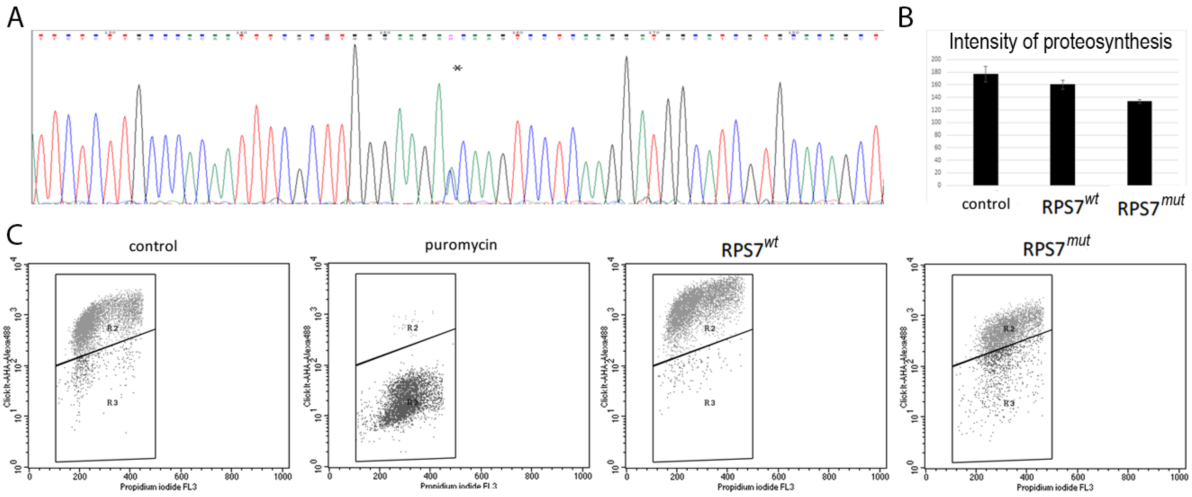

Fig. 2. Electrophoretogram from Sanger sequencing and translational activity: (A) Sanger sequencing electrophoretogram displaying level of *RPS7*^{mut} in a cellular model. (B, C) Protein synthesis assay showed decreased translational capacity of *RPS7*^{mut} cells compared to *RPS7*^{wt} transfectants or control cells. Puromycin treated control cells exhibit almost complete inhibition of protein synthesis.

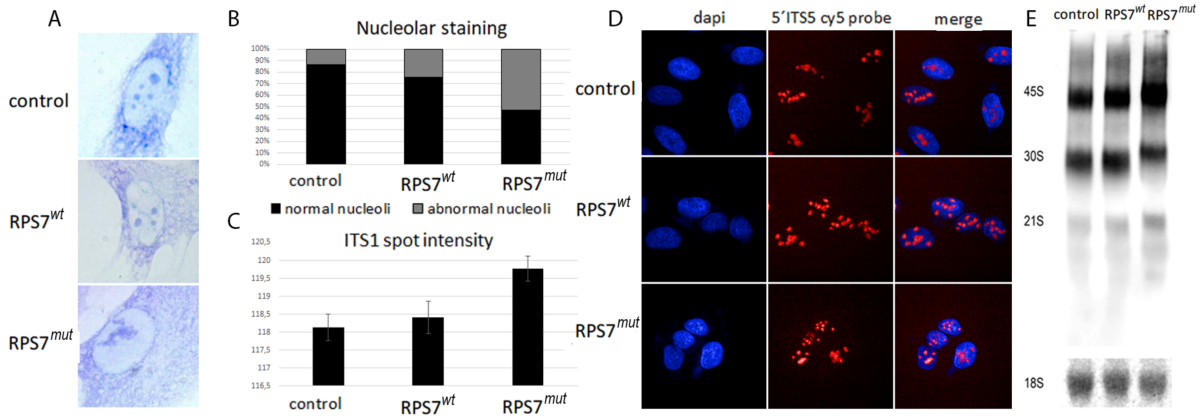

Fig. 3. Nucleolar morphology. (A) Toluidine blue nucleolar staining revealed abnormal nucleolar morphology in *RPS7*^{mut} transfectants compared to controls. (B) Proportion of nucleoli with abnormal morphology among 100 cells. (C, D) Increased intensity of pre-RNA precursors visible by 5‘ETS rRNA FISH. (E) Accumulation of 45S pre-rRNA was detected using Northern Blot.

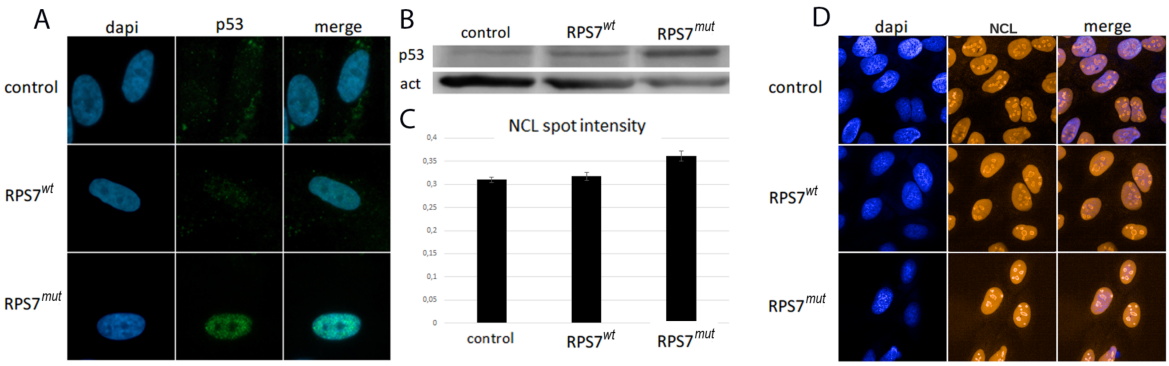

Fig. 4. TP53 activation and NCL staining. (A) Western blot analysis (three days after transfection) revealed increased levels of TP53 in *RPS7*^{mut} cells compared to *RPS7*^{wt} cells and control cells. (B) Immunostaining of TP53 showed increased TP53 translocation to nucleoli in *RPS7*^{mut} cells compared to controls. (C, D) Immunofluorescence staining of NCL showed increased protein amount in the nuclei of *RPS7*^{mut} transfectants compared to *RPS7*^{wt} cells or control cells.

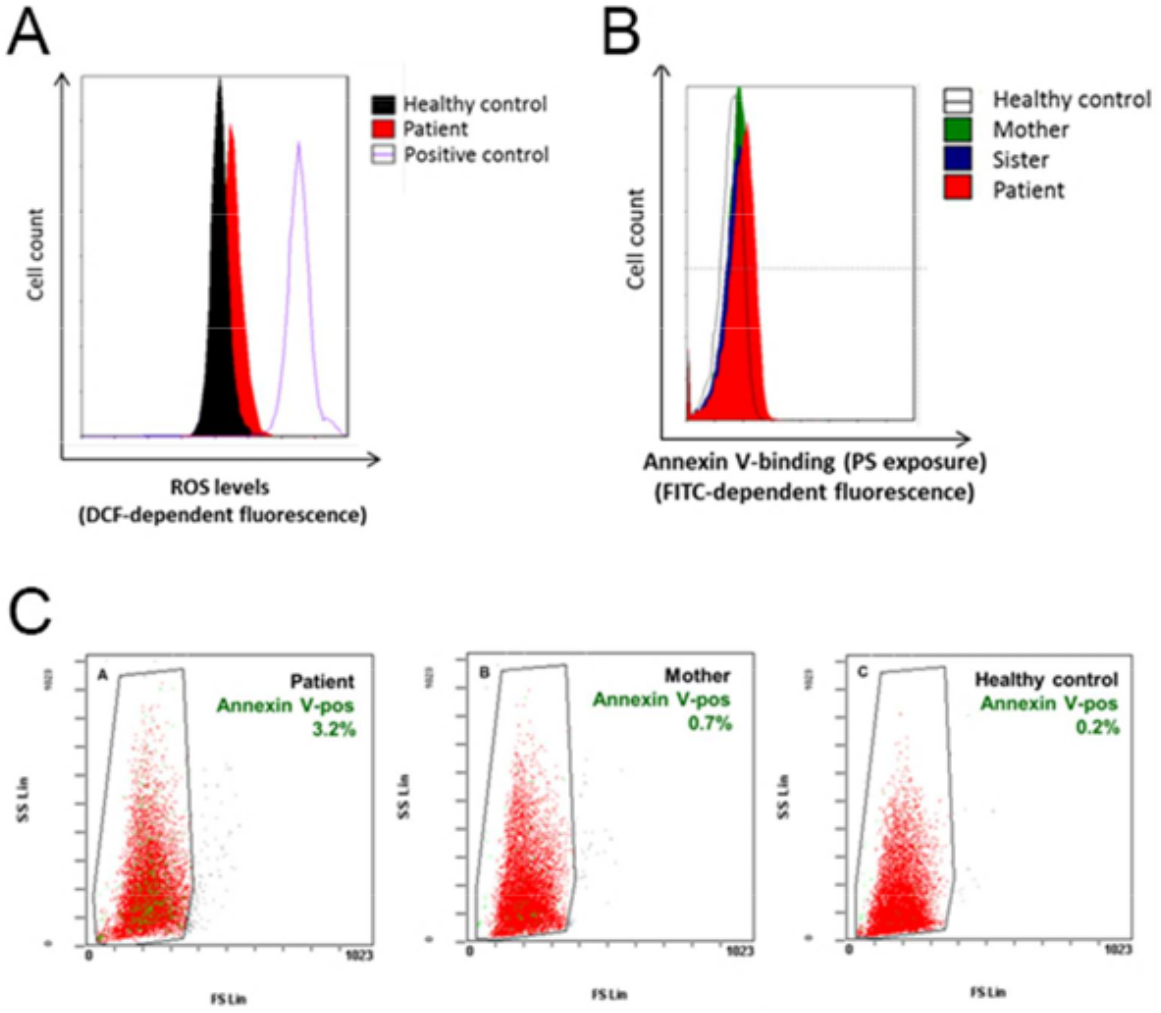

Fig. 5. Determination of ROS levels and Annexin V binding assay. Representative plots and histograms showing elevated levels of ROS (A), increased phosphatidylserine (PS) exposure on erythrocyte membrane (B) and increased percentage of Annexin V-positive erythrocytes (C) in the DBA patient compared to her asymptomatic family member and healthy control. In panel (A), DCF-dependent intensity of fluorescence is proportional to the concentration of ROS; erythrocytes of a healthy control treated with H2O2 served as a positive control for induced ROS formation. In panels (B) and (C), increased Annexin V-binding to RBC reflects increased exposure of PS on erythrocyte membrane.

	eADA	GSH	G6PD	PK	HK	ATP
	(IU/g Hb)	(μM)	(IU/g Hb)	(IU/g Hb)	(IU/g Hb)	(μmol/L)
Reference range	[0.8-2.5]	[1978-2888]	[5.4-7.0]	[5.1-5.8]	[0.8-1.6]	[188-334]
Patient	4.2±0.8	4356±44	10.3±0.6	14.8±0.8	4.4±0.05	775±96
Mother	3.5±0.2	2125	5.3±0.2	4.9±0.2	0.7±0.02	205±32
Sister	4.6±0.3	2450±35	6.5±0.1	6.8±0.5	0.9±0.13	251±45

Table 1. Levels of eADA, GSH and ATP and the activity of selected enzymes of anti-oxidative defence and anaerobic glycolysis in red blood cells.

RESEARCH PAPER

New Biotechnology • Volume 33, Number 5 • September 2016

Research Paper

Whole transcriptome analysis of transgenic barley with altered cytokinin homeostasis and increased tolerance to drought stress

Petr Vojta[1,2], Filip Kokáš[1], Alexandra Husičková[3], Jiří Grúz[4], Veronique Bergougnoux[1], Cintia F. Marchetti[1], Eva Jiskrová[1], Eliška Ježilová[3], Václav Mik[4], Yoshihisa Ikeda[1] and Petr Galuszka[1]

[1] Department of Molecular Biology, Centre of the Region Haná for Biotechnological and Agricultural Research, Faculty of Science, Palacký University in Olomouc, Šlechtitelů 27, 783 71 Olomouc, Czech Republic
[2] Institute of Molecular and Translational Medicine, Faculty of Medicine and Dentistry, Palacký University in Olomouc, Hněvotínská 1333/5, 779 00 Olomouc, Czech Republic
[3] Department of Biophysics, Centre of the Region Haná for Biotechnological and Agricultural Research, Faculty of Science, Palacký University in Olomouc, Šlechtitelů 27, 783 71 Olomouc, Czech Republic
[4] Department of Chemical Biology and Genetics, Centre of the Region Haná for Biotechnological and Agricultural Research, Faculty of Science, Palacký University in Olomouc, Šlechtitelů 27, 783 71 Olomouc, Czech Republic

Cytokinin plant hormones have been shown to play an important role in plant response to abiotic stresses. Herein, we expand upon the findings of Pospíšilová et al. [30] regarding preparation of novel transgenic barley lines overexpressing *cytokinin dehydrogenase 1* gene from Arabidopsis under the control of mild root-specific promotor of maize β-glycosidase. These lines showed drought-tolerant phenotype mainly due to alteration of root architecture and stronger lignification of root tissue. A detailed transcriptomic analysis of roots of transgenic plants subjected to revitalization after drought stress revealed attenuated response through the HvHK3 cytokinin receptor and up-regulation of two transcription factors implicated in stress responses and abscisic acid sensitivity. Increased expression of several genes involved in the phenylpropanoid pathway as well as of genes encoding *arogenate dehydratase/lyase* participating in phenylalanine synthesis was found in roots during revitalization. Although more precursors of lignin synthesis were present in roots after drought stress, final lignin accumulation did not change compared to that in plants grown under optimal conditions. Changes in transcriptome indicated a higher auxin turnover in transgenic roots. The same analysis in leaves revealed that genes encoding putative enzymes responsible for production of jasmonates and other volatile compounds were up-regulated. Although transgenic barley leaves showed lower chlorophyll content and down-regulation of genes encoding proteins involved in photosynthesis than did wild-type plants when cultivated under optimal conditions, they did show a tendency to return to initial photochemical activities faster than did wild-type leaves when re-watered after severe drought stress. In contrast to optimal conditions, comparative transcriptomic analysis of revitalized leaves displayed up-regulation of genes encoding enzymes and proteins involved in photosynthesis, and especially those encoded by the chloroplast genome. Taken together, our results indicate that the partial cytokinin insensitivity induced in barley overexpressing cytokinin dehydrogenase contributes to tolerance to drought stress.

Corresponding author: Galuszka, P. (petr.galuszka@upol.cz)

http://dx.doi.org/10.1016/j.nbt.2016.01.010

Introduction

Cytokinins (CKs) are plant hormones which together with auxins mainly influence plant morphology. Their role in other physiological processes, such as senescence and nutrient remobilization, is very well described [1]. Evidence, mostly from studies of Arabidopsis (*Arabidopsis thaliana*), suggests also an important role of CKs in the regulation of responses to environmental stresses [2]. CK-deficient Arabidopsis plants exhibited a strong stress-tolerant phenotype associated with increased cell membrane integrity and abscisic acid (ABA) hypersensitivity [3]. ABA's stress-related role consists mainly in induction of stomatal closure to prevent water losses under conditions of water limitation. Moreover, loss-of-function mutants of CK receptors and proteins involved in the CK-signaling pathway have been shown to be strongly tolerant to drought and salt stress because they up-regulated many stress-inducible genes [4,5]. Similarly, rice seedlings with knock-down proteins of the CK transduction pathway have been observed to be tolerant of osmotic stress but hypersensitive to salt stress [6]. Activated CK receptors negatively control osmotic stress responses and thus confirm that reduced CK status is a prerequisite for better drought tolerance.

On the other hand, increased drought tolerance or avoidance by stress-induced CK accumulation has been proven in several plant species [7–12]. A transgenic approach has exploited expression of the CK biosynthetic *isopentenyl transferase* (*IPT*) gene under a stress- and maturation-inducible promoter. Under drought-stress conditions, the transgenic plants maintained high photosynthetic activity in contrast to control plants due to the direct effect of CKs on delaying leaf senescence. The acquired drought tolerance was also due to CKs' effect on maintenance of nitrate acquisition from soil [13]. Thus, stress-induced CK synthesis in these transgenic plants promoted sink strengthening through the maintenance and coordination of N and C assimilation during water stress.

In abiotic stress responses, CKs can act in orchestration with other phytohormones. Auxin's role in drought tolerance has been demonstrated when increased activity of auxin conjugating enzyme, which reduces auxin maxima in leaves, led to the accumulation of late-embryogenesis abundant proteins responsible for the switch from plant growth to stress adaptation [14]. Auxin is able to induce the expression of genes encoding enzymes participating in biosynthesis of such stress-related hormones as ethylene [15]; vice versa, ethylene promotes local auxin biosynthesis and consequently reduces root cell elongation [16]. As CKs are known to affect production of both auxin and ethylene, coordinated regulation of hormonal biosynthetic pathways could play a crucial role in plants' adaptation to abiotic stresses [17]. Plants with stress-induced CK production showed up-regulation of brassinosteroid synthesis and signaling genes [11,18]. Brassinosteroids act synergistically with another group of plant hormones, gibberellins (GAs), due to shared components in their signaling pathways [19]. Transgenic Arabidopsis seedlings constitutively overexpressing GA-responsive genes exhibited improved tolerance to various abiotic stresses; stress tolerance was accompanied by biosynthesis of salicylic acid [20], another plant hormone mainly implicated in stress responses.

Plants exposed to drought stress show an alteration of CK content. Hormonal analysis of wild-type (WT) maize leaves subjected to drought showed a gradual decline in CK and GA contents during stress [21]. A comprehensive study on maize seedlings exposed to salt and osmotic stress also demonstrated rapid decline in some CK forms due to enforced CK catabolism. During acclimatization, however, accelerated CK metabolism led to a moderate increase in active CK forms [22]. Higher accumulation of all CK forms was also determined in tobacco exposed to severe drought stress [23]. Hence, accumulation of active CKs among other processes might contribute to the mechanisms by which plants overcome stress status and avoid growth inhibition. Regarding stress signaling, CKs do not, due to the slow response of their biosynthetic genes to stress induction, have a direct function similar to ABA, which directly affects stomatal closure [22].

Maintenance of high photosynthetic capacity is an important prerequisite for preserving crop yield under adverse environmental conditions. Although increasing CK content by senescence-regulated expression of a CK biosynthetic gene is an efficient tool for prolonging leaf photosynthetic activity [24], engineered wheat plants with senescence-regulated CK production showed no differences in yield-related parameters [25]. Shoot growth inhibition and promotion of root growth have been regarded as advantageous for crop stability under stressful conditions and constitute an integral part of plant stress tolerance [26,27]. Accordingly, plants with reduced shoot-to-root ratios as a consequence of CK deficiency showed greater tolerance to or avoidance of drought stress [28,29]. Hence, down- and up-regulation of CK levels *in planta* can have a synergistically positive effect on enhanced tolerance to water deficit: in the first case, through alteration of plant morphology to a root architecture that is better adapted to withstand water deprivation, and, in the second case, through activation of photosynthetic processes and source–sink relations.

Recently, we prepared several barley transgenic lines overexpressing a cytokinin catabolic enzyme–cytokinin dehydrogenase 1 (CKX) from Arabidopsis targeted to various subcellular compartments. Transgenic barley exhibited greater tolerance to or avoidance of drought stress that most probably was due to higher lignification and changes in root morphology [30]. While focusing primarily on post-stress revitalization, the in-depth transcriptomic analysis of our transgenic barley lines aimed to clarify and describe in detail all processes that enable CK-deficient barley plants to cope better with drought.

Material and methods

Plant material and cultivation

Transgenic and WT plants of the spring barley cultivar Golden Promise were grown in an environmental chamber with a photoperiod of 15°C/16 hours light and 12°C/8 hours darkness. The light source was a combination of mercury tungsten lamps and sodium lamps providing an intensity of 300 μmol m^{-2} s^{-1}. Plants were cultivated in a 2:1 mixture of soil and perlite (Perlit Ltd., Czech Republic). Soil composition was 1:1 professional substrate (peat type) for growing plants (Rašelina Soběslav, Czech Republic) and a muck-type arable soil from the Olomouc Region (Czech Republic).

Application of drought stress

For transcriptomic analysis of the root system exposed to drought stress, plants were grown hydroponically in a modified Hoagland solution [31] within an environmental chamber under the same

conditions as given above. The experiment was performed in the following arrangement: 2/3 of each vessel was filled with two transgenic genotypes and 1/3 with WT plants. In total, 27 plants from each genotype were cultivated together in three vessels. Three plants were pooled per biological replicate. Drought stress was induced on plants 4 weeks old by pouring the solution out of the growth vessel after the plants had been temporarily removed. Plants were then returned to the vessel, where they were further kept for another 24 hours, after which the solution was poured back into the vessel. The entire root system was collected after 24 hours of stress and after 14 days of revitalization. The youngest fully expanded leaves were collected for analyzing chlorophyll content every 2nd or 3rd day.

In order to perform transcriptome analysis of the upper part, barley plants were cultivated in shallow trays (30 cm × 20 cm with a depth of 5 cm) filled with soil and watered on a daily basis. Drought stress was applied to 4-week-old plants by keeping them without watering for 4 days, after which regularly watering on a daily basis was resumed. Photosynthetic parameters and relative water content [32] were determined on the youngest fully expanded leaves. Samples were collected 12 hours after the last watering, the 4th day of the stress application, 12 hours after re-watering, and after 14 days of revitalization.

Real-time PCR analysis

Isolation of total RNA was performed using an RNAqueous Kit (Life Technologies, USA). Isolated RNA was then treated using a TURBO DNA-free Kit (Life Technologies) and purified using magnetic beads (Agencourt RNA-CLEAN XP, Beckman Coulter, USA). cDNA was obtained using a RevertAid First Strand cDNA Synthesis Kit (Fermentas, Lithuania). Real-time PCR was set up with cDNA as template in total volume of 10 μL containing POWER SYBR Green PCR Master Mix (Life Technologies) and 300 nM of each primer. Reactions were run in the StepOnePlus™ Real-Time PCR System using the default program (Applied Biosystems, USA). Primers were designed using Primer Express 3.0 software (Supplemental Table S1).

The number of transcripts per ng of isolated total RNA was detected based on calibration curves made with genes cloned into the transformation vector. The relative quantification of most abundant endogenous genes involved in CK metabolism was made using the ΔΔCt method [33] with barley cyclophilin, actin, and elongation factor 1 (AK354091.1, AK248432.1, AK361008.1) analyzed as reference genes and then evaluated statistically using DataAssist v3.0 Software (Life Technologies). Each measurement consisted of four biological and two technical replicates.

RNA-seq analysis

Working with 2.5 μg of total RNA from each sample, extracted as described above, Illumina® TruSeq® Stranded mRNA Sample Preparation Kit (Illumina, USA) was used for cDNA library preparation. Library concentration was assessed using a Kapa Library Quantification Kit (Kapa Biosystems, USA) and all libraries were pooled to a final 8 pM concentration for cluster generation and sequencing. The clusters were generated using an Illumina® TruSeq® SR Cluster Kit v3 cBot HS and sequenced on a HiSeq SR Flow Cell v3 with a HiSeq 2500 Sequencing System. Two independent libraries were prepared for each genotype at each time point from two biological replicates (3 pooled plants in each).

The reads generated by sequencing were mapped to the reference genome of *Hordeum vulgare* v.25 (Ensembl, UK) using the TopHat2 v.2.0.12 splice-read mapper [34] with default parameters. The reads mapped to the transcripts annotated in the reference genome were quantified by using HTSeq v.0.6.0 [35] with respect to the stranded library. The tests for differential gene expression were performed using the DESeq2 package [36] implemented in R (R Development Core Team, 2008). The technical replicates were first analyzed as two independent experiments, which yielded similar results (see Figure 4 in Ref [37]). Thereafter, technical replicates were merged into one technical replicate to obtain higher coverage of the reference transcriptome. Gene ontology (GO) annotation of the reference genome was improved using the Blast2GO v.3.0 program [38], nt database (b2g_Jan15), the ncbi-blast+ v.2.2.28 program [39], as well as the UniProKB (http://www.uniprot.org/, 02.2015) and PGSB (http://pgsb.helmholtz-muenchen.de/plant/, 31.07.2014) databases (see Figure 1 in Ref [37]). This additional GO annotation helped to increase the number of GO annotated genes to 17,885 (from a total of 26,074 predicted genes in barley).

Quantification of lignin and its precursor

Lignin quantification was carried out in protein-free cell wall fractions using the acetyl bromide method [40]. Cinnamic and benzoic acids were determined by an LC–MS method described previously [41]. Monolignols and aromatic amino acids were analyzed with a UHPLC-QTOF-MS system (Synapt G2-Si, Waters, UK) operating in positive ion mode. Coumaryl, coniferyl and sinapyl alcohols were quantified by detecting product ions of the corresponding $[M-H_2O^+H]^+$ ions (i.e., 133 > 105.08, 163 > 131.06, and 193 > 105.08, respectively) while using $^{13}C_6$-isovanillic acid (157 > 114.05) as an internal standard. The relative levels of aromatic amino acids were estimated from peak area acquired in resolution MS mode. All compounds were identified and quantified based on authentic standards.

Measurement of chlorophyll content

Chlorophyll content was determined using a chlorophyll content meter (CCM-300, Opti-Sciences, Hudson, NH, USA) in plants 7–42 days old that were grown hydroponically under drought and control conditions. Measurement for each line consisted of at least 15 biological replicates and two technical replicates. Each transgenic genotype was grown together with the same number of WT barley plants in the same plastic vessel.

Chlorophyll fluorescence imaging

Chlorophyll fluorescence was monitored on the abaxial side of the youngest fully developed attached leaves using an imaging system (FluorCam 700 MF, Photon Systems Instruments, Czech Republic). All measurements were performed on at least four replicates. To measure fluorescence signal, short (microseconds in length) measuring flashes of red light placed 20 ms apart were applied and the signals detected during the measuring flash and just prior to the measuring flash were subtracted. The overall integral light intensity of the measuring flashes was low enough not to close the photosystem II reaction centers but still able to measure fluorescence. The minimum chlorophyll fluorescence yield (F_0) was determined after 40 min of dark adaptation by application of

the measuring flashes only. A saturating pulse of 1.6 s (white light, 2500 μmol m^{-2} s^{-1}) was applied to determine the maximum chlorophyll fluorescence yield in a dark-adapted state (F_M). The leaves were then exposed to red actinic light (200 μmol m^{-2} s^{-1}) for 8 min. After 5 s, the actinic light was accompanied by a series of saturating pulses placed 30 s apart to estimate the maximum fluorescence yield during light adaptation (F'_M). The non-photochemical quenching of chlorophyll fluorescence was calculated as $(F_M - F'_M)/F'_M$ and the coefficient of photochemical quenching (q_P) as $(F'_M - F_t)/(F'_M - F'_0)$, where F_t is the fluorescence yield measured just prior to application of the saturating pulse and F'_0 is the minimal fluorescence for a light-adapted state calculated as $F_0/((F_V/F_M) + (F_0/F'_M))$ [42].

Gas exchange parameters

Gas exchange parameters were measured on the youngest fully developed, attached leaves using an open gas-exchange system (Li-6400, LI-COR Biosciences Inc., Lincoln, NE, USA). Six to eight plants of each transgenic line were measured for each treatment (control, stress, and re-watering). The measurement was started after 3 min of adaptation to chamber conditions (380 μmol CO_2 mol^{-1}, 70% relative humidity, 16°C). The rate of CO_2 assimilation (A, mmol (CO_2) m^{-2} s^{-1}), stomatal conductance (g_s, mol (H_2O) m^{-2} s^{-1}), and transpiration rate (mol (H_2O) m^{-2} s^{-1}) were measured every 30 s over 5 min. Intrinsic water-use efficiency (mmol (CO_2) mol^{-1} (H_2O)) was calculated as the ratio of averaged values of A and g_s.

Water potential

The water potential was estimated on four leaves of each treatment and for each line using a Model 600 pressure chamber instrument from PMS Instrument Company (Albany, OR, USA).

Statistical analysis

Two-sample t-tests and ANOVA (Tukey and Bonferroni tests) at significance level 0.05 were performed using OriginPro 8.5.1 (OriginLab Corporation, Northampton, MA, USA). Some of the t-tests were carried out with STATISTICA 12 (StatSoft CR, Czech Republic).

Results and discussion

Two genotypes of *AtCKX1*-overexpressing transgenic barley, which were not affected in their yield parameters, were selected for detailed transcriptomic analysis: one targeting expressed recombinant CKX protein to vacuoles (*vAtCKX1*) and the other with predicted cytosolic localization (*cAtCKX1*). The genotype expressing a secreted CKX to apoplast (*aAtCKX1*) was negatively affected in its yield parameters and was used only for the analysis of photosynthetic parameters. To study differences in transcriptomes, 28 single-read sequencing libraries were prepared and sequenced on an Illumina Hi-Seq 2500 system. The basic features of all sequenced libraries are summarized in Supplemental Table S2.

Photosynthetic parameters of transgenic plants under optimal conditions and drought stress

Heterologous expression of *AtCKX1* negatively affected chlorophyll content, which was estimated in the developmental stage during which the highest expression of the transgene was detected [30]. In comparison to WT leaves of plants cultivated hydroponically, 25%, 11%, and 6% decreases were measured in 4- to 5-week-old leaves of *vAtCKX1*, *aAtCKX1*, and *cAtCKX1* plants, respectively (Fig. 1a). All transgenic genotypes maintained chlorophyll content around WT levels when exposed to two periods of drought stress and re-watering, and this was in contrast to their reduced levels observed under optimal conditions (Fig. 1b).

To examine changes in the photosynthetic apparatus, the chlorophyll fluorescence induction and gas exchange of leaves were examined in the plants cultivated in soil. Drought stress, detected as bending of the leaves, was accompanied by decreases in g_s and, consequently, decreases in transpiration rate and CO_2 assimilation (Table 1). Lower accessibility of CO_2 due to closed stomata led to lower usage of light excitations for photochemical reactions (i.e., a decrease in photochemical quenching and an induced increase in the regulated thermal dissipation of absorbed light) and a rise in the non-photochemical quenching of chlorophyll fluorescence (Table 1). Increases in non-photochemical quenching of chlorophyll fluorescence of light-adapted leaves is a known consequence of drought stress [43,44]. Such a response reflects the usage of absorbed excitation energy to regulate heat dissipation and serves as a protective mechanism against damage to photosystem II. As a consequence, drought stress induces a decrease in photochemical quenching [45] and reflects fewer photosystem II reaction centers being open for photosynthetic electron transport. Interestingly, both of these changes caused by water deficiency were least marked in the *cAtCKX1* and *aAtCKX1* genotypes despite the fact that they had lower g_s (Table 1).

The most notable changes were observed after 24 hours of re-watering: when plants had once again been watered, all measured parameters had a tendency to return to their initial values and the return of photochemical activities in all three transgenic lines was more noticeable in comparison to those for the WT plants (Table 1).

Gas exchange parameters did not differ between genotypes prior to stress treatment. Drought stress did, however, induce a more significant decrease in g_s in the transgenic *cAtCKX1* and *aAtCKX1* genotypes compared to WT. The strong decrease in g_s protects plants from unendurable loss of water through transpiration; on the other hand, it results in lower accessibility of CO_2 for photosynthesis. It is noteworthy that although the *cAtCKX1* plants still had significantly reduced g_s after 24 hours of re-watering, their rate of CO_2 assimilation had by that time completely recovered to its initial value. Our results indicate that *cAtCKX1* barley was the most effective in using water for photosynthesis (Table 1). While the water potential of WT plants after 24 hours of re-watering remained almost unchanged in comparison to stressed plants, all transgenic genotypes had significant increases in this value (Table 1). Transgenic plants with altered root morphology and stronger lignification therefore have greater ability to redistribute the necessary amount of water to the aerial parts during recovery from drought stress.

Effect of cytokinin deficiency on the aerial part of vAtCKX1 *plants under optimal conditions*

The mild expression of *AtCKX1* under the control of β-glycosidase promoter had a positive effect on root system development

(a)

Chlorophyll content in mg m^{-2}

Plant age in days	*vAtCKX1*			WT			*cAtCKX1*			WT			*aAtCKX1*			WT		
7	460	±	98	436	±	57	483	±	70	485	±	64	450	±	34	485	±	64
9	475	±	62	454	±	77	N.D.	±	N.D.	518	±	57	532	±	37	518	±	57
11	415	±	58	425	±	58	N.D.	±	N.D.	496	±	55	496	±	51	496	±	55
14	481	±	27	492	±	28	643	±	59	597	±	66	492	±	47	555	±	43
16	560	±	24	551	±	26	529	±	66	553	±	36	476	±	74	535	±	33
18	627	±	39	618	±	38	529	±	66	553	±	36	462	±	21	459	±	38
21	687	±	29	651	±	61	N.D.	±	N.D.	N.D.	±	N.D.	597	±	49	592	±	45
23	682	±	39	680	±	50	567	±	28	576	±	31	505	±	26	534	±	45
25	544	±	58	581	±	44	666	±	68	664	±	38	603	±	42	589	±	39
28	461	±	83	555	±	48	689	±	50	712	±	54	608	±	34	628	±	34
30	451	±	47	599	±	62	675	±	41	716	±	35	547	±	37	582	±	44
35	389	±	55	528	±	61	783	±	32	791	±	33	476	±	62	532	±	43
39	502	±	63	577	±	71	773	±	65	721	±	37	550	±	52	591	±	68
42	536	±	68	552	±	74	736	±	59	691	±	61	575	±	59	581	±	71

(b)

Plant age in days	*vAtCKX1*			WT			*cAtCKX1*			WT			*aAtCKX1*			WT		
	2 hours long drought						2 hours long drought						2 hours long drought					
7	404	±	98	395	±	80	N.D.	±	N.D.	N.D.	±	N.D.	467	±	30	435	±	58
11	450	±	31	430	±	82	N.D.	±	N.D.	N.D.	±	N.D.	517	±	44	483	±	64
14	437	±	33	442	±	30	648	±	67	550	±	47	504	±	40	472	±	34
16	540	±	48	562	±	40	493	±	81	494	±	80	473	±	53	422	±	66
18	619	±	46	587	±	71	494	±	81	494	±	60	425	±	62	413	±	48
21	646	±	37	664	±	48	N.D.	±	N.D.	N.D.	±	N.D.	489	±	71	508	±	62
23	669	±	38	687	±	34	569	±	69	517	±	41	459	±	28	453	±	40
26	698	±	34	696	±	37	581	±	47	572	±	31	N.D.	±	N.D.	N.D.	±	N.D.
27	766	±	38	713	±	38	686	±	49	648	±	36	500	±	39	488	±	41
28	24 hours long drought						24 hours long drought						24 hours long drought					
29	Revitalization						Revitalization						Revitalization					
30	N.D.	±	N.D.	N.D.	±	N.D.	N.D.	±	N.D.	N.D.	±	N.D.	582	±	60	680	±	42
35	754	±	41	722	±	44	726	±	78	741	±	57	615	±	48	663	±	60
39	786	±	61	751	±	74	672	±	57	660	±	64	663	±	64	675	±	53
42	756	±	74	801	±	68	647	±	90	686	±	62	674	±	47	721	±	48

FIGURE 1

Chlorophyll content in mg m^{-2} for WT, *vAtCKX1*, *cAtCKX1*, and *aAtCKX1* barley leaves. Plants were cultivated hydroponically (a) under optimal conditions (highlighted results indicate significant decreases in transgenic plants at chlorophyll level), and (b) under conditions of mild stress applied to 7-day-old seedlings and subsequent severe stress applied to 4-week-old plants with subsequent re-watering.

whereas the aerial part was not substantially affected [30]. The height of *vAtCKX1* plants was slightly reduced (Fig. 2a,d), while *cAtCKX1* plants exhibited no visible changes in their aerial part during the first 4 weeks of development. Differential expression examination revealed that approximately 400 genes were significantly affected in the 6-week-old aerial part in contrast to more than 2400 genes affected in the roots of hydroponically cultivated *vAtCKX1* plants [30]. In order to understand those mechanisms only regulated by the altered hormonal status during leaf development, we performed an in-depth transcriptomic analysis of *vAtCKX1* plants of the same age but cultivated in the soil. In contrast to hydroponically cultivated plants, approximately four times more genes were found to be affected by altered CK content. Of the total 26,067 annotated genes, 988 and 609 genes were significantly down- or up-regulated, respectively (adjusted P-value ≤ 0.01; Supplemental Table S3). GO terms at level 6 of the most significantly affected genes from both sequencing experiments were compared and those 15 most affected and which overlap in the two environments are summarized in Table 2.

The four most negatively affected processes in leaves of *vAtCKX1* plants were linked to photosynthesis (Table 2). The fluorescence photosynthetic parameters, suggesting a decrease in energy transfer to the photosystem II core complexes (Table 1), together with lower chlorophyll content in non-stressed leaves (Fig. 1a), indicated that the photosynthetic apparatus and photosynthesis were slightly affected in transgenic plants. On the transcriptomic level, the effect was much more pronounced in those plants cultivated in the shallow soil (Table 2).

TABLE 1

Transgenic and wild type (WT) barley plants grown in shallow soil tested for ability to recover after 4 days of drought stress. Plants were stressed by drought in the 4th week of growth. Physiological parameters were determined directly prior to stress, on the 3rd day of the stress period, and 24 hours after the stress period. Quenching characteristics of chlorophyll fluorescence determined after drought stress and during revitalization were calculated as percentages of their values prior to stress

	WT	*vAtCKX1*	*cAtCKX1*	*aAtCK1*
Prior to stress				
CO_2 assimilation (mmol (CO_2) m^{-2} s^{-1})	2.00 ± 0.70	2.60 ± 0.70	1.60 ± 0.90	2.10 ± 0.70
Stomatal conductance (mol (H_2O) m^{-2} s^{-1})	0.06 ± 0.03	0.08 ± 0.02	0.05 ± 0.02	0.04 ± 0.01
Transpiration rate (mol (H_2O) m^{-2} s^{-1})	0.30 ± 0.13	0.38 ± 0.09	0.24 ± 0.10	0.20 ± 0.05
Non-photochemical quenching	0.72 ± 0.12	0.85 ± 0.10	0.99 ± 0.08*	0.87 ± 0.13
Photochemical quenching	0.41 ± 0.06	0.38 ± 0.04	0.32 ± 0.03*	0.36 ± 0.05
Drought stress				
CO_2 assimilation (mmol (CO_2) m^{-2} s^{-1})	1.30 ± 0.94	1.19 ± 1.13	−1.33 ± 0.77*	−1.77 ± 0.75*
Stomatal conductance (mol (H_2O) m^{-2} s^{-1})	0.036 ± 0.026	0.031 ± 0.019	0.005 ± 0.003*	0.005 ± 0.003*
Transpiration rate (mol (H_2O) m^{-2} s^{-1})	0.18 ± 0.13	0.16 ± 0.09	0.03 ± 0.02*	0.03 ± 0.01*
Non-photochemical quenching (%)	137 ± 23	171 ± 21	121 ± 16	102 ± 24
Photochemical quenching (%)	71 ± 12	57 ± 12	82 ± 15	76 ± 11
Water potential (MPa)	−1.11 ± 0.09	−1.25 ± 0.15	−1.69 ± 0.11*	−1.73 ± 0.04*
Re-watering				
CO_2 assimilation (mmol (CO_2) m^{-2} s^{-1})	2.21 ± 0.47	1.43 ± 0.53*	1.31 ± 0.87*	1.03 ± 0.99*
Stomatal conductance (mol (H_2O) m^{-2} s^{-1})	0.09 ± 0.03	0.07 ± 0.02	0.04 ± 0.01*	0.05 ± 0.02*
Transpiration rate (mol (H_2O) m^{-2} s^{-1})	0.43 ± 0.11	0.36 ± 0.08	0.19 ± 0.07*	0.23 ± 0.09*
Non-photochemical quenching (%)	126 ± 18	101 ± 20	95 ± 16*	93 ± 5*
Photochemical quenching (%)	86 ± 9	104 ± 12*	108 ± 11*	103 ± 6*
Water potential (MPa)	−1.04 ± 0.21	−0.59 ± 0.02*	−0.59 ± 0.04*	−0.46 ± 0.07*
Relative water content (%)	78.38 ± 7.64	94.97 ± 1.02*	97.82 ± 2.06*	91.84 ± 5.05*

* Significant difference between WT and transgenic tissue according to unpaired Student's *t*-test at $P \leq 0.05$.

Three of four putative genes coding for prephenate/arogenate dehydratase, an enzyme participating in the final steps of the aromatic amino acid pathway that produces tyrosine and phenylalanine [46], were up-regulated in the leaves of *vAtCKX1* plants. Phenylalanine is the primary substrate for the phenylpropanoid pathway that gives rise to lignin, flavonoids, and anthocyanins. Accordingly, the most up-regulated GO terms were GO:0009963 'Positive regulation of flavonoid biosynthetic process' and GO:0009718 'Anthocyanin-containing compound biosynthetic process.' Enforced production of phenylalanine thus might serve as a pool for the larger amount of flavonoids and anthocyanins in transgenic leaves, where these compounds participate in protection mechanisms against various stresses. However, four of eight genes encoding phenylalanine ammonia lyases, whose activity is considered a key switch between the phenylpropanoid pathway and primary aromatic amino acid metabolism [47], were significantly down-regulated. Nevertheless, all four genes, *MLOC_4684*, *MLOC_62322*, *MLOC_79728* and *MLOC_477*, were found to be up-regulated (by 3.6-, 3.0-, 2.7-, and 1.9-fold, respectively) in the roots of *vAtCKX1* plants [30]. Hence, and inasmuch as the aromatic amino acid metabolism was not affected in *vAtCKX1* transgenic roots, surplus phenylalanine might be translocated from leaves to roots, where it can supply enhanced lignin deposition.

The third most enriched process in *vAtCKX1* leaves was linked to the activity of lipoxygenases, which enzymes participate in the release of volatile compounds, including jasmonates (JAs), from intracellular lipids [48]. These compounds are usually released during plant defense against various pathogens. As the result is based on two independent experiments in which two biological replicates were sequenced and compared to the respective WT plants, it is not very likely that the observed lipoxygenase activation was merely a response to an undetected biotic stressor. In addition to plant defenses, JAs participate in several developmental processes such as trichome formation and leaf senescence [49]. Interestingly, JA-dependent formation of trichomes is accompanied by production of such secondary compounds as flavonoids, anthocyanins, and terpenoids [49,50]. Although there is not enough evidence to indicate cross-talk between JAs and CKs, it is predicted that their interaction might be antagonistic inasmuch as JAs strongly inhibit the CK-induced callus growth [51]. Nevertheless, the interplay of both phytohormone groups probably depends not only on the CK:JA ratio but also on other hormones [52]. In total, 12 of 55 and 8 of 39 genes categorized as GO:0009753 'Response to jasmonic acid' and GO:0010026 'Trichome differentiation,' respectively, were found to be significantly upregulated in the roots of two independent *vAtCKX1* lines [30]. Hence, predicted JA production in the upper part of transgenic plants might affect mainly roots and their fine architecture. Volatile methyl JA can be translocated as a rapid chemical signal from shoot to root and function there as a gene expression inducer [53]. Nevertheless, enforced JA production directly in roots is also feasible inasmuch as GO:0016165 'Linoleate 13S-lipoxygenase activity' is among enriched terms in transgenic roots during revitalization (see below).

Whole transcriptome response of vAtCKX1 *plants during revitalization after drought stress*

In addition to optimal conditions, three other kinds of sequencing libraries were generated from the upper part of *vAtCKX1* and WT plants cultivated in the shallow soil: the first from plants exposed

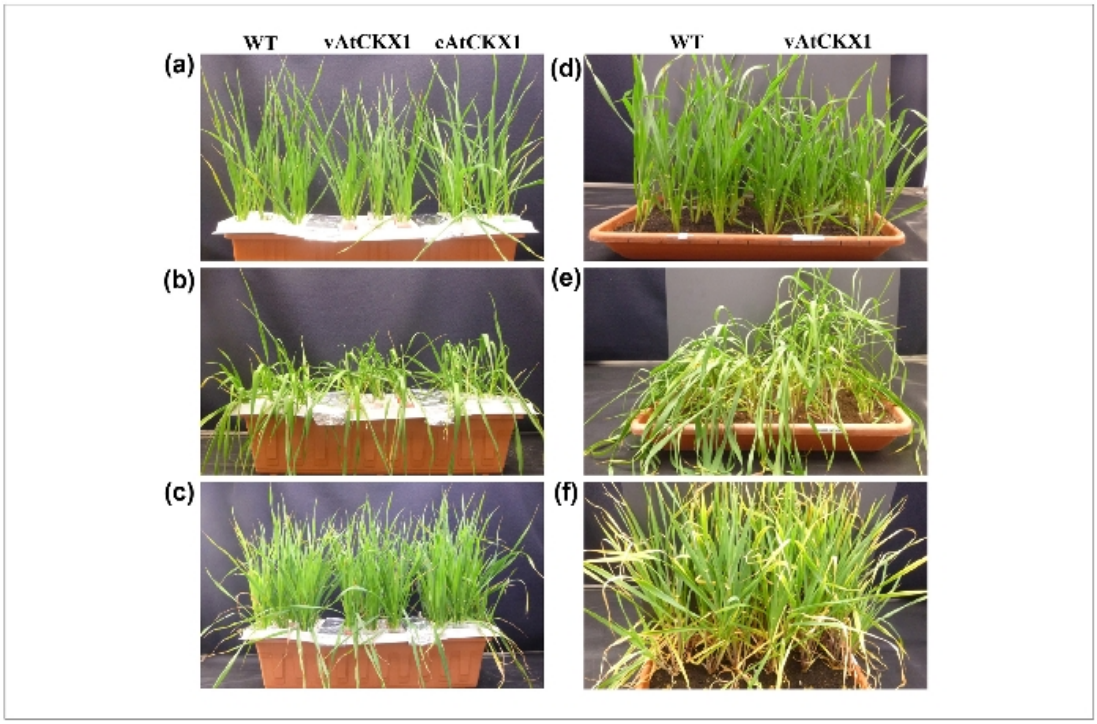

FIGURE 2

Photographs of transgenic and wild-type (WT) barley plants cultivated in hydroponic system (left) or shallow soil (right). (a,d) optimally watered 4-week-old plants, (b,e) plants suffering from severe drought stress, (c,f) regenerated plants 2 weeks after the application of drought stress.

to 4-day drought (Fig. 2e), the second from material 12 hours after re-watering, and the third from leaves having undergone 14-day revitalization (Fig. 2f). Unsurprisingly, only five genes were significantly altered (adjusted *P*-value ≤ 0.05) between stressed transgenic and WT leaves, thereby indicating that transcriptomes of both genotypes were strongly affected by the water deficit (Supplemental Table S3, see Supplemental Table S2 in Ref [37]). Twelve hours after re-watering, 10 and 9 genes were significantly up- and down-regulated, respectively, between *vAtCKX1* and WT leaves (Supplemental Table S3). Additionally, 5 of these 19 genes were not altered between the libraries made from optimally cultivated versus stressed leaves of either transgenic or WT leaves. Two putative *F-box-like proteins* (*MLOC_75620*, *MLOC_43997*), which have been shown to play an essential role in multiple phytohormone-signaling pathways [54], and one *receptor-like protein kinase* (*MLOC_17138*) were detected among them. The protein MLOC_17138 contains in addition to the kinase domain, a pfam01657 domain associated with a role in salt stress response and antifungal activity.

Transgenic plants overexpressing *AtCKX1* exhibit better growth parameters (e.g., biomass production and yield) when encountering drought stress [30]. To understand processes attributed to the beneficial growth of *vAtCKX1* plants, a comparative transcriptomic analysis was carried out examining transgenic versus WT leaves 2 weeks after revitalization from stress. Of the total 26,067 barley genes, 301 and 31 genes were significantly up- and down-regulated, respectively, in revitalized *vAtCKX1* leaves in contrast to WT (Supplemental Table S3). The enriched GO terms in up-regulated genes of *vAtCKX1* are summarized in Table 3A.

Products of many genes up-regulated by *vAtCKX1* participate as structural proteins or enzymes of the photosynthetic apparatus. Accordingly, the measured photosynthetic parameters of transgenic plants were better in the early stage of revitalization (Table 1), and chlorophyll content reached WT levels 2 weeks after re-watering (Fig. 1b), as compared to plants of the same age grown for their entire life span under optimal conditions. Interestingly, the most activated genes comprised those encoded by the barley chloroplast genome (indicated by the prefix EPIHVUG). In total, 14 of 112 translatable chloroplast genes were 2- to 3-fold up-regulated with high significance (adjusted *P*-value ≤ 0.05). Real-time PCR was performed on six selected genes to confirm the accuracy of the transcriptomic data (Supplemental Fig. S1). Chloroplasts are a known target of CK action. Indeed, exogenously applied CK is able directly to activate the expression of several chloroplast-encoded genes in detached barley leaves which accumulated also the stress hormone ABA [55]. Because it is not yet clear whether CK acts directly on chloroplast transcription, we can only speculate that the increase in chloroplast transcripts observed

TABLE 2

The most affected gene ontology (GO) terms in the upper part of *vAtCKX1* plants cultivated hydroponically or in soil compared to wild-type plants. Percentages are shown of differentially expressed genes (adjusted *P*-value ≤ 0.05) at GO level 6 and higher from total number of genes with the same GO number. MF, molecular function; BP, biological process. Genes affected in both culture conditions are in bold. Genes in several GO terms are not listed because the term parsed to several other child terms

GO number	Category	GO term	Total #	% of affected genes		Accession of affected genes in format *MLOC_XXXXX*
				Hydrop.	Soil	
Up-regulated						
GO:0004664	MF	Prephenate dehydratase activity	4	50.0	25.0	*23316, 65725, 56414*
GO:0008131	MF	Primary amine oxidase activity	6	16.7	50.0	***70980**, 4986, 17390*
GO:0016165	MF	Linoleate 13S-lipoxygenase activity	16	31.3	18.8	***64972**, 54031, **55029**, 71275, 51884, 69572*
GO:0005544	MF	Calcium-dependent phospholipid binding	10	20.0	20.0	*54932, 40592, 55134, 15770*
GO:0004834	MF	Tryptophan synthase activity	5	20.0	20.0	*59863, 61188*
GO:0009963	BP	Positive regulation of flavonoid biosynthetic process	9	11.1	22.2	*81070, 54366, 19988*
GO:0004034	MF	Aldose 1-epimerase activity	7	14.3	14.3	***5638***
GO:0005337	MF	Nucleoside transmembrane transporter activity	7	14.3	14.3	***55464***
GO:0009718	BP	Anthocyanin-containing compound biosynthetic process	11	18.2	9.1	*61512, 65788, 64248*
GO:0009407	BP	Toxin catabolic process	27	7.4	18.5	***17760**, 73593, **68101**, 57709, 72489*
GO:0047262	MF	Polygalacturonate 4-α-galacturonosyltransferase activity	8	12.5	12.5	*11661, 57229*
GO:0031418	MF	L-Ascorbic acid binding	13	15.4	7.7	***77814**, 64248*
GO:0004806	MF	Triglyceride lipase activity	41	9.8	12.2	***17298**, **18031**, **80878**, **80586**, 58940*
GO:0006569	BP	Tryptophan catabolic process	14	14.3	7.1	*12847, 57323, 69262*
GO:0015996	BP	Chlorophyll catabolic process	33	3.3	15.2	*80455, 34851, 55009, 21175, **64277***
Down-regulated						
GO:0008937	MF	Ferredoxin-NAD(P) reductase activity	4	25.0	50.0	*7761, 53537, 40355*
GO:0010027	BP	Thylakoid membrane organization	106	2.8	61.3	***58382***; not listed
GO:0051667	BP	Establishment of plastid localization	63	4.8	55.6	Not listed
GO:0045548	MF	Phenylalanine ammonia lyase activity	7	28.6	28.6	*79728, 62322, 477, 4684*
GO:0009658	BP	Chloroplast organization	137	2.2	54.0	Not listed
GO:0019682	BP	Glyceraldehyde-3-phosphate metabolic process	202	1.5	51.5	Not listed
GO:0006720	BP	Isoprenoid metabolic process	237	1.3	46.0	Not listed
GO:0010310	BP	Regulation of hydrogen peroxide metabolic process	15	6.7	26.7	*33774, 1518, 15501, 65632, 1340*
GO:0030855	BP	Epithelial cell differentiation	7	14.3	14.3	*38181, 54366*
GO:0016054	BP	Organic acid catabolic process	153	3.9	14.4	Not listed
GO:0008544	BP	Epidermis development	9	11.1	11.1	*38181, 54366*
GO:0009699	BP	Phenylpropanoid biosynthetic process	22	9.1	9.1	*4684, 477, 57736, 79728*
GO:0070726	BP	Cell wall assembly	11	9.1	9.1	*52864, 67760*
GO:0032870	BP	Cellular response to hormone stimulus	205	8.8	5.7	Not listed
GO:0007166	BP	Cell surface receptor signaling pathway	30	3.3	10.0	*63541, 17680, 44275, 72162*

in revitalized *vAtCKX1* transgenic plants relays an accumulation of CK in leaves upon water stress. Our hypothesis is supported by the strong activation of endogenous *IPT* genes in *vAtCKX1* leaves at several developmental time points as a consequence of CK depletion [30]. Hence, increased local maxima of CKs, produced by IPT activity localized in chloroplasts, might trigger similar machinery as was described in CK-treated detached leaves to activate the chloroplast genome. The analysis of endogenous CK content in chloroplasts under these conditions would provide support for our hypothesis. It is noteworthy that none of the chloroplast-encoded genes were down-regulated in *vAtCKX1* plants cultivated under optimal conditions when as many nucleus-encoded genes participating in photosynthesis were down-regulated compared to those in WT plants (Table 2). Nevertheless, eight chloroplast-encoded genes were significantly up-regulated (Supplemental Fig. S1), indicating that the phenomenon is linked rather to CK imbalance than to activation by drought.

Among other interesting genes significantly up-regulated in revitalized *vAtCKX1* leaves were these coding for four putative aquaporins (*MLOC_56278*, *MLOC_71237*, *MLOC_552*, *MLOC_22808*), which are channel proteins facilitating the transport of water through plasma and intracellular membranes. The increased expression of several genes encoding barley aquaporins had already been observed in plants exposed to salinity stress [56]. Those authors had hypothesized that an increase in water channel activity would facilitate maintenance or recovery of growth during or after the stress period.

Two genes classified under the GO term 'phenylpropanoid catabolic process' encode putative laccases – aromatic compound:oxygen oxidoreductase (Table 3A), which might participate in lignin degradation or its polymerization. Nevertheless, in contrast to root tissue, significantly altered lignin content in the upper part of *vAtCKX1* plants was not determined in comparison to that in WT plants (Fig. 4a).

TABLE 3A

The most enriched GO terms in up-regulated genes (adjusted *P*-value ≤ 0.05) in the aerial part of *vAtCKX1* plants collected 2-weeks after re-watering. Percentages are shown of differentially expressed genes at GO level 6 and higher from total number of genes with the same GO number. MF, molecular function; BP, biological process; CC, cellular component.

GO number	Category	GO term	Total #	% of affected genes	Accession of affected genes in format *MLOC_XXXXX* or *EPlHVUG000000XXXX*
GO:0016984	MF	Ribulose-bisphosphate carboxylase activity	5	40.0	*EPlHVUG00000010074, MLOC_21811*
GO:0009765	BP	Photosynthesis, light harvesting	32	34.4	Not listed
GO:0030076	CC	Light-harvesting complex	8	25.0	*EPlHVUG00000010021, MLOC_57061*
GO:0009718	BP	Anthocyanin-containing compound biosynthetic process	10	20.0	*MLOC_5324, 19814*
GO:0016165	MF	Linoleate 13S-lipoxygenase activity	16	18.8	*MLOC_37378, 51884, 71948*
GO:0045259	CC	Proton-transporting ATP synthase complex	27	14.8	*EPlHVUG00000010007, 10016, 10047, MLOC_26730*
GO:0009767	BP	Photosynthetic electron transport chain	56	14.3	*EPlHVUG00000010010, 10072, 10065, 10026, 10021, MLOC_52515, 22512, 39436*
GO:0046271	BP	Phenylpropanoid catabolic process	20	10.0	*MLOC_15203, 61189*
GO:0052716	MF	Hydroquinone:oxygen oxidoreductase activity	20	10.0	*MLOC_15203, 61189*
GO:0009579	CC	Thylakoid	331	9.9	Not listed
GO:0016597	MF	Amino acid binding	31	9.7	*MLOC_62844, 19879, 80634*
GO:0004499	MF	*N,N*-Dimethylaniline monooxygenase activity	22	9.1	*MLOC_11897, 11896*
GO:0009637	BP	Response to blue light	48	8.3	*MLOC_43394, 22512, 11312, 52515*
GO:0055082	BP	Cellular chemical homeostasis	47	6.4	*MLOC_22808, 65878, 69460*
GO:0034754	BP	Cellular hormone metabolic process	38	5.3	*MLOC_6666, 73942*

Furthermore, genes significantly affected between non-stressed and revitalized leaves were evaluated separately for *vAtCKX1* and WT plants. Those from the transgenic plants that did not overlap with WT plants were further compared with genes differentially regulated between the two genotypes (i.e., the 301 up- and 31 down-regulated genes). Only seven up-regulated genes remained as being not developmentally dependent but genotype dependent. None of the down-regulated genes meet both criteria (Table 3B). Two genes coding for putative enzymes of the flavonoid biosynthesis pathway – chalcone isomerase and isoflavone 2′-hydroxylase – were found to be up-regulated in *vAtCKX1* plants. These two genes combine with two other genes found to be up-regulated in revitalized *vAtCKX1* leaves and participating in the regulation of flavonoid metabolism (*chalcone isomerase*: *MLOC_5324*; *zinc-finger (B-box) protein*: *MLOC_19814*), indicating an enforced production of isoflavonoids and anthocyanins. Recently, an unambiguous positive effect of flavonoid and anthocyanin production in improving tolerance to drought stress has been shown [57]. Due to their antioxidative activity, the over-accumulation of flavonoids mitigates the negative effect of reactive oxygen species released under stress conditions. Peroxiredoxin (MLOC_74367) belongs to a family of cysteine-dependent peroxidases which also participate in detoxification of plant cells by scavenging reactive oxygen species [58]. An orthologue of peroxiredoxin has been found among another 25 over-accumulated proteins in wheat seedlings of a cultivar that is drought-stress tolerant in comparison to a

TABLE 3B

Significantly up-regulated genes in *vAtCKX1* leaves 2 weeks after re-watering (adjusted *P*-value ≤ 0.05) which are not developmentally dependent and also significantly up-regulated between revitalized and non-stressed leaves of *vAtCKX1* genotype but not in wild-type plants (adjusted *P*-value ≤ 0.001); R2W, 2-week revitalization; NS, non-stressed

Gene number	Gene annotation	Mean expression (R2W)	Fold change	
			***vAtCKX1* (R2W) versus WT (R2W)**	***vAtCKX1* (R2W) versus *vAtCKX1* (NS)**
MLOC_8529	Nematode-resistance protein	1471	4.28	2.21
MLOC_14310	GDSL esterase/lipase	1163	2.51	2.62
MLOC_74636	tolB protein (WD40-like Beta Propeller)	185	2.38	3.60
MLOC_30661	Putative isoflavone 2′-hydroxylase	78	2.31	6.66
MLOC_70609	unknown protein located in chloroplast stroma	104	2.30	4.30
MLOC_74367	Peroxiredoxin (Thioredoxin-like fold)	2443	2.23	2.66
MLOC_80571	Chalcone isomerase	598	2.19	2.86

drought-sensitive one [59]. MLOC_14310 belongs to a large family of GDSL-type esterase/lipases with hydrolytic activity toward triacylglycerols. Members of this family are involved in plant development, morphogenesis, secondary metabolite synthesis, and defense responses, and some members are activated by JAs. The closest rice orthologue of MLOC_14310 (LOC_Os01g46080) was found to be activated by desiccation stress in rice leaves [60]. Moreover, pepper GDSL lipase caused higher susceptibility to pathogens but increased tolerance to osmotic stress when overexpressed in Arabidopsis [61].

Taken together, the differential expression study in *vAtCKX1* and WT leaves before and after the stress period reveal several genes whose increased expression initiated by the CK imbalance may lead to better drought tolerance and/or faster growth after rewatering.

Response of vAtCKX1 *and* cAtCKX1 *roots during stress and revitalization*

Due to the impossibility of collecting root tissues from soil without causing mechanical stress, transcriptome of the root system was studied from plants grown hydroponically. Twelve sequencing libraries were generated from *vAtCKX1*, *cAtCKX1*, and WT roots collected at two time points: during the severe drought stress (Fig. 2b) and 2 weeks after revitalization (Fig. 2c). Similarly as in the aerial part, stress induced a strong response at the transcriptome level (see Supplemental Table S1 in Ref [37]). Between transgenic plants and WT plants, only a few genes were deregulated during the stress (Supplemental Table S4). Just seven genes were significantly up-regulated in both *vAtCKX1* and *cAtCKX1* genotypes, including, for example, putative *nicotianamine synthase* (*MLOC_71596*) and *4-coumarate CoA ligase* (*MLOC_18901*) involved in lignification. Fifty-seven genes were significantly down-regulated. The most strongly down-regulated gene in both lines was a putative *F-box-like protein* (*MLOC_75620*; 12.6- and 5.3-fold), which was found also among the most strongly down-regulated genes in the early and late phases of leaf revitalization. The unambiguous and strong depletion of *MLOC_75620* transcripts in all transgenic samples indicates that this F-box protein might play a crucial role in regulating responses in CKX-overexpressing plants via cross-talk with other hormones. F-box proteins represent one of the largest superfamilies in plants, that is, involved in the process of ubiquitination and protein degradation. To date, only a limited number of F-box proteins have been functionally characterized. Most of them are involved in regulating hormone signaling pathways, where they degrade repressors or activators of auxin, GA, ethylene, and JA response [54].

Analysis of differentially expressed genes in revitalized 6-week-old roots (Supplemental Table S4) revealed that the gene encoding one of the cytokinin receptors (*HvHK3*; *MLOC_44452*) was significantly down-regulated in both transgenic genotypes (Fig. 3a,c). The gene was also down-regulated in 6-week-old *vAtCKX1* and *cAtCKX1* roots cultivated under optimal conditions (see Figure 3B in Ref [30]), thus leading to the conclusion that cessation of CK perception via HvHK3 is a developmental consequence rather than a response to stress. The addition of one *CKX* gene to the barley genome led to a hormonal imbalance which plants tend to buffer by regulation of endogenous CKX and IPTs, which are CK biosynthetic enzymes, in a very sensitive way [30]. Plant *IPT* genes are generally very weakly expressed, and the enzyme's activity is regulated by farnesylation [62]. Significant up-regulation of two abundant endogenous CKX enzymes – HvCKX4 and HvCKX5 – was observed in both independent experiments with 6-week-old *AtCKX1*-overexpressing plants, while other HvCKXs were down-regulated or unchanged in comparison to WT plants. Although it is difficult to estimate the final CK homeostasis, one might expect a local minimum in CK content that leads to cessation in *HvHK3* transcription and CK perception through this receptor.

CK receptors belong to a small group of histidine kinases. The Arabidopsis genome encompasses three real CK receptors binding CKs (AHK2, AHK3, and AHK4/CRE1) and three others implicated in CK transduction cascade and osmosensing without the ability directly to bind CKs (AHK1, CKI1, and CKI2) [4]. In contrast to other genes participating in CK signal transduction, phosphotransfer proteins, and response regulators (RR, Fig. 3d), CK receptors show lineage-specific expansion between dicot and monocot species that implies their specific and evolutionarily old function among all green plants [63]. Thus, in the barley genome, HvHK3 is an orthologue of AHK3, while the orthologue of AHK2 is missing and AHK4 has otherwise two duplicated orthologues (Fig. 3a). A similar representation of CK receptors was found in rice [63].

Interestingly, Arabidopsis knock-outs of AHK3 and AHK2 or double knock-out manifest strong drought-tolerance phenotype [4]. This is the first direct evidence demonstrating that CKs might be a negative regulator of the stress signaling pathway. Tran et al. explained the phenomenon by the up-regulation of many stress and ABA responsive genes in *ahk2/ahk3* double knock-out already under non-stress conditions. To check if the response of *AtCKX1*-overexpressing barley was similar, we blasted the barley orthologous genes closest to these significantly up-regulated genes in the Arabidopsis double knock-out (Supplemental Table S5). In total, 23 and 25 orthologues of the 40 genes presented in Tran et al. were also significantly up-regulated in *vAtCKX1* and *cAtCKX1* transgenic barley, respectively. Among them, we found several regulatory genes implicated in responses to stress, such as *MLOC_37104* (an orthologue of *ANAC055*), *NAC* (no apical meristem) transcription factor [64], and *MLOC_71611* (an orthologue of *AtMYC2*). Overexpression of both transcription factors in Arabidopsis led to drought-tolerance and increased sensitivity to ABA [65]. Both genes have been shown to be activated by JAs [66], the overproduction of which is expected in the upper part of *AtCKX1* transgenic plants. While it is interesting that both genes have relatively strong expression in barley and are more abundant in roots than in leaves, their action has been studied mainly in Arabidopsis leaves [64,65]. Hence, drought tolerance mediated via these two transcription factors might be universal for the entire plant body. Recently, rice plants overexpressing *OsNAC9*, the closest orthologue of *MLOC_37104*, under the control of a root-specific promoter have been shown to be more drought tolerant during vegetative development due to their enlarged root diameter and aerenchyma formation [67].

Altered homeostasis of CKs in *AtCKX1*-overexpressing barley, which influences root system architecture, might anticipate changes in auxin levels, transport, and perception. There exist several groups of auxin response genes in plant genomes that react sensitively to auxin imbalance. Auxin early response genes are divided into two categories – the Aux/IAA and SAUR (small auxin

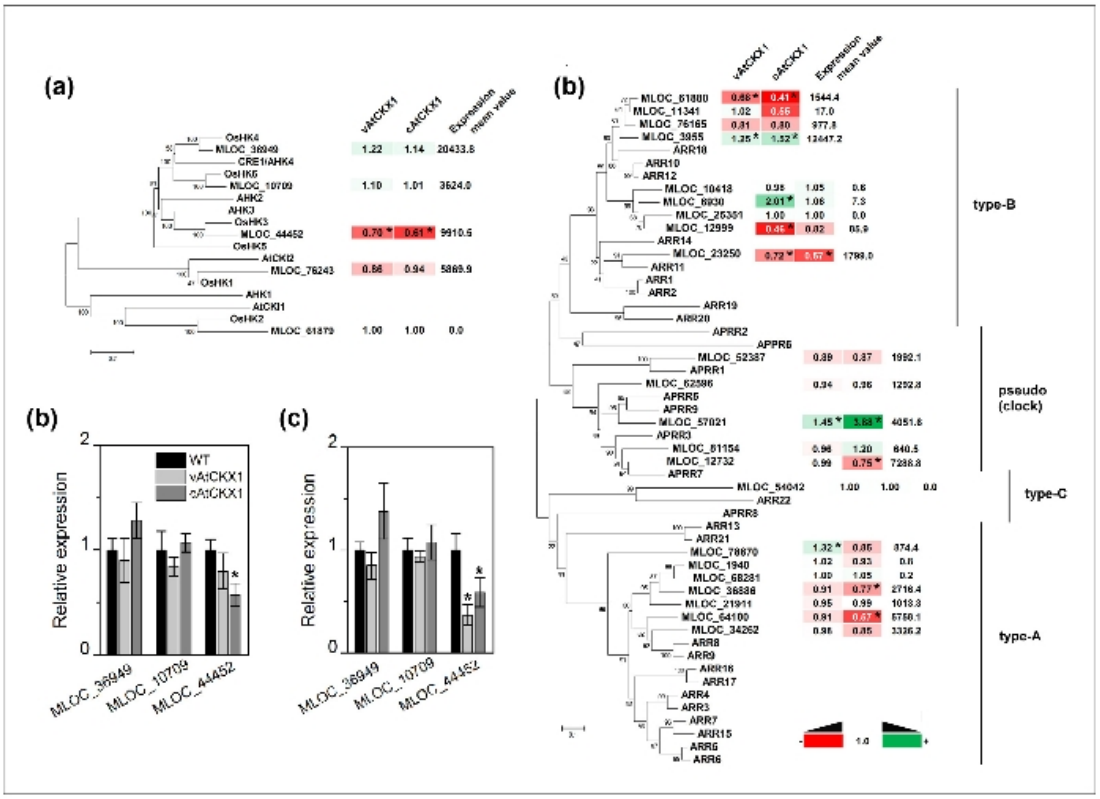

FIGURE 3

Cytokinin perception in *vAtCKX1* and *cAtCKX1* plants. (a) Phylogenetic relationship of barley, rice, and Arabidopsis histidine kinases implicated in CK perception. Expression relative to wild-type (WT) of all homologues found in the annotated barley genome are depicted in up- and down-regulation color code together with their mean expression values. Real-time PCR analysis of three CK receptors in roots cultivated (b) under optimal conditions or (c) 2 weeks after re-watering following the drought stress. (d) Phylogenetic relationship of all CK response regulators found in the barley genome and their Arabidopsis counterparts. Expression relative to WT plants is shown in the color code. Unrooted trees were generated using ClustalW by neighbor-joining method. *Significant difference between WT and transgenic tissue according to unpaired Student's *t*-test at $P \leq 0.05$.

up RNA) – and all regulate plant physiology by modulating the interaction with auxin response elements of other transcription factors, such as a major group of auxin response factors (ARFs). Auxin action is influenced by its polar transport that is mediated by auxin efflux carriers (PINs). Its homeostasis is also regulated by *GH3* (*Gretchen Hagen3*) genes encoding mainly auxin–amino acid synthetases that form from surplus auxin its inactive conjugates [68]. AtCKX1/WT comparative data indicated that transgenic roots contain elevated levels of auxin, inasmuch as 3 of 12 predicted and expressed PIN transporters and 3 of 7 *GH3* genes were significantly up-regulated in *cAtCKX1* roots (Supplemental Table S6). Analysis of *vAtCKX1* roots showed a similar but slightly weaker tendency.

Many of the 48 significantly down-regulated genes in Arabidopsis *ahk2/ahk3* double knock-out with higher stress tolerance are auxin early responsive genes (*SAUR* and *IAA/AUX*). The dwarf phenotype of *ahk2/ahk3* plants was attributed to the observed down-regulation of auxin response [4]. Because *vAtCKX1* and *cAtCKX1* plants were not substantially affected in their aerial part but had positively altered root system morphology, a different way of auxin response might be expected. In contrast to *ARF* and *GH3* genes, several *SAUR* and *IAA/AUX* genes exhibited lower expression in transgenic plants than in WT plants. Nevertheless, no straightforward comparison can be made between the auxin response of Arabidopsis *ahk2/ahk3* mutant and *AtCKX1*-overexpressing barley (Supplemental Tables S5 and S6). Particularly noteworthy was that two type-A *AtRR* genes were found among the down-regulated genes of the *ahk2/ahk3* mutant [4]. Two of seven *HvRR* genes were significantly down-regulated in *cAtCKX1* transgenic barley, thus implicating reduced CK sensing due to decreased CK content and/or silenced HvHK3 receptor (Fig. 3d). Taken together, the comparison of our transcriptomic data with the previous work of Tran et al. [4] suggests that the general mechanism of drought-stress tolerance relates in part to CK insensitivity, which can be acquired by receptor knock-out or CKX overexpression in all species across the plant kingdom.

Up-regulation of genes in the phenylpropanoid biosynthesis pathway leads to higher lignification of AtCKX1 *transgenic roots exposed to drought stress*

Our pilot whole-transcriptome characterization of *vAtCKX1* transgenic roots revealed strong up-regulation of many genes encoding proteins involved in the phenylpropanoid biosynthesis pathway [30]. Lignin content was quantified by the acetyl bromide method in protein-free cell wall samples prepared separately from whole root and leaf mass of hydroponically cultivated plants. Both transgenic genotypes showed systematic increase in total lignin content in roots from the 2nd week after germination (data not shown). Approximately up to 20% higher lignin content was determined in roots of transgenic compared to WT plants cultivated under optimal conditions 6 weeks after germination, while lignin content in leaves was not significantly altered (Fig. 4a).

Analysis of lignin precursors in 4-week-old transgenic plants showed that *cAtCKX1* accumulated significantly greater amounts of cinnamates and monolignols than did WT tissue (Fig. 4b). Four-week-old roots of *vAtCKX1* genotype contained a larger amount of sinapyl alcohol, similarly as 2 weeks later, when grown under optimal conditions. The exposure to drought stress and the following revitalization resulted in more pronounced accumulation

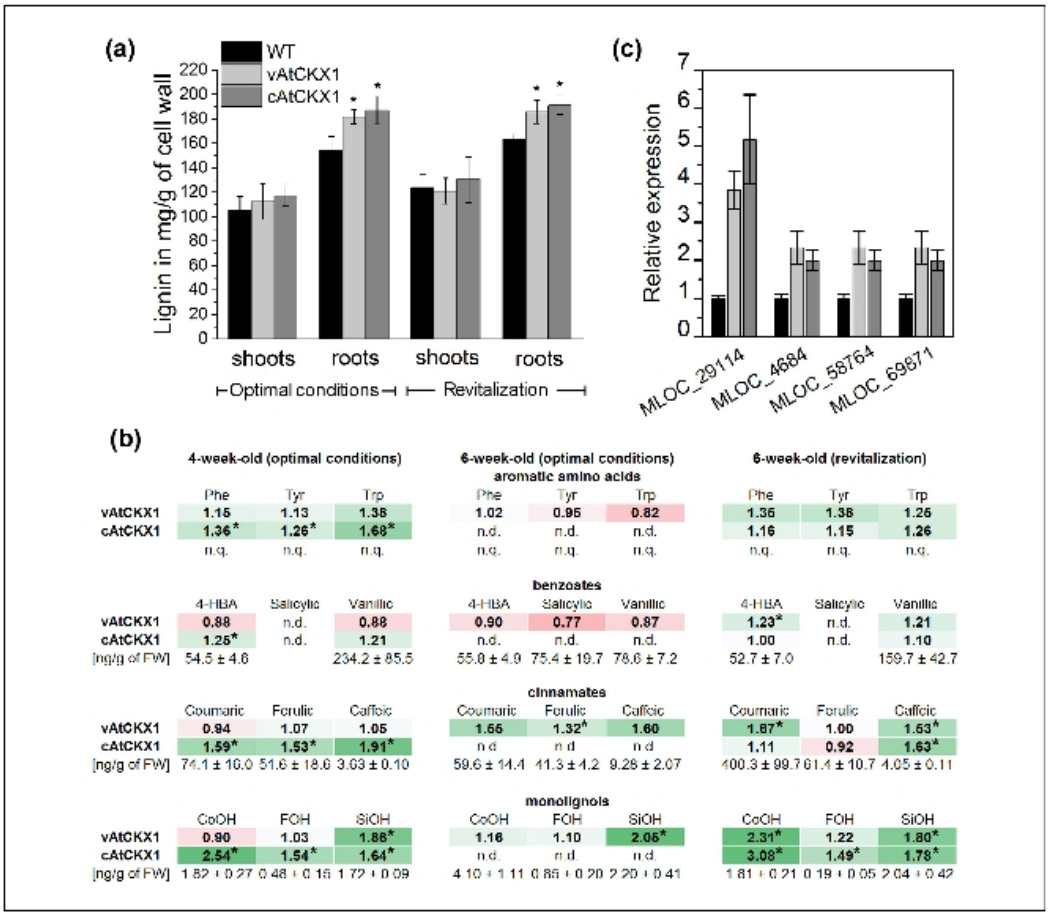

(b)

4-week-old (optimal conditions)	Phe	Tyr	Trp
vAtCKX1	1.15	1.13	1.38
cAtCKX1	1.36*	1.26*	1.68*
	n.q.	n.q.	n.q.

6-week-old (optimal conditions) aromatic amino acids	Phe	Tyr	Trp
	1.02	0.95	0.82
	n.d.	n.d.	n.d.
	n.q.	n.q.	n.q.

6-week-old (revitalization)	Phe	Tyr	Trp
	1.35	1.38	1.25
	1.16	1.15	1.26
	n.q.	n.q.	n.q.

benzoates	4-HBA	Salicylic	Vanillic
vAtCKX1	0.88	n.d.	0.88
cAtCKX1	1.25*	n.d.	1.21
[ng/g of FW]	54.5 ± 4.6		234.2 ± 85.5

benzoates	4-HBA	Salicylic	Vanillic
	0.90	0.77	0.87
	n.d.	n.d.	n.d.
	55.8 ± 4.9	75.4 ± 19.7	78.6 ± 7.2

benzoates	4-HBA	Salicylic	Vanillic
	1.23*	n.d.	1.21
	1.00	n.d.	1.10
	52.7 ± 7.0		159.7 ± 42.7

cinnamates	Coumaric	Ferulic	Caffeic
vAtCKX1	0.94	1.07	1.05
cAtCKX1	1.59*	1.53*	1.91*
[ng/g of FW]	74.1 ± 16.0	51.6 ± 18.6	3.63 ± 0.10

cinnamates	Coumaric	Ferulic	Caffeic
	1.55	1.32*	1.60
	n.d.	n.d.	n.d.
	59.6 ± 14.4	41.3 ± 4.2	9.28 ± 2.07

cinnamates	Coumaric	Ferulic	Caffeic
	1.87*	1.00	1.63*
	1.11	0.92	1.63*
	100.3 ± 99.7	61.4 ± 10.7	4.05 ± 0.11

monolignols	CoOH	FOH	SiOH
vAtCKX1	0.90	1.03	1.88*
cAtCKX1	2.54*	1.54*	1.64*
[ng/g of FW]	1.82 ± 0.27	0.48 ± 0.15	1.72 ± 0.09

monolignols	CoOH	FOH	SiOH
	1.16	1.10	2.06*
	n.d.	n.d.	n.d.
	4.10 ± 1.11	0.85 ± 0.20	2.20 ± 0.41

monolignols	CoOH	FOH	SiOH
	2.31*	1.22	1.80*
	3.08*	1.49*	1.78*
	1.81 ± 0.21	0.19 ± 0.05	2.04 ± 0.42

FIGURE 4

Lignin content and intermediates of the phenylpropanoid pathway in *vAtCKX1* and *cAtCKX1* transgenic barley. (a) Total lignin content of hydroponically cultivated plants under optimal conditions (6th week) and during 2-week revitalization (6th week); each value represents the mean of four biological replicates. (b) Quantification of aromatic amino acids, phenylpropanoid intermediates, and benzoic acids in roots of hydroponically cultivated plants (each in three biological replicates) collected during 4th and 6th weeks of growth under optimal conditions and 2nd week of revitalization after drought stress; n.q., not quantified due to lack of internal standard; n.d., not determined; Phe, phenylalanine; Tyr, tyrosine; Trp, tryptophan; 4-HBA, 4-hydroxybenzoic acid; CoOH, coumaryl alcohol; FOH, coniferyl alcohol; SiOH, sinapyl alcohol; *significant difference between WT and transgenic tissue according to unpaired Student's *t*-test at $P \leq 0.05$. (c) Real-time PCR analysis of four selected genes encoding enzymes involved in the phenylpropanoid pathway in transgenic barley roots 2 weeks after re-watering following the drought stress; *MLOC_29114, cinnamoyl-CoA reductase; MLOC_4684, phenylalanine ammonia lyase; MLOC_58764, 4-coumarate:CoA ligase; MLOC_69871, cinnamate 4-hydroxylase*.

of all quantified intermediates of the phenylpropanoid pathway (Fig. 4b) as well as in higher lignin content of the root cell wall fraction in both transgenic genotypes compared to WT plants. However, lignification in transgenic roots having passed through severe stress was not greater than in the transgenic roots cultivated under optimal conditions (Fig. 4a). Measurement confirmed that decreased CK sensitivity has a positive impact on root lignification but that the effect is not augmented by exposure to stress, even though more precursors are formed. Thus, the inability to produce more lignin after revitalization from stress may consist in limiting of specific peroxidases participating in monolignol polymerization. The most enriched GO terms in revitalized roots of both transgenic genotypes nicely corresponded to the observed increased amount of phenylpropanoid pathway intermediates and

TABLE 4

The most affected gene ontology (GO) terms in the roots of *vAtCKX1* and *cAtCKX1* plants cultivated hydroponically 2 weeks after re-watering compared to wild-type plants. Percentages are shown of differentially expressed genes (adjusted *P*-value ≤ 0.05) at GO level 6 and higher from total number of genes with the same GO number. MF, molecular function; BP, biological process. Genes affected in both genotypes are in bold. Genes in several GO terms are not listed because the term parsed to several other child terms

GO number	Category	GO term	Total #	% of affected genes		Accession of affected genes in format *MLOC_XXXXX*
				vAtCKX1	*cAtCKX1*	
Up-regulated						
GO:0008792	MF	Arginine decarboxylase activity	2	100.0	100.0	***58866***, ***39205***
GO:0047987	MF	Hydroperoxide dehydratase activity	2	100.0	100.0	***8106***, ***21933***
GO:0004664	MF	Prephenate dehydratase activity	4	75.0	100.0	*23316*, ***65725***, ***56414***, ***60716***
GO:0009916	MF	Alternative oxidase activity	4	75.0	50.0	***34173***, *82029*, ***53632***
GO:0045548	MF	Phenylalanine ammonia lyase activity	7	71.4	71.4	***79728***, ***62322***, ***4684***, ***19798***, ***67067***
GO:0003979	MF	UDP-glucose 6-dehydrogenase activity	3	66.7	100.0	***5287***, ***70967***, *63077*
GO:0005345	MF	Purine nucleobase transmembrane transporter activity	3	66.7	66.7	***66246***, ***32910***
GO:0004470	MF	Malic enzyme activity	6	50.0	83.3	***11548***, ***75667***, ***35785***, *64502*, *51144*
GO:0009805	BP	Coumarin biosynthetic process	9	55.6	55.6	*66898*, *20110*, *17364*, *19988*, *52497*
GO:0009699	BP	Phenylpropanoid biosynthetic process	26	53.9	46.2	Not listed
GO:0016165	MF	Linoleate 13S-lipoxygenase activity	16	50.0	56.3	Not listed
GO:0052542	BP	Defense response by callose deposition	10	50.0	50.0	***57937***, ***51297***, ***42826***, ***17648***, ***59580***
GO:0006986	BP	Response to unfolded protein	25	40.0	40.0	Not listed
GO:0035967	BP	Cellular response to topologically incorrect protein	25	40.0	40.0	Not listed
GO:0042538	BP	Hyperosmotic salinity response	10	40.0	40.0	***69262***, ***52084***, ***42826***, ***2170***
GO:0004348	MF	Glucosylceramidase activity	5	40.0	40.0	***398***, *53162*, *13522*
GO:0010942	BP	Positive regulation of cell death	5	40.0	40.0	***12681***, ***75133***
GO:0003885	MF	D-Arabinono-1,4-lactone oxidase activity	9	33.3	44.4	***31769***, ***34835***, ***68610***, *59091*
GO:0003978	MF	UDP-glucose 4-epimerase activity	6	33.3	33.3	***70713***, ***10406***
GO:0015020	MF	Glucuronosyltransferase activity	12	25.0	41.7	***4722***, *54026*, *65730*, ***8254***, ***56928***
Down-regulated						
GO:0004650	MF	Polygalacturonase activity	32	21.9	12.5	*6444*, *4738*, *68357*, *67885*, ***51158***, ***53562***, *75889*, *13213*, *72199*
GO:0001666	BP	Response to hypoxia	13	7.7	23.1	***36714***, *1340*, *65221*
GO:0042886	BP	Amide transport	28	3.6	25.0	*22335*, *59508*, *20029*, *71333*, *10510*, ***56891***, *58935*
GO:0009735	BP	Response to cytokinin	13	7.7	15.4	***23250***, *58762*
GO:0008375	MF	Acetylglucosaminyltransferase activity	36	2.8	19.4	*38958*, ***37085***, *65593*, *74430*, *5087*, *63430*, *60533*
GO:0016307	MF	Phosphatidylinositol phosphate kinase activity	18	5.6	16.7	***81640***, *62872*, *5875*
GO:0008509	MF	Anion transmembrane transporter activity	104	4.8	16.4	Not listed
GO:0042594	BP	Response to starvation	44	6.8	13.6	***56127***, ***7416***, ***44452***, *16652*, *4685*, *57969*
GO:0005667	CC	Transcription factor complex	30	3.3	16.7	***76757***, *67781*, *7755*, *36554*, *62730*
GO:0045786	BP	Negative regulation of cell cycle	25	8.0	12.0	***57670***, ***65158***, *62665*
GO:0031669	BP	Cellular response to nutrient levels	45	6.7	13.3	***56127***, ***7416***, ***44452***, *16652*, *4685*, *57969*
GO:0042559	BP	Pteridine-containing compound biosynthetic process	15	6.7	13.3	***74131***, *10075*
GO:0008643	BP	Carbohydrate transport	41	4.9	14.6	*65088*, *13612*, *17903*, *280*, *63767*, *67524*, *10342*, *59161*
GO:0019901	MF	Protein kinase binding	36	5.6	13.9	*46471*, ***57670***, *66940*, *51179*
GO:0010565	BP	Regulation of cellular ketone metabolic process	16	6.3	12.5	***36714***, *14398*
GO:0004672	MF	Protein kinase activity	1099	4.3	14.5	Not listed
GO:0000272	BP	Polysaccharide catabolic process	43	7.0	11.6	*40915*, *54306*, *59047*, *49756*, *4022*
GO:0009751	BP	Response to salicylic acid	54	5.6	13.0	*21464*, *1340*, ***36714***, *14398*, ***43518***, *71936*, *10787*
GO:0003950	MF	NAD+ ADP-ribosyltransferase activity	11	9.1	9.1	*66554*, *72444*
GO:0009723	BP	Response to ethylene	35	8.6	8.6	*44452*, *53881*, *64636*

stronger lignification. Indeed, about half of the genes assigned as participating in the phenylpropanoid pathway were significantly up-regulated, as were 5 of 7 genes encoding phenylalanine ammonia lyases and all four genes encoding prephenate dehydratase. The up-regulation of the four selected genes was confirmed by real-time PCR (Fig. 4c). Lignin synthesis depends on precursors the same as those for benzoic acids. The levels of the three most abundant benzoic acids were reduced in the *vAtCKX1* roots cultivated under optimal conditions (Fig. 4b). Hence, a metabolic switch between lignin and benzoic acid production seems to be a downstream process of reduced CK status. Nevertheless, a more precise analysis of all possible products needs to be conducted in the future to elucidate all consequences of the observed dramatic regulation of genes involved in the phenylpropanoid pathway.

Among other up-regulated processes, we could identify also hydroperoxide dehydratase and linoleate 13S-lipoxygenase activity, which may stimulate the production of JAs or other volatile compounds, the biosynthesis of coumarin, and the response to hyperosmotic salinity (Table 4).

Conclusions

Here, we presented one of the first whole-transcriptome studies done on barley plants. Although a rough draft of the barley genome has been available for several years [69], its precise annotation and the classification of predicted genes into GO categories are still incomplete and in some aspects unsatisfying. For instance, the GO term 'response to cytokinin' counts only 13 putative genes and none of the type A-RR are included. Nevertheless, the

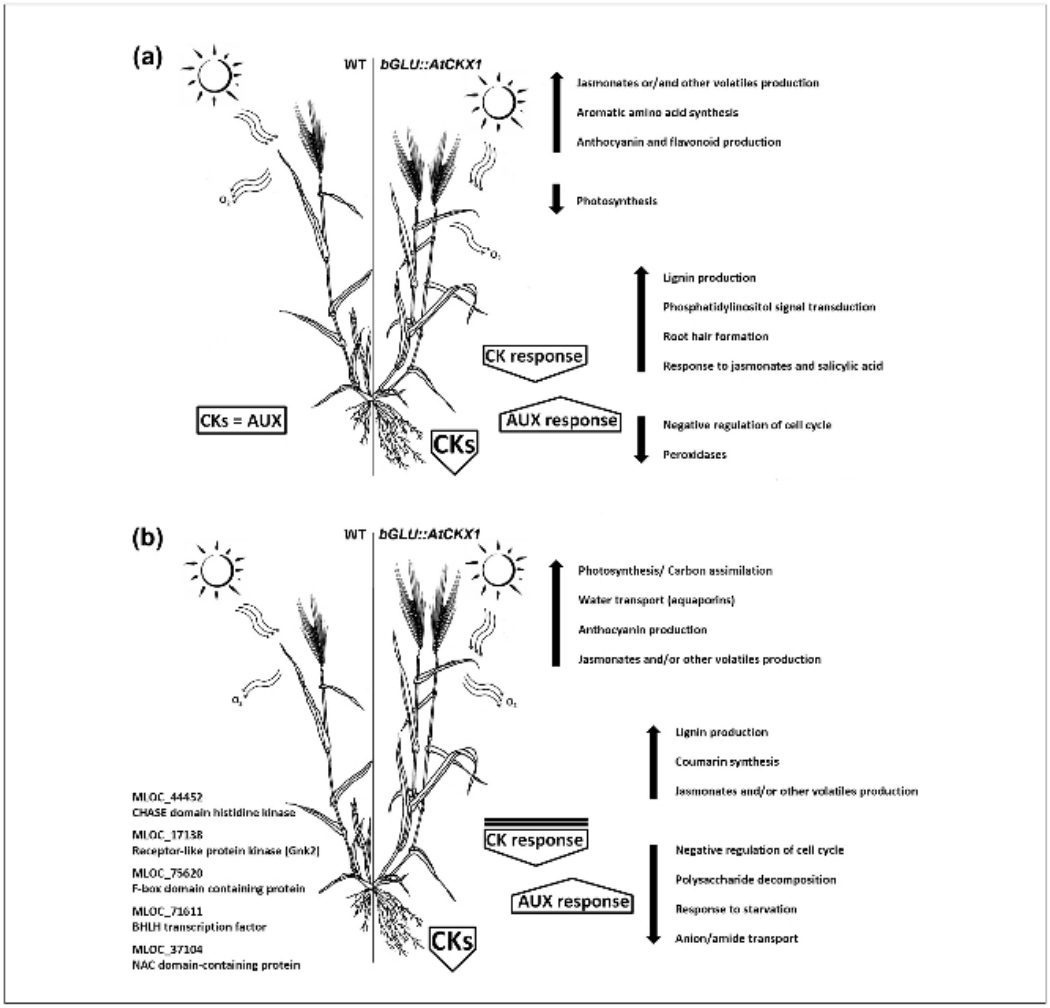

FIGURE 5

Conceptual diagram of main physiological responses in transgenic barley overexpressing *CKX* gene under the control of mild root-specific promotor (a) under optimal conditions or (b) during revitalization after drought stress. Predicted key regulatory genes are listed.

challenging RNA-seq method enabled us to comprehensively inspect all processes occurring in plant tissue with CK imbalance and suggest a new context especially toward other phytohormones. In addition to the fact that the described transgenic plants showed better drought avoidance due to modified root morphology, probably as a consequence of an altered cytokinin-to-auxin ratio, partial CK insensitivity due to down-regulation of HvHK3 receptor expression influenced also other physiological processes leading to drought tolerance (Fig. 5). Up-regulation of four *aquaporin* genes might have contributed to the fact that all transgenic genotypes were able to increase water potential faster than were WT plants. The process of leaf revitalization is accompanied by up-regulation of genes implicated in photosynthesis, and especially those encoded by the chloroplast genome. This aspect leads to faster regeneration of transgenic plants that is observed as higher biomass accumulation. Altered CK status noticeably accelerates secondary metabolism derived from phenylalanine and leads to accumulation of intermediates of the phenylpropanoid pathway in the roots. In this manner, more lignin is deposited in the root tissue and formation of such other compounds as anthocyanins and flavonoids can be expected. The comparative transcriptomic analyses disclosed several genes that might play a crucial role in the drought-tolerant phenotype of *AtCKX1*-overexpressing barley plants. In addition to two transcription factors of the MYB and NAC families shown to increase sensitivity to ABA, the expression of a putative F-box-like protein (MLOC_75620) was strongly depleted in all transgenic tissues. This protein might be involved in ubiquitination of repressors or activators of other phytohormone transduction pathways and thus mediate cross-talk of CKs with auxins, GAs, or JAs. Enforced production of JAs or other volatile compounds might be another process attributed to *AtCKX1*-overexpression phenotype inasmuch as linoleate 13S-lipoxygenase activity is among the most enriched GO terms in both transgenic leaves as well as roots after re-watering. In conclusion, introduction of one CK-degradation enzyme into the barley genome under the control of a mild promoter resulted in a CK-insensitive phenotype that activates processes enabling plants to regenerate better after a water deficit (Fig. 5).

Acknowledgements

The authors thank Hana Pospíšilová for providing plant material. This work was supported by the Czech Science Foundation (grant no. 14-12355S) as well as the Czech Ministry of Education, Youth and Sports through the National Programme for Sustainability I (project no. LO1204), and Mobility (project no. 7AMB15AR011) programs.

Appendix A. Supplementary data

Supplementary data associated with this article can be found, in the online version, at http://dx.doi.org/10.1016/j.nbt.2016.01.010.

References

[1] Zalabák D, Pospíšilová H, Šmehilová M, Mrízová K, Frébort I, Galuszka P. Genetic engineering of cytokinin metabolism: prospective way to improve agricultural traits of crop plants. Biotechnol Adv 2013;31:97–117.
[2] Ha S, Vankova R, Yamaguchi-Shinozaki K, Shinozaki K, Tran LSP. Cytokinins: metabolism and function in plant adaptation to environmental stresses. Trends Plant Sci 2012;17:172–9.
[3] Nishiyama R, Watanabe Y, Fujita Y, Le DT, Kojima M, Werner T, et al. Analysis of cytokinin mutants and regulation of cytokinin metabolic genes reveals important regulatory roles of cytokinins in drought, salt and abscisic acid responses, and abscisic acid biosynthesis. Plant Cell 2011; 23:2169–83.
[4] Tran LSP, Urao T, Qin F, Maruyama K, Kakimoto T, Shinozaki K, et al. Functional analysis of AHK1/ATHK1 and cytokinin receptor histidine kinases in response to abscisic acid, drought, and salt stress in Arabidopsis. Proc Natl Acad Sci U S A 2007;104:20623–28.
[5] Nishiyama R, Watanabe Y, Leyva-Gonzalez MA, Ha CV, Fujita Y, Tanaka M, et al. *Arabidopsis* AHP2, AHP3, and AHP5 histidine phosphotransfer proteins function as redundant negative regulators of drought stress response. Proc Natl Acad Sci U S A 2013;110:4840–5.
[6] Sun L, Zhang Q, Wu J, Zhang L, Jiao X, Zhang S, et al. Two rice authentic histidine phosphotransfer proteins, OsAHP1 and OsAHP2, mediate cytokinin signaling and stress responses in rice. Plant Phys 2014;165:335–45.
[7] Rivero RM, Kojima M, Gepstein A, Sakakibara H, Mittler R, Gepstein S, et al. Delayed leaf senescence induces extreme drought tolerance in a flowering plant. Proc Natl Acad Sci U S A 2007;104:19631–36.
[8] Zhang P, Wang WQ, Zhang GL, Kaminek M, Dobrev P, Xu J, et al. Senescence-inducible expression of isopentenyl transferase extends leaf life, increases drought stress resistance and alters cytokinin metabolism in cassava. J Integr Plant Biol 2010;52:653–69.
[9] Ghanem ME, Albacete A, Smigocki AC, Frébort I, Pospíšilová H, Martinez-Andújar C, et al. Root-synthesized cytokinins improve shoot growth and fruit yield in salinized tomato (*Solanum lycopersicum* L.) plants. J Exp Bot 2011; 62:125–40.
[10] Merewitz EB, Gianfagna T, Huang B. Photosynthesis, water use, and root viability under water stress as affected by expression of *SAG12-ipt* controlling cytokinin synthesis in *Agrostis stolonifera*. J Exp Bot 2011;62:383–95.
[11] Peleg Z, Reguera M, Tumimbang E, Walia H, Blumwald E. Cytokinin-mediated source/sink modifications improve drought tolerance and increase grain yield in rice under water-stress. Plant Biotechnol J 2011;9:747–58.
[12] Kuppu S, Mishra N, Hu R, Sun L, Zhu X, Shen G, et al. Water-deficit inducible expression of a cytokinin biosynthetic gene *IPT* improves drought tolerance in cotton. PLoS ONE 2013;8:e64190.
[13] Reguera M, Peleg Z, Abdel-Tawab YM, Tumimbang EB, Delatorre Ca, Blumwald E. Stress-induced cytokinin synthesis increases drought tolerance through the coordinated regulation of carbon and nitrogen assimilation in rice. Plant Physiol 2013;163:1609–22.
[14] Zhang SW, Li CH, Cao J, Zhang YC, Zhang SQ, Xia YF, et al. Altered architecture and enhanced drought tolerance in rice via the down-regulation of indole-3-acetic acid by *TLD1/OsGH3.13* activation. Plant Physiol 2009;151:1889–901.
[15] Tsuchisaka A, Theologis A. Unique and overlapping expression patterns among the Arabidopsis 1-amino-cyclopropane-1-carboxylate synthase gene family members. Plant Physiol 2004;136:2982–3000.
[16] Růžička K, Ljung K, Vanneste S, Podhorská R, Beeckman T, Friml J, et al. Ethylene regulates root growth through effects on auxin biosynthesis and transport-dependent auxin distribution. Plant Cell 2007;19:2197–212.
[17] Peleg Z, Blumwald E. Hormone balance and abiotic stress tolerance in crop plants. Curr Opin Plant Biol 2011;14:290–5.
[18] Rivero RM, Gimeno J, Van Deynze A, Walia H, Blumwald E. Enhanced cytokinin synthesis in tobacco plants expressing P_{SARK}::*IPT* prevents the degradation of photosynthetic protein complexes during drought. Plant Cell Physiol 2010;51:1929–41.
[19] Wang L, Wang Z, Xu Y, Joo SH, Kim SK, Xue Z, et al. *OsGSR1* is involved in crosstalk between gibberellins and brassinosteroids in rice. Plant J 2009; 57:498–510.
[20] Alonso-Ramírez A, Rodríguez D, Reyes D, Jiménez JA, Nicolás G, López-Climent M, et al. Evidence for a role of gibberellins in salicylic acid-modulated early plant responses to abiotic stress in Arabidopsis seeds. Plant Physiol 2009;150:1335–44.
[21] Wang C, Yang A, Yin H, Zhang J. Influence of water stress on endogenous hormone contents and cell damage of maize seedlings. J Integr Plant Biol 2008;50:427–34.
[22] Vyroubalová Š, Václavíková K, Turečková V, Novák O, Šmehilová M, Hluska T, et al. Characterization of new maize genes putatively involved in cytokinin metabolism and their expression during osmotic stress in relation to cytokinin levels. Plant Physiol 2009;151:433–47.
[23] Havlová M, Dobrev PI, Motyka V, Štorchová H, Libus J, Dobrá J, et al. The role of cytokinins in responses to water deficit in tobacco plants over-expressing *trans*-zeatin O-glucosyltransferase gene under *35S* or *SAG12* promoters. Plant Cell Environ 2008;31:341–53.
[24] Gan S, Amasino RM. Inhibition of leaf senescence by autoregulated production of cytokinin. Science 1995;270:1986–8.
[25] Sýkorová B, Kurešová G, Daskalova S, Trčková M, Hoyerová K, Raimanová I, et al. Senescence-induced ectopic expression of the *A. tumefaciens ipt* gene in wheat delays leaf senescence, increases cytokinin content, nitrate influx, and nitrate reductase activity, but does not affect grain yield. J Exp Bot 2008;59:377–87.

[26] Sharp RE, LeNoble ME. ABA, ethylene and the control of shoot and root growth under water stress. J Exp Bot 2002;53:33–7.
[27] Albacete AA, Martínez-Andújar C, Pérez-Alfocea F. Hormonal and metabolic regulation of source–sink relations under salinity and drought: from plant survival to crop yield stability. Biotechnol Adv 2014;32:12–30.
[28] Werner T, Nehnevajova E, Köllmer I, Novák O, Strnad M, Krämer U, et al. Root-specific reduction of cytokinin causes enhanced root growth, drought tolerance, and leaf mineral enrichment in *Arabidopsis* and tobacco. Plant Cell 2010; 22:3905–20.
[29] Macková H, Hronková M, Dobrá J, Turečková V, Novák O, Lubovská Z, et al. Enhanced drought and heat stress tolerance of tobacco plants with ectopically enhanced cytokinin oxidase/dehydrogenase gene expression. J Exp Bot 2013;64:2805–15.
[30] Pospíšilová H, Jiskrová E, Vojta P, Mrízová K, Kokáš F, Majeská Čudejková M, et al. Transgenic barley overexpressing a cytokinin dehydrogenase gene shows greater tolerance to drought stress. New Biotechnol 2016;33:692–705.
[31] Vlamis J, Williams DE. Ion competition in manganese uptake by barley plants. Plant Physiol 1962;37:650–5.
[32] Turner NC, Abbo S, Berger JD, Chaturvedi SK, French RJ, Ludwig C, et al. Osmotic adjustment in chickpea (*Cicer arietinum* L.) results in no yield benefit under terminal drought. J Exp Bot 2007;58:187–94.
[33] Livak KJ, Schmittgen TD. Analysis of relative gene expression data using real-time quantitative PCR and the 2−ΔΔCT method. Methods 2001;25: 402–8.
[34] Kim D, Pertea G, Trapnell C, Pimentel H, Kelley R, Salzberg SL. TopHat2: accurate alignment of transcriptomes in the presence of insertions, deletions and gene fusions. Genome Biol 2013;14:R36.
[35] Anders S, Pyl PT, Huber W. HTSeq – a Python framework to work with high-throughput sequencing data. Bioinformatics 2014;31:166–9.
[36] Love MI, Huber W, Anders S. Moderated estimation of fold change and dispersion for RNA-Seq data with DESeq2. Genome Biol 2014;15:550.
[37] Kokáš F, Vojta P, Galuszka P. Comparative transcriptome analysis of barley (*Hordeum vulgare*) exposed to drought and subsequent re-watering. Data Brief 2016 [submitted for publication].
[38] Conesa A, Götz S, García-Gómez JM, Terol J, Talón M, Robles M. Blast2GO: a universal tool for annotation, visualization and analysis in functional genomics research. Bioinformatics 2005;21:3674–6.
[39] Camacho C, Coulouris G, Avagyan V, Ma N, Papadopoulos J, Bealer K, et al. BLAST+: architecture and applications. BMC Bioinform 2009;10:421.
[40] Moreira-Vilar FC, Siqueira-Soares RDC, Finger-Teixeira A, De Oliveira DM, Ferro AP, Da Rocha GJ, et al. The acetyl bromide method is faster, simpler and presents best recovery of lignin in different herbaceous tissues than klason and thioglycolic acid methods. PLoS ONE 2014;9:e110000.
[41] Gruz J, Novák O, Strnad M. Rapid analysis of phenolic acids in beverages by UPLC–MS/MS. Food Chem 2008;111:789–94.
[42] Oxborough K, Baker NR. Resolving chlorophyll *a* fluorescence images of photosynthetic efficiency into photochemical and non-photochemical components – calculation of *qP* and *Fv′/Fm′* without measuring *Fo′*. Photosynth Res 1997;54:135–42.
[43] Hassan IA. Effects of water stress and high temperature on gas exchange and chlorophyll fluorescence in *Triticum aestivum* L.. Photosynthetica 2006;44: 312–5.
[44] Roostaei M, Mohammadi SA, Amri A, Majidi E, Nachit M, Haghparast R. Chlorophyll fluorescence parameters and drought tolerance in a mapping population of winter bread wheat in the highlands of Iran. Russ J Plant Physiol 2011;58:351–8.
[45] Robredo A, Pérez-López U, Miranda-Apodaca J, Lacuesta M, Mena-Petite A, Muñoz-Rueda A. Elevated CO_2 reduces the drought effect on nitrogen metabolism in barley plants during drought and subsequent recovery. Environ Exp Bot 2011;71:399–408.
[46] Rippert P, Matringe M. Molecular and biochemical characterization of an *Arabidopsis thaliana* arogenate dehydrogenase with two highly similar and active protein domains. Plant Mol Biol 2002;48:361–8.
[47] Cass CL, Peraldi A, Dowd PF, Mottiar Y, Santoro N, Karlen SD, et al. Effects of *PHENYLALANINE AMMONIA LYASE* (*PAL*) knockdown on cell wall composition, biomass digestibility, and biotic and abiotic stress responses in *Brachypodium*. J Exp Bot 2015;66:4317–35.
[48] Feussner I, Wasternack C. The lipoxygenase pathway. Annu Rev Plant Biol 2002;53:275–97.
[49] Wasternack C. Action of jasmonates in plant stress responses and development – applied aspects. Biotechnol Adv 2014;32:31–9.
[50] Tian D, Tooker J, Peiffer M, Chung SH, Felton GW. Role of trichomes in defense against herbivores: comparison of herbivore response to *woolly* and *hairless* trichome mutants in tomato (*Solanum lycopersicum*). Planta 2012;236:1053–66.
[51] Ueda J, Kato J. Identification of jasmonic acid and abscisic acid as senescence-promoting substances from *Cleyera ochnacea* DC. Agric Biol Chem 1982; 46:1975–6.
[52] O'Brien JA, Benková E. Cytokinin cross-talking during biotic and abiotic stress responses. Front Plant Sci 2013;4:451.
[53] Baldwin IT, Schemelz EA, Ohnmeiss TE. Wound-induced changes in root and shoot jasmonic acid pools correlate with induced nicotine synthesis in *Nicotiana sylvestris* spegazzini and comes. J Chem Ecol 1994;20:2139–57.
[54] Moon J, Parry G, Estelle M. The ubiquitin–proteasome pathway and plant development. Plant Cell 2004;16:3181–95.
[55] Zubo YO, Yamburenko MV, Selivankina SY, Shakirova FM, Avalbaev AM, Kudryakova NV, et al. Cytokinin stimulates chloroplast transcription in detached barley leaves. Plant Physiol 2008;148:1082–93.
[56] Wei W, Alexandersson E, Golldack D, Miller AJ, Kjellbom PO, Fricke W. HvPIP1;6, a barley (*Hordeum vulgare* L.) plasma membrane water channel particularly expressed in growing compared with non-growing leaf tissues. Plant Cell Physiol 2007;48:1132–47.
[57] Nakabayashi R, Yonekura-Sakakibara K, Urano K, Suzuki M, Yamada Y, Nishizawa T, et al. Enhancement of oxidative and drought tolerance in Arabidopsis by overaccumulation of antioxidant flavonoids. Plant J 2014;77:367–79.
[58] Cha JY, Barman DN, Kim MG, Kim WY. Stress defense mechanisms of NADPH-dependent thioredoxin reductases (NTRs) in plants. Plant Signal Behav 2015;10:e1017698.
[59] Cheng Z, Dong K, Ge P, Bian Y, Dong L, Deng X, et al. Identification of leaf proteins differentially accumulated between wheat cultivars distinct in their levels of drought tolerance. PLoS ONE 2015;10:e0125302.
[60] Jiang Y, Chen R, Dong J, Xu Z, Gao X. Analysis of GDSL lipase (GLIP) family genes in rice (*Oryza sativa*). Plant Omics 2012;5:351–8.
[61] Hong JK, Choi HW, Hwang IS, Kim DS, Kim NH, Choi DS, et al. Function of a novel GDSL-type pepper lipase gene, *CaGLIP1*, in disease susceptibility and abiotic stress tolerance. Planta 2008;227:539–58.
[62] Galichet A, Hoyerová K, Kamínek M, Gruissem W. Farnesylation directs AtIPT3 subcellular localization and modulates cytokinin biosynthesis in Arabidopsis. Plant Physiol 2008;146:1155–64.
[63] Tsai YC, Weir NR, Hill K, Zhang W, Kim HJ, Shiu SH, et al. Characterization of genes involved in cytokinin signaling and metabolism from rice. Plant Physiol 2012;158:1666–84.
[64] Tran LSP, Nakashima K, Sakuma Y, Simpson SD, Fujita Y, Maruyama K, et al. Isolation and functional analysis of Arabidopsis stress-inducible NAC transcription factors that bind to a drought-responsive *cis*-element in the *early responsive to dehydration stress 1* promoter. Plant Cell 2004;16:2481–98.
[65] Abe H, Urao T, Ito T, Seki M, Shinozaki K, Yamaguchi-Shinozaki K. Arabidopsis AtMYC2 (bHLH) and AtMYB2 (MYB) function as transcriptional activators in abscisic acid signaling. Society 2003;15:63–78.
[66] Bu Q, Jiang H, Li CB, Zhai Q, Zhang J, Wu X, et al. Role of the *Arabidopsis thaliana* NAC transcription factors ANAC019 and ANAC055 in regulating jasmonic acid-signaled defense responses. Cell Res 2008;18:756–67.
[67] Redillas MCFR, Jeong JS, Kim YS, Jung H, Bang SW, Choi YD, et al. The overexpression of *OsNAC9* alters the root architecture of rice plants enhancing drought resistance and grain yield under field conditions. Plant Biotechnol J 2012;10:792–805.
[68] McSteen P. Auxin and monocot development. Cold Spring Harb Perspect Biol 2010;2:a001479.
[69] Mayer KFX, Waugh R, Langridge P, Close TJ, Wise RP, et al. A physical, genetic and functional sequence assembly of the barley genome. Nature 2012; 491:711–6.